Simulating the Sydney hailstorm of 9 December 2007 using WRF

Benjamin McBurney

A Thesis Submitted in Fulfilment
of the Requirements for the Masters of Research Degree

FACULTY OF SCIENCE AND ENGINEERING

23rd October 2015

Department of Environmental Sciences
Macquarie University
Sydney, Australia

CONTENTS

Abstract

This study first extended Sydney's most comprehensive hybrid hailstorm database until the end of the 2014/2015 June-May hail season to discern whether an apparent decline in hailstorm frequency over the 1991-2010 period (8.45 ± 1.57 hailstorms per annum) has continued in recent years. Hailstorm numbers were found to average 10.89 ± 1.20 per annum from 1950-2014. However, the average became 12.00 ± 4.68 hailstorms per annum during 2011-2014. This suggests that the apparent decline may be attributed to inter-annual and inter-decadal variability, rather than a long-term reduction in frequency.

As a case study, a high-resolution numerical simulation of the 9th of December, 2007 hailstorm was undertaken in order to assess advancements in Numerical Weather Prediction (NWP) models for such local-scale hazardous weather. The storm was simulated using version 3.6.1 of the Weather Research and Forecasting (WRF) Model. Sensitivity tests on cloud microphysics and radiation schemes were performed to determine their impacts. Microphysics options that included hail as one of their hydrometeors reproduced the hailstorm significantly better than those that did not. The Goddard microphysics scheme using the hail option coupled with the Goddard shortwave radiation scheme simulated the event most accurately, although the storm arrived approximately 1.5 hours earlier than the actual event.

ACKNOWLEDGEMENTS

I would like to thank Dr Kevin Cheung for being my supervisor again this year, for keeping me on the right track amongst the frustrating times trying to learn WRF.

Thank you very much to Christina Macgill, my co-supervisor who was happy to help out with whatever issues I had!

A very big thanks to Yubin Li and Guoping Zhang (Ben) for helping me out with my WRF problems. I don’t know where I would be without the advice of both of you – I would have had a much more difficult and stressful year otherwise!

Finally, a big thanks to William Farebrother again for continual support and feedback throughout the year! I don’t know many other people out there who are as willing to help out as you are. Best of luck in your Masters of Research, I know you’ll go far!

LIST OF FIGURES

LIST OF TABLES

DECLARATION

I certify that the work in this thesis “Simulating the Sydney hailstorm of 9 December using WRF” has not previously been submitted for a degree nor has it been submitted as part of requirements for a degree to any other university or institution other than Macquarie University.

I also certify that the thesis is an original piece of research and has been written by me. The assistance and help I have received in my research have been acknowledged.

I declare that all literature and sources of information are appropriately reference in the thesis.

Benjamin McBurney (41190548)

October 2015

CHAPTER 1 INTRODUCTION AND LITERATURE REVIEW

1.1 Introduction

Hail is a weather phenomenon that significantly impacts people through casualties and often extensive property damage. Globally, the most intense hailstorms have been documented in the United States, Argentina, Bangladesh and central Africa (Cecil and Blankenship, 2012). Australia has only recently been recognised as a place that endures frequent severe hail, particularly in the nation's east (Cecil and Blankenship, 2012), and is the country's most expensive type of natural disaster, accounting for one-third of total insured losses (Schuster *et al.,* 2005). Arguably, Australia's most hail-prone city is Sydney where approximately 45% of all severe thunderstorms contain severe hail (Schuster *et al.,* 2005; Crompton, 2011). In Australia, severe thunderstorms are defined as any storm that produces one or a combination of: wind gusts in excess of 90 km h^{-1}, heavy rainfall leading to flash flooding, tornadoes, and hail equal to or greater than 2 cm in diameter (Bureau of Meteorology, 2011). Sydney has experienced a number of very large hail events across the past three decades (Schuster *et al.*, 2005). The most damaging of these was the Sydney hailstorm of April 1999, where hailstones up to 9 cm in diameter (unofficial reports of up to 13 cm) caused an estimated AUD$2 billion dollars of damage (Speer *et al.*, 2004). However, despite the incidence of severe hailstorms in eastern Australia and Sydney, there has been little research done on this area of study. Accurately studying hail is difficult as it is a small-scale phenomenon with a spatial scale typically of several hundreds of metres or a few kilometres, with durations in the order of minutes (Sokol *et al.,* 2014). This can make it especially difficult in countries such as Australia where vast areas of the country are sparsely populated. Schuster *et al.* (2005) constructed the first hail climatology of the Sydney metropolitan area between 1791 and 2003, using reports from the public obtained from the Australian Bureau of Meteorology (BoM), and the Risk Frontier's PerilAus database that was developed using a combination of newspaper articles and scientific reports (Risk Frontiers, 2011). They found that hailstorm frequency averaged approximately 10 hailstorms per annum (P.a.) over the preceding 50 years, with significant inter-annual and inter-decadal variability, but a reduction in hailstorm frequency since 1989. This hailstorm climatology was extended and updated in McBurney (2012) until the 2010/2011 June-May hail season, observing a similar reduction in hailstorm frequency since the early 90s, although this was partly attributed due to missing data from 1991-1999. Rasuly *et al.* (2015) found that severe hail events had sharply declined over the 2011-2013 period in Sydney.

The required conditions for hailstorm formation in other parts of the globe have been studied at length (Mills and Colquhoun, 1998; Tucker, 2002), however a study by Tucker (2002) suggested that some parameters used elsewhere in the world to forecast hailstorms were not as useful in eastern Australia. Notably, only small or moderate amounts of Convective Available Potential Energy (CAPE, refer to Appendix I for definition) were frequently found during hailstorms events, which also had little impact on severity. These findings were supported by McBurney (2012), which noted only low or moderate CAPE combined with strong vertical wind shear (see Appendix I for definition) and a cold and dry upper level atmosphere led to most severe hailstorm events in Sydney. However, whilst the mechanisms that precipitate hailstorm development are becoming more understood, it is extremely difficult to predict the position and time of hail occurrence with satisfactory precision due to its complex and dynamic nature (Sokol *et al.*, 2014). There has been a focus in recent years on trying to successfully simulate hailstorms using high resolution models. Studies using very high resolution models in the order of hundreds of metres to a kilometre have examined individual storms, including squall lines (Jewett *et al.*, 2001; French & Parker, 2014) with some encouraging results. Many studies (several of these will be analysed here) have also attempted simulations of large hailstorm events using slightly coarser resolutions (1-50 km) using a variety of mesoscale Numerical Weather Prediction (NWP) models complemented by cloud microphysics schemes (Sokol *et al.*, 2014; Garcia-Ortega *et al.*, 2007; Chevuturi *et al.*, 2014; Buckley *et al.*, 2001; Speer *et al.*, 2004; Leslie *et al.*, 2008). Forecasting hail using these models can be very complex as they can be highly sensitive to primary data controlling the model initial condition and closely rely on the parameterisation of microphysical processes (Sokol *et al.*, 2014). However, despite these complexities, severe hail events have been successfully simulated in various parts of the globe, including Australia.

Initially, the most detailed hailstorm database of the Sydney Metropolitan Region (compiled by Schuster *et al.*, 2005 and McBurney, 2012) for the period 1950-2010 was updated to May 2015. This was done in order determine whether an apparent decline in hailstorm frequency over the 1990-2010 period found in McBurney (2012) had continued, and whether the low frequency of severe hail events found in Rasuly *et al.* (2015) for the 2011-2013 period had continued in recent years.

To this end, a case study of a giant hailstorm event that impacted Sydney in the last several decades was simulated. This was accomplished through initially conducting a literature review that examined three of Sydney's most damaging hailstorm events: the 18 March 1990 hailstorm, the 14 April 1999 hailstorm and the 9 December 2007 hailstorm. These events were analysed in detail, focusing on the synoptic setup, thunderstorm track, meteorological observations and damage. This literature review also investigated studies that have simulated hailstorm events using mesoscale NWP models (resolutions of 1-50 km), focusing on the accuracy of the simulations and the types of methods used to achieve the outcomes. Australian simulations in particular were examined in order to determine how research in in this field compared internationally, improvements that are required, and the exploration of data limitations in the country.

This allowed a severe hailstorm event in Sydney to be simulated using The Weather Research and Forecasting (WRF) model; a next-generation numerical weather prediction system, with the Advanced Research WRF (ARW) solver. Through examining the cases in the literature review, it was determined that the 9th of December, 2007 hailstorm that impacted western and northern parts of Sydney was suitable for this study. This case was selected as it has not yet been studied in detail, despite it being one of Sydney's most costly and devastating hailstorms. This paper aimed to build on the research undertaken by Buckley *et al.* (2001) and Leslie *et al.* (2008) to help improve high-resolution forecasting of severe hailstorms, particularly in Australia.

1.2 Literature Review: Sydney Historical Cases

Literature describing three of Sydney’s most damaging hailstorms; the 18 March 1990 hailstorm, the 14 April 1999 hailstorm and the 9 December 2007 hailstorm were examined in detail, focusing on the synoptic setup, observations and damage.

1.2.1 18 March 1990 event

Mitchell and Griffiths (1993) from the BoM conducted an in-depth analysis of the 18 March 1990 hailstorm event, which had an insurance payout of AUD$400 million dollars (Andrews and Blong, 1997). The supercell thunderstorm produced hailstones as large as 8 cm around Liverpool, very heavy rainfall leading to flash flooding and wind gusts of 109 km h^{-1} at Bankstown Airport Automatic Weather Station (AWS), although damage suggested stronger gusts. The storm developed 53 km west-southwest of Camden on the Great Diving Range and moved on an east-northeast path (left of the mean steering flow) across the Sydney Basin, reaching maximum intensity at approximately 4 pm. Fig. 1.1 demonstrates the path of the storm and observed hail sizes across Sydney, which was adapted from a report by Andrews and Blong (1997), who assessed damage across the Sydney region from the storm.

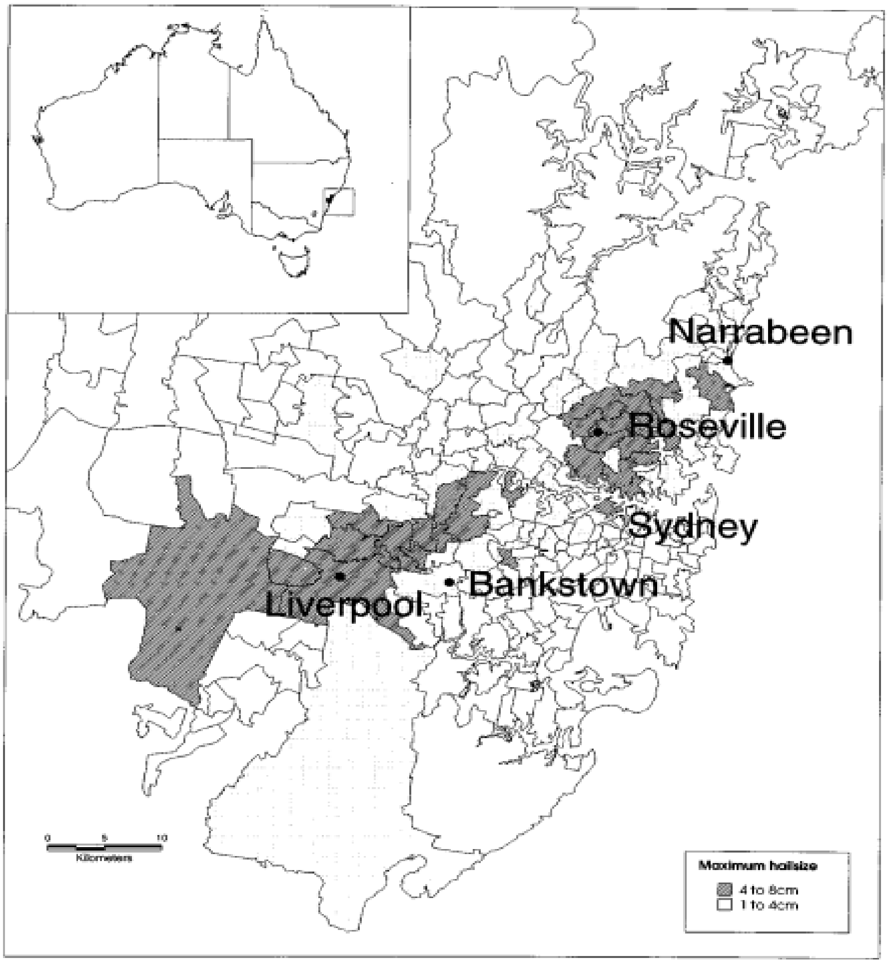

Fig. 1.1. Maximum reported hailsize by postcode on 18 March, 1990 [adapted from Figure 1 of Andrews and Blong (1997)].

As discussed in Mitchells & Griffiths (1993), a trough stretched roughly from Nyngan to Tumut (Fig. 1.2). This trough marked the boundary between moist-low level air sourced from the Tasman Sea (directed by a high pressure system near New Zealand) and dry, stable air caused by a high pressure system in the Great Australian Bight. An upper trough sloping with height from 600-300 hPa complemented a cold pool of upper level air which approached Sydney from the west during the day.

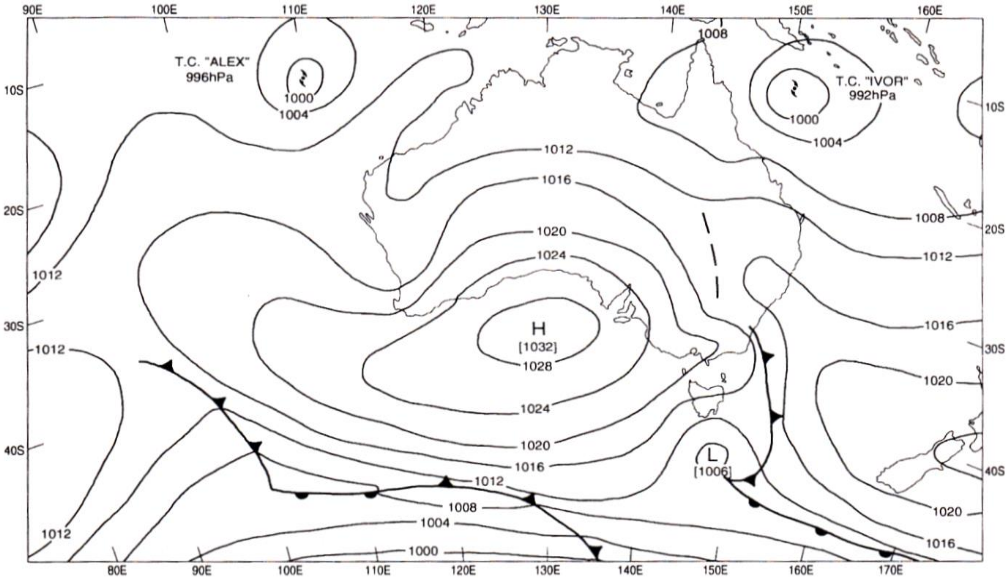

Fig. 1.2. Synoptic chart at 9 am EDT on 18 March, 1990 [adapted from Fig. 8 of Mitchell and Griffiths (1993)].

A weak south-southeast wind change moved through Sydney around midday, however due to retardation of the front along the ranges, light easterly winds persisted along the eastern ranges. The 2300 Coordinated Universal Time (UTC) sounding (9 am Eastern Daylight Time (EDT)) showed that while linear shear was not strong, there was significant directional shear (wind backing with height). There were 16 kt southeasterly winds at the surface, 15 kt southwesterly winds at 850 hPa, 20 kt west-northwesterly winds at 500 hPa and a strong west-northwest jet of 110 kts at 200 hPa. Wind shear intensified during the day as the surface trough and upper level cold pool approached. As the upper level trough and cold pool approached, lapse rates and adiabatic cooling intensified with 500 hPa temperatures cooling from -12 to -18 °C between 3 pm and 4 pm, around the height of the storm. CAPE values across Sydney averaged 1200 J kg^{-1}, with the highest values (1400 J kg^{-1}) to the southwest of the Sydney region. The storm originated in Sydney's southwest on the frontal boundary and close to the 600 hPa upper trough in steep topography, approximately 1050 m above sea level (ASL). The role of topography as a mechanism for storm formation has been documented in a few hail studies in Europe (Spanos, 1993; Manzato, 2012) and was a significant trigger for this hailstorm event. The Bulk Richardson Value (a value that incorporates both wind shear and CAPE, see Appendix I for definition) of 14 was recorded, which is well within the 10-40 range required for supercell formation (Mitchell and Griffiths, 1993). Helicity (see Appendix I) values were obtained from planes but were inconsistent. One flight recorded helicity as low as -18 m^2s^{-2}, but another flight noted an increase from -186 m^2s^{-2} to -427 m^2s^{-2} within 40 minutes. As seen in Fig. 1.3, an intrusion of dry air was located in the mid-troposphere, a factor that is commonly associated with severe hail events (Colquhoun, 1987).

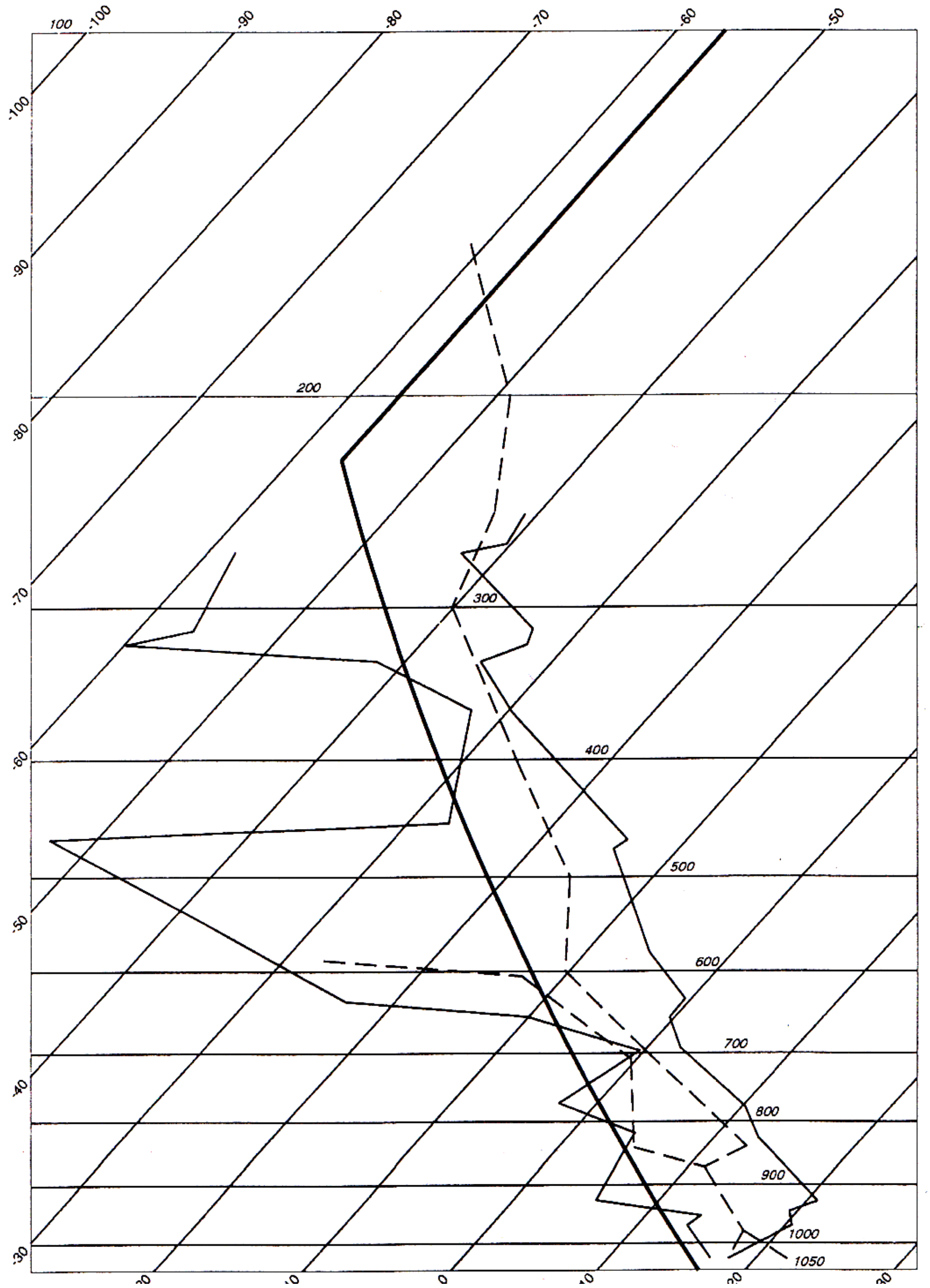

Fig. 1.3. Skew-T diagram showing temperature and dewpoint profile for Sydney airport at 6 am on 18 March 1990 [adapted from Fig. 16 of Mitchell and Griffiths (1993)].

The combination of moderate levels of CAPE, strong directional wind shear, a dry slot (see Appendix I) in the mid-troposphere and steepening lapse rates were all considered fundamental in allowing the storm to have become intense enough to produce giant hail. The strong upper level jet was also believed to have played a role in the storms severity.

1.2.2 14 April 1999 Event

Buckley *et al.* (2001) undertook a study of the meteorological conditions that led to the 14th April 1999 Sydney hailstorm, the most costly and damaging hailstorm in Australia's history. The storm led to insured losses of AUD$1.7 billion dollars, with total damage estimated at around AUD$2 billion (Speer *et al.,* 2004). The largest measured hail stone was 9 cm at Kensington in Sydney's eastern suburbs, with some reports and damage surveys suggesting hail closer to 11 cm was likely. Strong winds and heavy rainfall were also reported over the northern suburbs. Notably, the thunderstorm was poorly forecasted, with conditions in the morning unfavourable for severe thunderstorm development. The storm track was very unusual for severe thunderstorms in the Sydney Basin, developing west of Kiama (to the south of Sydney) and moving north-northeast up the coastline, eventually moving offshore. As the storm underwent transition into a supercell it veered to the left of the steering flow (a more northerly path) towards eastern Sydney (Fig. 1.4).

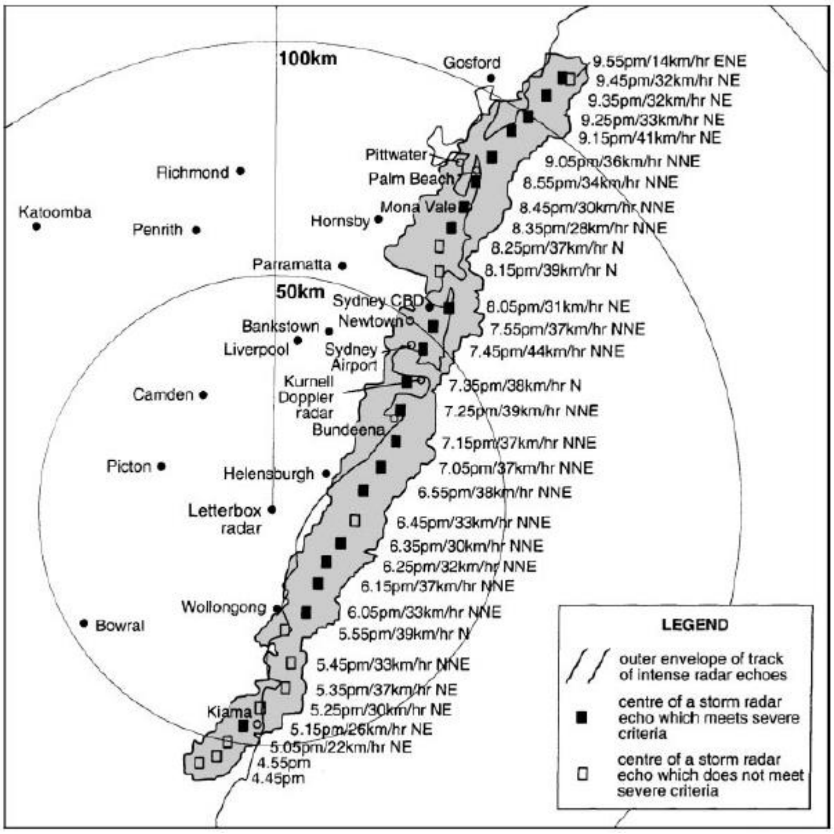

Fig. 1.4. Path of the 14th April, 1999 Sydney hailstorm [adapted from Fig.6 of Buckley *et al.* (2001)].

It is evident in Fig. 1.5 that a weak cold front moved up the NSW coastline, associated with a pre-frontal trough, with a high pressure ridge situated over the Great Australian Bight behind the front. A deep layer of moderately strong and relatively stable west-southwest winds were located ahead of the front, which extended from 1000 m above the ground through to the tropopause. A cold pool of upper level air and an associated upper-level trough approached from the west during the day, destabilising the atmosphere and affecting Sydney later in the evening.

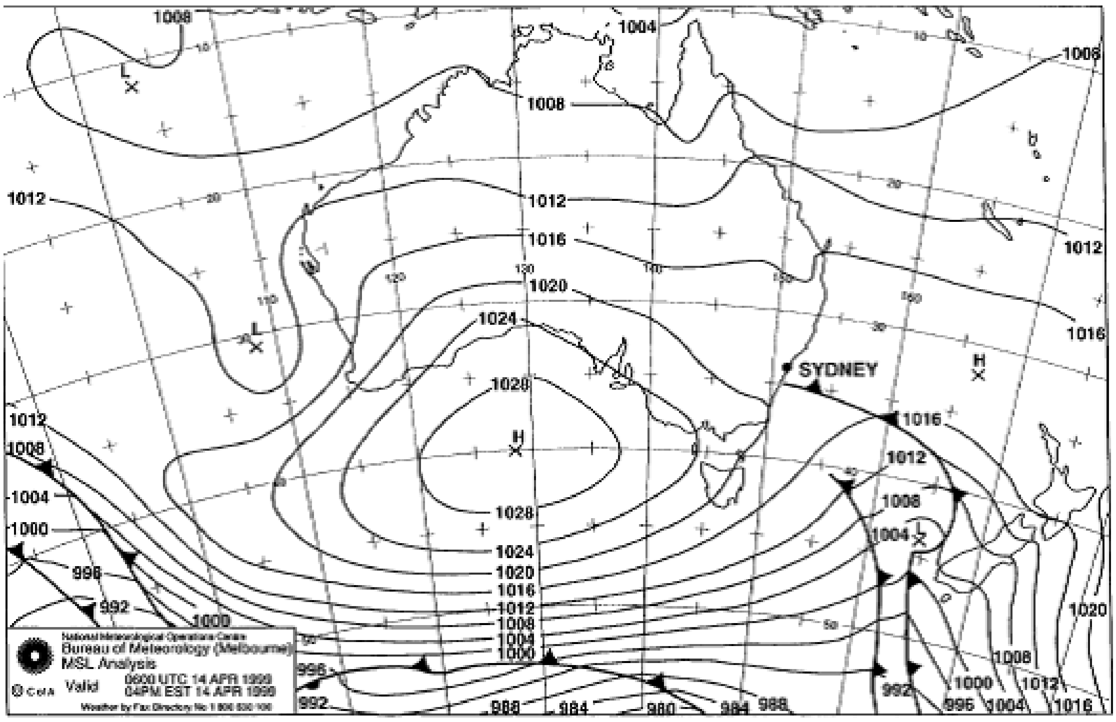

Mean sea-level pressure pattern at 4pm 14 April, 1999

Fig. 1.5. Surface analysis chart at 4 pm (EST) 14 April, 1999 [adapted from Fig.8a of Buckley *et al.* (2001)].

Temperatures at the surface were 26 °C in western Sydney and 21 °C on the coast, while dewpoints at the surface were approximately 16 °C. The dewpoint declined rapidly with height with little moisture above 1000 m ASL. A significant inversion was also located around this layer. However, easterly winds strengthened and deepened due to the approach of the front. At midday these easterly winds were light and only 300 m deep, but reached 16 kts at 1500 m (850 hPa) by 7 pm. This provided sufficient moisture to trigger hail coalescence. There was significant directional wind shear, with west-southwest winds 24 kts at 600 hPa and 34 kts at 500 hPa. CAPE values were moderate at approximately 1700 J kg^{-1} and lifted index (refer to A1 for definition) values peaked at -4 (Bureau of Meteorology, 2006). As seen in the Skew-T diagram below (Fig. 1.6), lapse rates were steep due to the approaching cold pool and upper trough, while there was also dry air located in the mid-troposphere around 650 hPa.

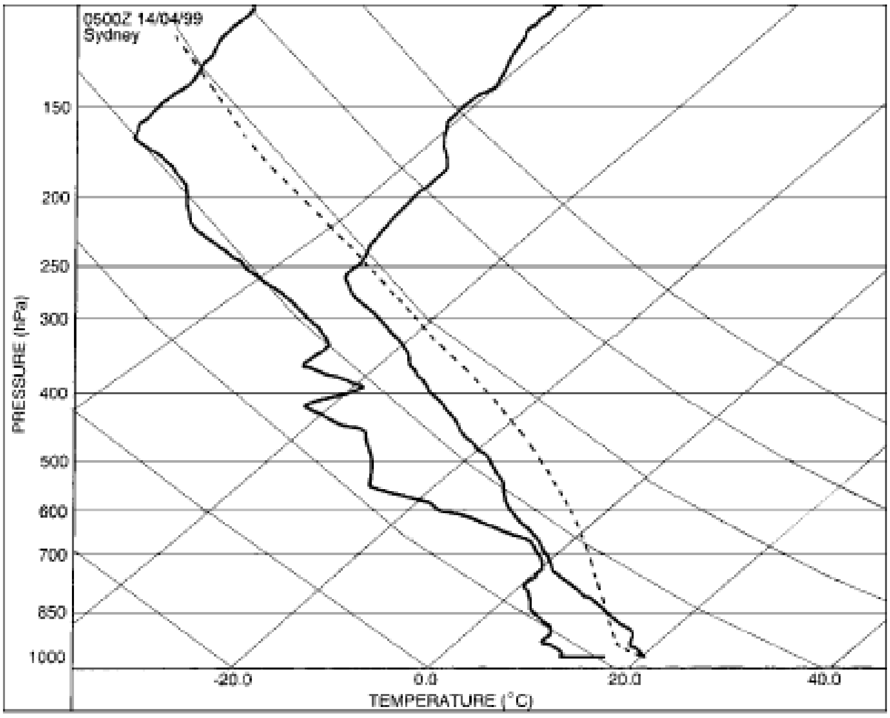

Fig. 1.6. Skew-T Diagram at Sydney airport at 3 pm, 14th April 1999 [adapted from Fig.8c of Buckley *et al.* (2001)].

Helicity at 3 pm was recorded at -180 m^2s^{-2} and continued to increase throughout the afternoon. The Bulk Richardson value was recorded at 37 (Bureau of Meteorology, 2006). While conditions were unfavourable for supercell development in the morning, meteorological parameters became more favourable throughout the day in response to the approaching cold pool and front, playing a significant role in the storm's intensity. Helicity, wind shear and moisture values reached their peaks right on the change, considerably aiding the formation of the supercell. It was inferred that the non-severe storm ran into strengthening easterly winds, which provided inflow and increased vertical wind shear on the change. These conditions combined with the increased low level moisture provided by unseasonably warm sea surface temperatures (SSTs), allowing the storm to evolve into a supercell. The enhanced upper-level shear and cooler, drier air in the mid-troposphere helped sustain the supercell structure for over five hours.

1.2.3 9 December 2007 Event

Sydney's most recent giant hailstorm event was analysed by Davies *et al.* (2008), and had a total insurance payout estimated to be AUD$470 million. The thunderstorm developed over the lower Blue Mountains near Warragamba Dam and as it transitioned into a supercell thunderstorm took on an east-northeast path, left of the mean steering flow. The storm peaked as it moved over the Blacktown area with a secondary focus across the Castle Hill area. The official maximum recorded hailstorm size was 8.5 cm, although members of the public reported stones as large as 11 cm. Fig. 1.7 shows the path of the storm and distribution of hail size in the Sydney Basin.

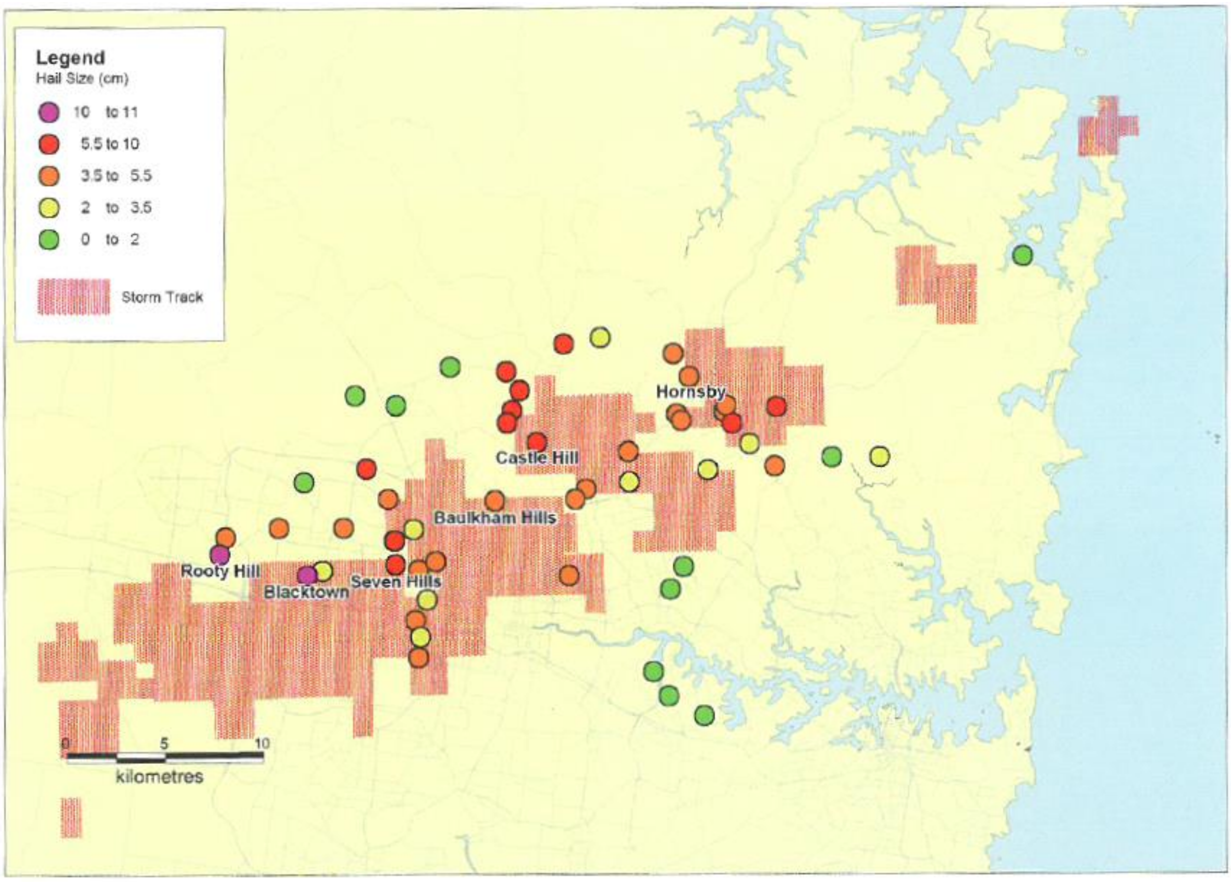

Fig. 1.7. Footprints of high reflectivity radar echoes and observed hailstone sizes of the 9th December, 2007 hailstorm [adapted from Figure 5 of Davies *et al.* (2008)].

As seen in the surface analysis chart at 00:00 UTC (11am EDT) in Fig. 1.8, a surface trough approached from the west during the day, enhancing instability, while a high pressure ridge over the Tasman Sea directed a humid northeasterly wind flow across the Sydney Basin. A cold front was crossing Victoria and Tasmania.

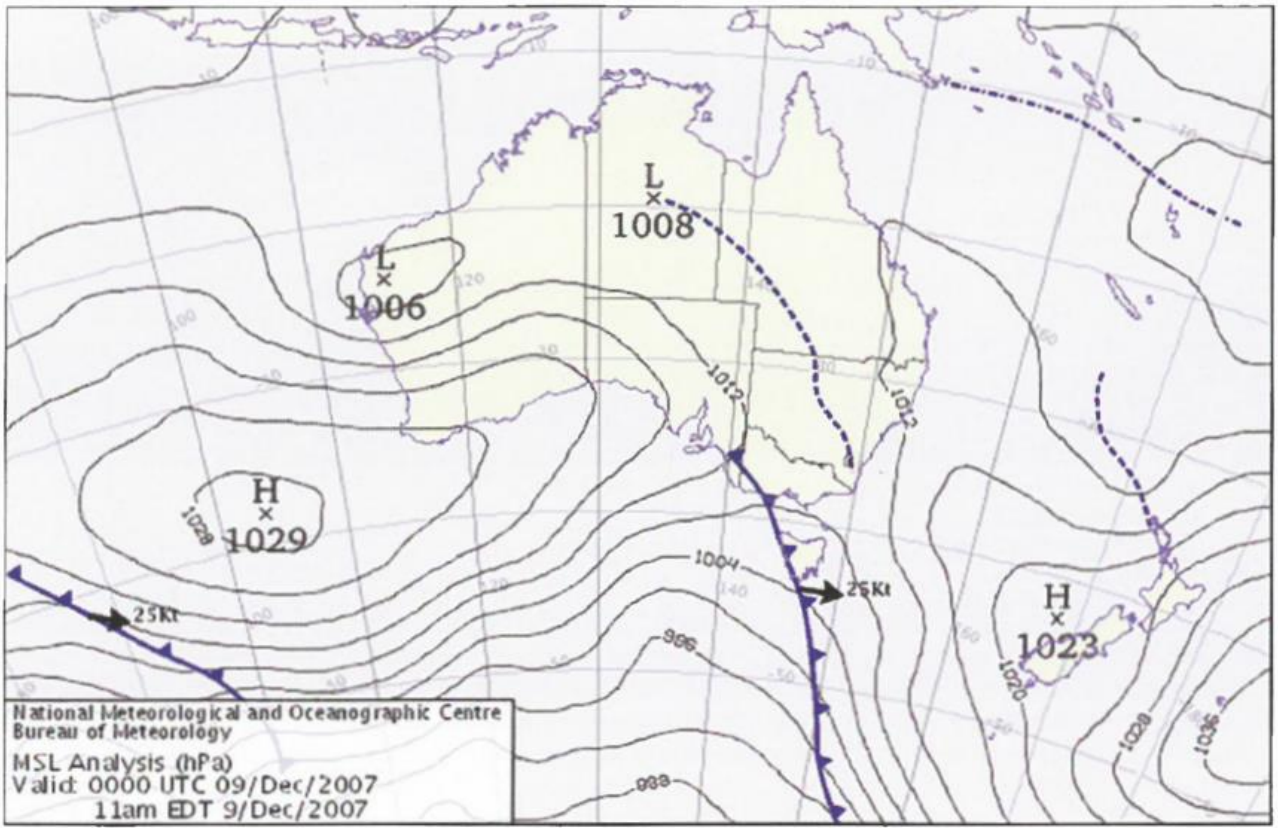

Fig. 1.8. Mean Sea Level Pressure Chart at 11 am on 9 December 2007 [adapted from Figure 2 of Davies *et al.* (2008)].

Unfortunately, Davies *et al.*, (2008) lacked the exact meteorological conditions of the day, although several important dynamics were noted. Temperatures were cool enough in the mid-levels so that the rising humid air was significantly warmer than its surrounding environment, encouraging strong updrafts to develop. Northeasterly winds in the low-levels backed to westerly winds in the mid-levels to create sufficient shear for the thunderstorm to transition into a supercell and to steer the storm across Sydney. These northeasterly winds helped cause a deep layer of low-level moisture, which is believed to be a fundamental factor in the severity of this storm (Davies *et al.*, 2008).

1.3 Model simulations

1.3.1 International studies

Predicting the position and time of hail occurrence with adequate precision is extremely difficult. High-resolution NWP models in conjunction with cloud microphysics schemes have the ability to be used to predict severe thunderstorms and hail (Sokol *et al.*, 2014; Leslie *et al.*, 2008; Chevuturi *et al.*, 2014). Cloud microphysics schemes consist of a variety of hydrometeors to help simulate the processes controlling the development and growth of ice crystals and cloud droplets and their end as precipitation (Morrison, 2010). Many of the currently operational NWP models do not consider hail to be one of the hydrometeors in model microphysics, limiting hail forecasts to warnings indicating the possibility of hail producing severe convection (Sokol *et al.*, 2014). However, there are some high-resolution NWP models that do include hail as one of the hydrometeors, and can be used to simulate hailstorms to an extent (Sokol *et al.*, 2014). Simulations of hailstorm events using a variety of NWP models and techniques have been performed in numerous studies with varying degrees of success; a selection of these will be discussed here.

Sokol *et al.* (2014) performed a simulation of the 15th August 2010 severe hailstorm in Prague, Czech Republic, where hail 5 cm in diameter was recorded. The study used a non-hydrostatic Consortium for Small-Scale Modelling (COSMO) NWP Model to simulate the event in conjunction with the two-moment Seifert–Beheng cloud microphysical scheme. Compared to one-moment schemes that only predict the mixing ratios of the hydrometeors by representing the hydrometeor size from each class with a distribution function, two-moment schemes predict the mixing ratio of the hydrometeors as well as their number concentrations (Lim and Hong, 2010). The model also assimilated radar reflectivity. The model was run at horizontal resolutions of 2.8 km and 1.1 km to decipher the importance of resolution on the quality of output. Model forecasts with a lead time of 90 minutes were found to accurately simulate the hailstorm, although beyond this time it declined, with factors such as hail size being overestimated. Despite overestimating hail size even with a 90 minute lead time, the 1.1 km model outperformed the 2.8 km model, with the 2.8 km model generally forecasting only small amounts of hail over a large areas. The higher resolution model also had more accurate predictions of the location and intensity of precipitation, and was improved with the incorporation of radar assimilation, unlike the lower resolution model.

Garcia-Ortega *et al.* (2007) undertook a simulation of a severe hailstorm occurring on 16th August, 2003 in the town of Alcañiz, located in the Ebro Valley in northeast Spain that produced hailstones up to 12 cm in diameter. The non-hydrostatic Mesoscale Model (MM5) was used, developed by the Pennsylvania State University–National Centre for Atmospheric Research. The model was multiply nested with the smallest domain a 0.67 km grid, supported by the Kain and Fritch (1990) convective parametrisation scheme and the Reisner graupel (Reisner *et al*., 1998) moisture scheme. While the model output did not reproduce hailstone size, it predicted the storm track and precipitation. As displayed in Fig. 1.9, the storm was well simulated with the most intense precipitation aligning well to radar signatures, although total precipitation was underestimated. The storm was also well captured by the model on temporal scales.

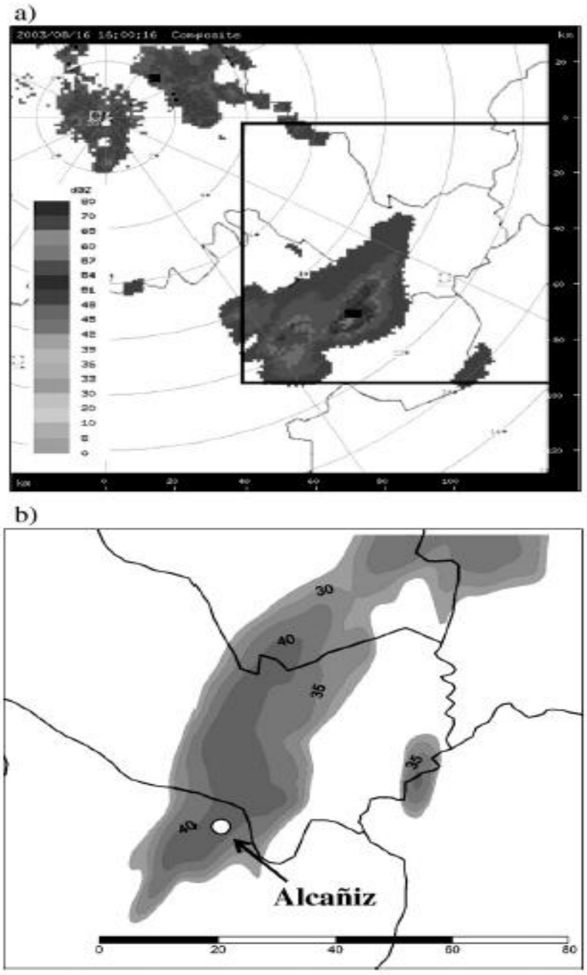

Fig. 1.9. a) Composite reflectivity factor (dBZ on scale), provided by the radar at 1600 UTC and b) the MM5 simulated reflectivity factor average between 1530 UTC and 1600 UTC [adapted from Fig. 10 a) and b) of Garcia-Ortega *et al*. (2007)].

Notably, a sensitivity experiment was also performed in Garcia-Ortega *et al.* (2007) to study the effects of solar radiation and topography, removing one or both features during model runs. It was found that both these variables were required in order for the model to perform accurately, but on their own had little impact.

Chevuturi *et al.* (2014) simulated an unusual winter hailstorm over Delhi, India on 17th January 2013 using the Weather Research and Forecasting Model (WRF), supported by the Goddard Cumulus Ensemble (GCE) microphysics scheme with six hydrometeors, including hail. The aim of the study was to understand the hailstorm event using a comparative analysis between the options of hail and graupel in the microphysics scheme. The hail option more accurately simulated observed precipitation intensity compared to the graupel option, and can also be used to simulate hail precipitation that the graupel option handled poorly. The model also simulated well the synoptic patterns leading to the hail event, although wind and geopotential heights patterns were slightly overestimated when compared to observational values.

1.3.2 Australian Studies

Within Australia, there are only a limited amount of studies that focus on simulating hailstorm events (Buckley *et al.,* 2001; Speer *et al.,* 2004; Leslie *et al.,* 2008). A significant reason behind the lack of studies is the sparse availability of surface and upper air observations over the oceans surrounding the country (Buckley *et al.,* 2001). The studies that have been done are becoming dated as model technology and cloud microphysics schemes improve, such as the incorporation of the WRF model in recent years. There are no known simulations of hailstorm events using this technology in Australia, although projected changes in future rainfall over the Sydney metropolitan region were investigated using WRF in Ji *et al.* (2013). A simulation of the 14th April 1999 Sydney hailstorm event was carried out by Buckley *et al.* (2001), the first successful simulation of its kind in Australia. Operational NWP models suggested the environment on the day was not conducive to supporting severe thunderstorms over land, and was hence poorly forecasted. Buckley *et al.* (2001) used the High Resolution numerical model (HIRES), developed by the School of Mathematics at the University of New South Wales (NSW), Australia which took into account Land – Sea and terrain interactions. The model included a six water-ice phase microphysics scheme, which was necessary for the simulation of hail growth linked with supercell development. A supercell thunderstorm was successfully simulated close to the observed radar track (Fig. 1.10), although hail size was underestimated by the time it reached Sydney.

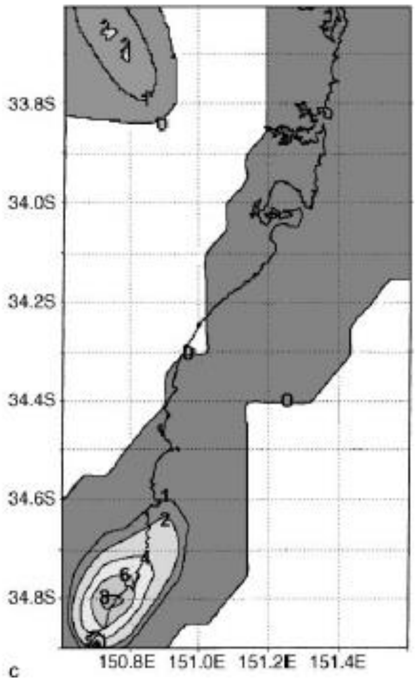

Fig. 1.10. One kilometre horizontal resolution HIRES model output showing the accumulated maximum hail size, at the surface, for the 10 hour period ending 2200 AEST (1200 UTC) April 14, 1999 [adapted from Fig. 10c of Buckley *et al*. (2001)].

Convection was initiated within a couple of hours of the observed storm, as was the time of the arrival at Sydney Airport. Precipitation was slightly overestimated and was positioned to the west of where it was recorded.

Speer *et al.* (2004) recognised the deficiencies in the Buckley *et al.* (2001) model, particularly the discrepancies in hail size over the Sydney Basin. The hailstorm was re-simulated using the same model (HIRES), with several improvements. One of these improvements was an increased resolution of 15 km in the largest domain (in a triply nested scheme to 1 km), compared to 50 km in Buckley *et al.* (2001). Modifications were also made to the cloud microphysics scheme, including reducing the mean diameter of graupel particles in a given cloud volume, but increasing the mean number of graupel particles per unit volume, as well as re-casting conservation equations in the 5th-order conservation form instead of the second-order, The simulation of the hailstorm event by the updated model configuration can be seen in Fig. 1.11.

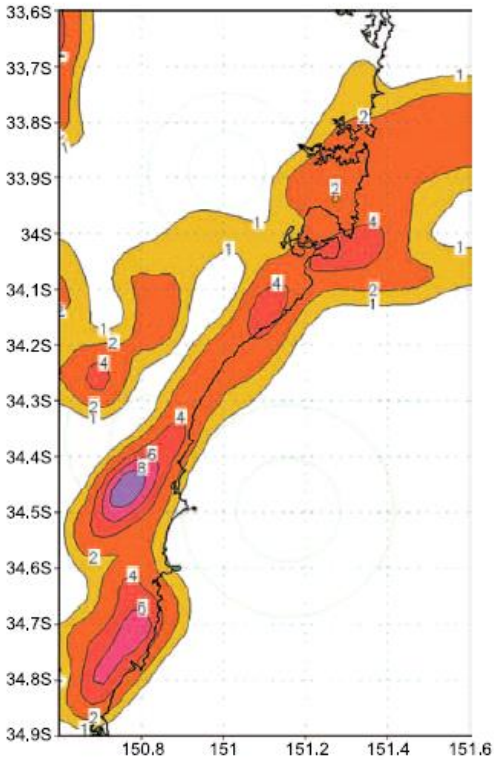

Fig. 1.11. Simulation of the 14th April 1999 hailstorm using an updated version of the HIRES model [adapted from Fig. 4c of Speer *et al.* (2004)].

The hail patterns and track were very close to the actual event and outperformed both the operational NWP model used by the BoM on the day, and the simulation by Buckley *et al.* (2001). However, it was noted that further improvements were required. Notably, the margin for error was likely large with the chance the model could have predicted the storm to be a little further east or west, which could have had significantly different impacts. Hail size was also underestimated in Sydney, although still an improvement over Buckley *et al.* (2001).

The latest study that has simulated hailstorms in Australia was conducted by Leslie *et al.* (2008), which examined future hailstorm trends over the Sydney Basin using the University of Oklahoma Coupled General Circulation Model (OU-CGM). The model was high resolution and multiply-nested, with the finest domain having a horizontal grid spacing of 1 km and was complemented by a 10-ice phase cloud microphysics scheme. Three events – the 21st January 1991 hailstorm, the 3rd November 2000 hailstorm and the 16th February 2002 hailstorm were simulated. The 21st January simulation suffered from coarse resolution, with the operational model run at 125 km horizontal grid spacing, and limited vertical levels. Despite these limitations, the model suggested an environment capable of supporting multiple severe hailstorms with diameters up to 5-6 cm. However, these hailstorms were simulated outside the

Sydney Basin (west of Sydney in the Lithgow area), and within Sydney the simulated hail size did not reach 2 cm, in contrast to the observed size of 7 cm. The 3rd November 2000 event, which was associated with three distinct hail areas (Fig. 1.12), was simulated much more accurately with reports, weather and satellite imagery showing strong similarities to the observed storm.

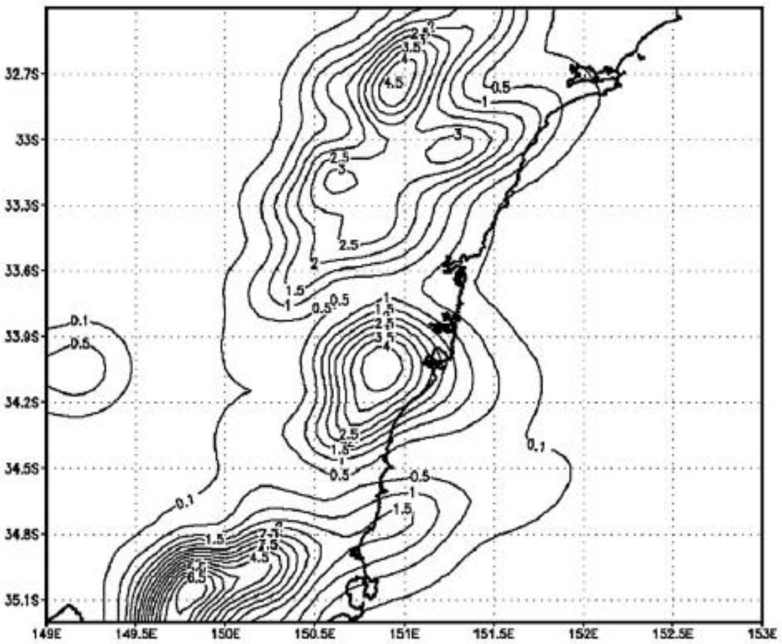

Fig. 1.12. 1 km resolution control run showing hail size (in cm) for the 3rd November, 2000 severe hailstorm [adapted from Fig. 3 of Leslie *et al.* (2008)].

The model predicted a maximum hail size of around 4 cm in western Sydney when the storm was at its most intense, before weakening as it moved into the northern suburbs, which was similar to the actual storm. The model simulation also accurately depicted the more intense Illawarra hailstorm with sizes to 6.5 cm (close to that observed), before weakening as it approached the coast. The 16th February 2002 simulation predicted the size of the cell well, as were hail sizes as large as 6 cm (close to the observed 5 cm); however the forecast hail was about 60 km west of where the storm occurred. It was inferred that coarse resolution of the numerical analysis of a trough over central NSW contributed to this displacement. These simulations aimed to be representative of the conditions of the present climate, and provide a benchmark for further tests in increasing greenhouse gas scenarios and no greenhouse gas scenarios. This thesis focuses mainly on simulations of observed events, rather than using idealised configurations for hailstorm cases in the future. However, it is worth noting that using idealised configurations of the model with the Intergovernmental Panel on Climate Change

(IPCC) A1B future climate scenario, Sydney was projected to experience more intense hailstorms. It was concluded by Leslie *et al.* (2008) that the model used could simulate giant hail events in the present day climate, although small changes in resolution and meteorological parameters can influence the results significantly.

CHAPTER 2 METHODS

2.1 Overview

This study first extended Sydney's most comprehensive and detailed hybrid hailstorm database. The database, which was originally compiled for the 1950-2010 period (Schuster *et al.*, 2005 and McBurney, 2012), was updated until the end of the 2014/2015 June-May hail season. As a case study, the 9th December, 2007 severe hailstorm that affected western and northern parts of Sydney was simulated. This was done with a high resolution NWP model, which is the Weather Research and Forecasting (WRF) model with the Advanced Research WRF (ARW) dynamical core. WRF is a next-generation mesoscale numerical weather model developed by a collaborative partnership (Wang *et al.*, 2010), including the US National Centre for Atmospheric Research (NCAR), the National Centre for Environmental Prediction (NCEP) run by the National Oceanic and Atmospheric Administration (NOAA), and the Air Force Weather Agency (AFWA). The ARW dynamical core was developed largely by NCAR (Skamarock *et al.*, 2008). Using WRF allows generation of simulations based on real data, including observations and analyses.

2.2 Extending the Sydney hail climatology

The most comprehensive and complete hail database for the Sydney Metropolitan Region compiled in McBurney (2012) for the period from 1950-2010 was updated through until May 2015 (the end of the defined June-May hailstorm season which was established in Schuster *et al.*, 2005 and continued in McBurney (2012). This database was originally developed by obtaining two separate databases and combining them. The first database was the Bureau of Meteorology hailstorm database (dated back to 1900), which mostly documented severe hailstorm events, largely through reports from the public, particularly from 1990 when the storm spotter network was established (Schuster *et al.*, 2005). The second database (PerilAus) was compiled by the Risk Frontiers Natural Hazards Research Centre at Macquarie University, which completed the database for the 1791-2003 period. This database documented hailstorm events through journal articles, newspaper reports and media releases. In McBurney (2012), the hailstorm database was extended until 2010, although the Sydney region was defined as extending north to Maroota, west to Springwood, and south to Helensburgh (Fig 2.1), which is a slightly larger area to that of Schuster *et al.* (2005).

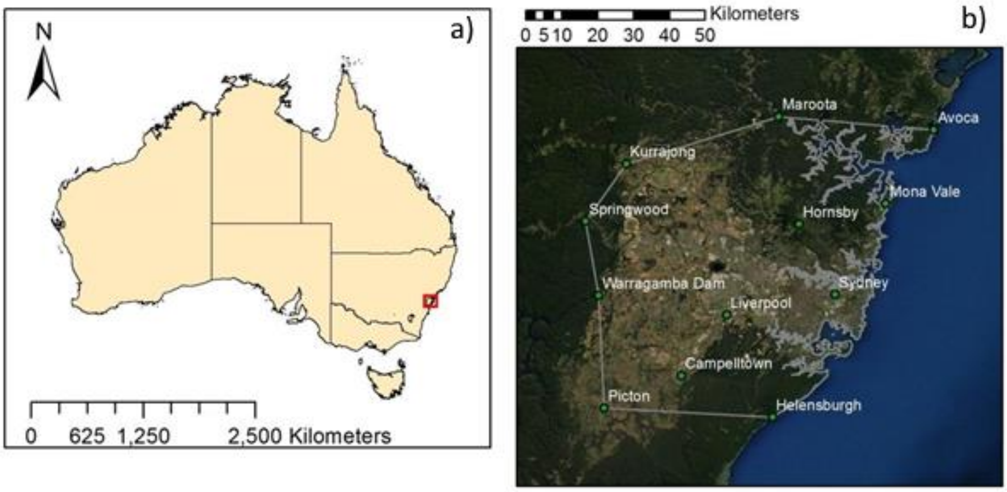

Fig. 2.1. a) Regional setting of the study area. b) Boundaries of the study area used to compile the hail database in McBurney (2012). The region extends north to Maroota, west to Springwood and Picton, and south to Helensburgh [adapted from Fig. 2.1 of McBurney (2012)].

McBurney (2012) used similar methods to Schuster *et al.* (2005) to extend the database until 2010, whilst also removing any duplicate events and cases outside the Sydney Basin. These methods were applied in this paper in order to extend the database until the 2014/2015 hail season, including BoM reports, journal articles, social media reports and media releases. It is worth noting that hail sizes were not included without correlation to official reports when using social media, with the public often having the tendency to inaccurately report hail sizes. Information such as the location, time, date, diameter and any damage the event may have caused was included in all hailstorm entries when possible. Basic statistical tests were conducted from 1950 until present (due to increasingly inaccurate data prior to 1950) using Microsoft Excel to calculate the means of annual hail days and annual severe hail days, whilst also analysing trends.

2.3 Installing and configuring WRF

The version of WRF used was 3.6.1 as it had a greater variety of cloud microphysics options (inc1uding a hail option) than the 3.6.0 version, while also being more stable than the 3.7 version. The experimental process involved selecting a multitude of cloud microphysics schemes, boundary layer conditions and radiation options to see their effects on the model's simulation of the storm, including the synoptic environment, storm track, timing and intensity.

Three domains were selected for the WRF simulation, with one parent domain and two nested domains (Fig. 2.2). The parent domain was run over the Australian region at a horizontal resolution of 15 km, extending approximately between 5 °S and 50 °S and 100 °E and 165 °E. Domain 2 was nested within the parent domain at a resolution of 5 km over southeastern Australia, roughly between 24 °S and 43 °S, and 137 °E and 159 °E. The third domain was nested within domain 2 at a resolution of 1 km over the Sydney, Lower Hunter, Central Tablelands, Illawarra, northern South Coast and northern Southern Tablelands regions, between 32 °S and 36 °S and 147.8 °E and 152.7 °E. Domains 2 and 3 had 2-way feedbacks to the parent domain.

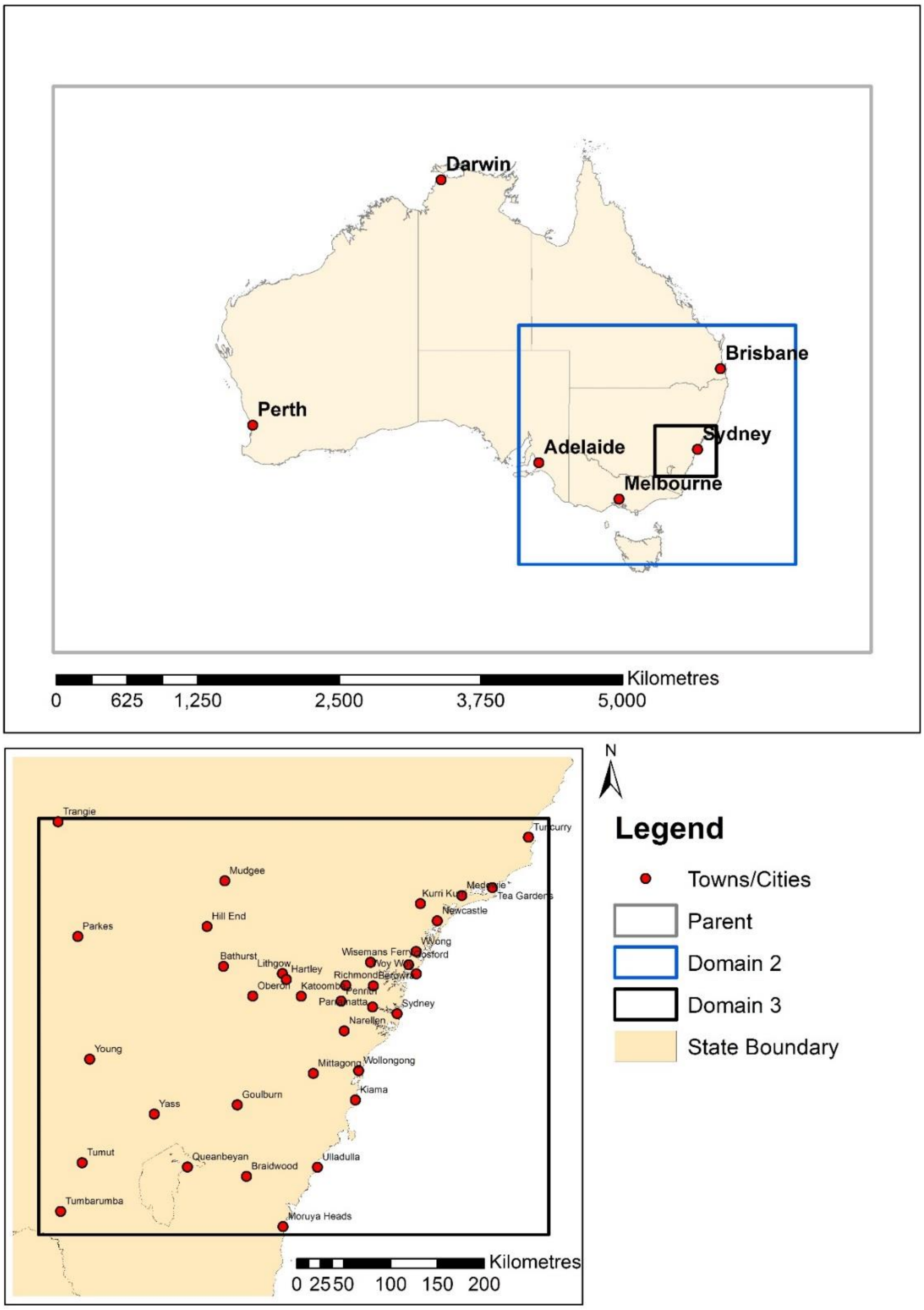

Fig. 2.2. a) Regional setting of the study area, displaying the parent domain (15 km resolution), domain 2 (5 km resolution) and domain 3 (1 km resolution) b) A higher resolution view of domain 3 (1 km resolution).

The NCEP Final Analysis, with 1 degree resolution, from the Global Forecast System (GFS) was used as the initial and boundary condition of WRF. Domains 1 and 2 were set to run from 12:00 UTC (11 pm Eastern Daylight Time or EDT) on the 6th of December until 12:00 UTC on the 9th of December to ensure the model ingested enough data to calculate the correct boundary conditions, synoptic patterns and the meteorological conditions leading up to the hailstorm event, while domain 3 (the smallest domain) was run from 18:00 UTC (4am EDT) on the 8th of December until 12:00 UTC on the 9th of December.

The Kain-Fritsch Cumulus Parameterisation scheme was used on domain 1, with no cumulus scheme used for domains 2 and 3. Cumulus parameterisation is generally not required for resolutions coarser than 10 km, as presumptions for convective eddies being sub-grid-scale break down for finer grid scales (Skamarock *et al.*, 2008). The Noah Land Surface Model was used for the surface physics. Vertical levels were set to 30 for all three domains.

2.4 Cloud microphysics and radiation options

Among the simulations performed, shortwave (SW) and longwave (LW) radiation options, which control the fluxes of incoming and outgoing radiation that provide atmospheric heating (Skamarock *et al.*, 2008), and in particular, cloud microphysics schemes were altered to determine their impacts on the model's portrayal of the hailstorm. Rain, ice, snow and graupel processes were common hydrometeors in the microphysics schemes, with only a few including hail. Simulations were run using a multitude of microphysics schemes, as displayed in Table 2.1.

Table 2.1. Microphysics schemes (including descriptions) used for WRF simulations (The Mesoscale and Microscale Meteorology Division, 2015a)

Scheme	Hail option?	Description	Reference
Kessler	No	A warm-rain (no ice) scheme	Kessler (1969)
Lin *et al.*	No	Sophisticated scheme with ice, snow and graupel processes	Lin *et al.* (1983)
WRF Single-Moment 3-class (WSM3)	No	Simple scheme with ice and snow processes	Hong *et al.* (2004)
WRF Single-Moment 6-class (WSM6)	Yes	More complex scheme with ice, snow and graupel processes	Hong and Lim (2006)
Goddard	Yes	Scheme with ice, snow and graupel processes	Tao *et al.* (1989)
Thompson *et al.*	No	Scheme with ice, snow and graupel processes	Thompson *et al.* (2008)
Morrison Double-Moment	Yes	Scheme with double-moment ice, snow, rain and graupel	Hong and Pan (1996)
WRF Double-Moment 6-class	Yes	Double-Moment rain, otherwise same as WSM6	Lim and Hong (2010)

Half of these microphysics schemes included hail as a hydrometeor, and those that did were run once with a graupel option and once with a hail option. It has been shown that including the hail hydrometeor in cloud microphysics significantly improves model portrayal of hailstorms **(**Chevuturi *et al.,* 2014). The Milbrandt-Yau Double-Moment 7-class scheme (Milbrandt and Yau, 2005) also included hail as a hydrometeor; however, simulations using this scheme were not included due to incompatibility with our computing hardware. For most simulations the Rapid Radiative Transfer Model longwave radiation scheme (Mlawer *et al.*, 1997) and the Dudhia shortwave radiation scheme (Dudhia, 1989) were used. However, in the Goddard microphysics hail and graupel schemes, the New Goddard shortwave scheme (Chou and Suarez, 1999) and New Goddard longwave scheme (Chou and Suarez, 1999) were also tested as it has been suggested that model output is improved when used with the microphysics scheme (Shi and Tao, 2006). The Yonsei University planetary boundary layer scheme (Hong *et al.*, 2006) was used for all simulations. Simulation data from WRF were analysed using the NCAR Command Language (NCL). AFWA diagnostics were used to compute maximum hail diameter. The first diagnostic, AFWA_HAIL, computed diameter based on vertical velocity, mid-level humidity, temperature and duration (Fig 2.3.)

$$\text{Updraft} = (\text{Vertical Velocity [m s-1]} \,/\, 1.4)\ 1.25$$
$$\text{MidRH} = \text{3.5 km AGL RH [\%]} - 70\text{; min of } 0$$
$$\text{Melt} = \text{2 meter temperature [K]} - 288.15\text{; min of } 0$$
$$\text{Duration} = (\text{2-5 km updraft helicity [m2 s-2]} \,/\, 100) + 0.25$$
$$\text{Hail [mm]} = (\text{Updraft} - \text{Melt} - \text{MidRH}) \times \text{Duration}$$

Fig. 2.3. Formula for computing AFWA_HAIL from the AFWA diagnostics package [adapted from The Mesoscale and Microscale Meteorology Division, 2015b).

The second diagnostic, AFWA_HAILCAST, computed mean hail diameter based on five hail embryos which undergo typical hail formation and fallout processes (The Mesoscale and Microscale Meteorology Division, 2015b).

CHAPTER 3 EXTENDING THE SYDNEY HAIL CLIMATOLOGY

3.1 Introduction

Hail climatologies are important as they document past events and enable the analysis of trends that help severe weather forecasting, research on the effects of climate change, estimates of insurance liabilities, agricultural impacts, and risks to the public (Cintineo *et al.*, 2012). Assembling an accurate hail climatology is difficult due to the spatial and temporal nature of hail. It is not atypical to have hail falls confined to an area of several hundred metres, with durations in the order of minutes (Sokol *et al.*, 2014). To help combat these spatial and temporal constraints, hailpads have been frequently used across Europe, the Unites States, Canada, and more recently Argentina and New Zealand, although it has been argued that distances between hailpads are still several kilometres, which is generally not adequate to capture all events (Sokol *et al.,* 2014). Nonetheless, several hail climatologies have been constructed across the globe using hailpads as their foundations, particularly in Italy (Baldi *et al.*, 2014) and France (Bertet *et al.*, 2011) where hailpad records and coverage are more complete. More often, hail databases are constructed using a variety of methods, such as instrumental data from meteorological stations, hailpads, radar data, or reports from the public. This has meant a number of countries such as Great Britain (Webb *et al.,* 2001), Germany (Kunz *et al.*, 2009), the United States (Changnon and Changnon, 2000), Switzerland (Houze *et al.*, 1993), Argentina (Mehzer *et al.*, 2012), France (Vinet, 2001), Finland (Tuovinen *et al.*, 2008) and China (Xie *et al.*, 2008) have been able to develop long-term hailstorm climatologies that have been considered accurate.

In countries such as Australia, creating a reliable hail climatology outside urban centres is impossible due to the spatial discontinuities of the populace (low population densities across large expanses of the country) and therefore lack of reports. Australia does not have a hailpad network, and as such relies heavily on reports. In 1990, the BoM storm spotter network was founded which greatly improved reporting of severe thunderstorms (including rural areas), although data was still heavily skewed towards densely populated urban centres (Schuster *et al.*, 2005). The first in-depth hail climatology for NSW, Australia was constructed by Schuster *et al.* (2005), with a focus on the Sydney Metropolitan region. This database from 1791 to 2003 was constructed largely from reports; firstly by collecting hail data from the BoM (mostly consisting of large hail (≥ 2 cm) reports), before using the PerilAus database to extend the database and to include small hail cases. In McBurney (2012), the database for Sydney was extended through to the 2010/2011 June-May hail season using similar methods (although for a slightly modified area, see Fig 2.1), whilst also incorporating social media reports. It is worth noting that social media has the possibility of negatively skewing trends computed from hailstorm databases constructed by reports, due to much higher chances of isolated and brief hailstorm events being reported. Despite inaccuracies in the database prior to at least 1950 due to missing data and the influence of social media, this database is considered the most detailed and comprehensive in Australia, containing four times as many entries as the BoM database. Schuster *et al.* (2005) found a statistically significant decrease in hail frequency from 1989-2003, with only 7.6 ± 2.8 P.a compared to an average of 10.3 ± 1.5 hailstorms P.a. for the 1953-2003 period. A similar trend was observed by McBurney (2012) with an average of 8.45 ± 1.57 hailstorms P.a. from 1991-2010, although it was suggested that the apparent low frequency of hail in this period was at least partly due to a lack of small hail reports from 1991-1999. It was noted that total hail numbers recovered somewhat from 2000-2010 (but still below average), although it was also found in Rasuly *et al.* (2015) that severe hail events declined in the period 2011-2013. To examine whether the apparent decline in total hail numbers and severe hail numbers continued in recent years, the hail database was put through quality control analyses and extended through until the 2014/2015 June-May hail season using the same methods and area as McBurney (2012). It is important to note that only records from post-1950 were used to compute trends and statistics, as the database prior to this time was considered inaccurate due to inconsistent data and lack of primary data.

3.2 Results: Trends in hailstorm frequency and variability

3.2.1 Total hail frequency

Basic statistical tests (including calculating trendlines) were performed to determine means, confidence intervals (CI), variability and trends of hail frequency for the Sydney area from 1950-2014. Hailstorm numbers for this period were found to average 10.89 ± 1.20, although significant temporal variability was found to exist. As shown in Fig. 3.1, the 1991-1999 period exhibited lower than average hailstorm frequency (6.22 ± 1.75 P.a), whilst the 1983-1990 period showed higher than average hailstorm frequency (19.00 ± 3.22 hailstorms P.a). Since 2000, hailstorm frequency has been close to the mean, with an average of 10.73 ± 1.67 hailstorms P.a. There is clear inter-annual and inter-decadal variability, although there is no defined trend in total hail numbers (m (slope) = 0.0072).

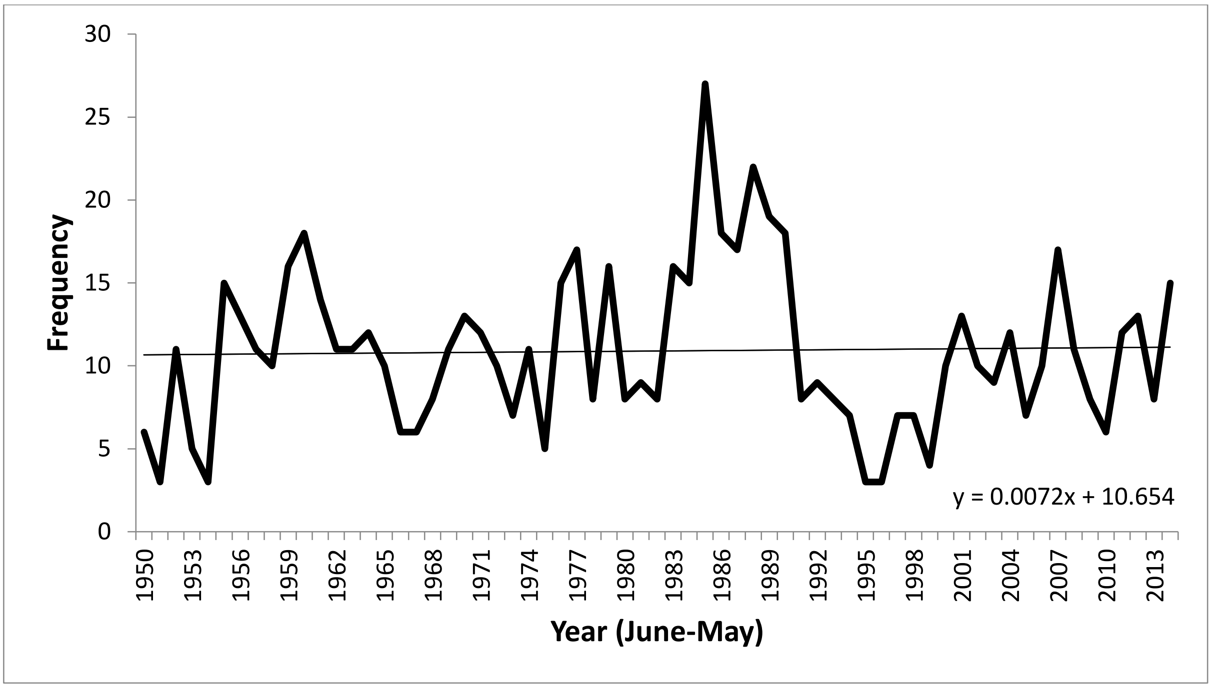

Fig. 3.1. Total hail numbers (with trendline) for the Sydney Metropolitan region for the 1950-2014 period.

3.2.2 Severe hail

In Australia, severe hail is defined as hail measuring a diameter of 2 cm or greater (Bureau of Meteorology, 2011). For the period of 1950-2014, there was an average of 3.58 ± 0.63 severe hailstorms Pa, with significant temporal variability again evident as seen in Fig 3.2. 1972-1982 saw the lowest severe hail frequencies with an average of 1.55 ± 0.87 storms P.a., whilst 1985-1994 was the most active period with 7.0 ± 1.26 severe hailstorms P.a. Notably, severe hailstorm frequencies were greater in the second half of the database (5.09 ± 0.89 from 1983-2014) than the first half (2.00 ± 0.53 from 1950-1982), although numbers have declined somewhat in recent years (3.00 ± 1.19 from 2008-2014). Statistics generally suggest that severe hailstorm numbers have increased (m (slope) = 0.0584), particularly from the 1980s, but have tapered off since the mid-to-late 2000s.

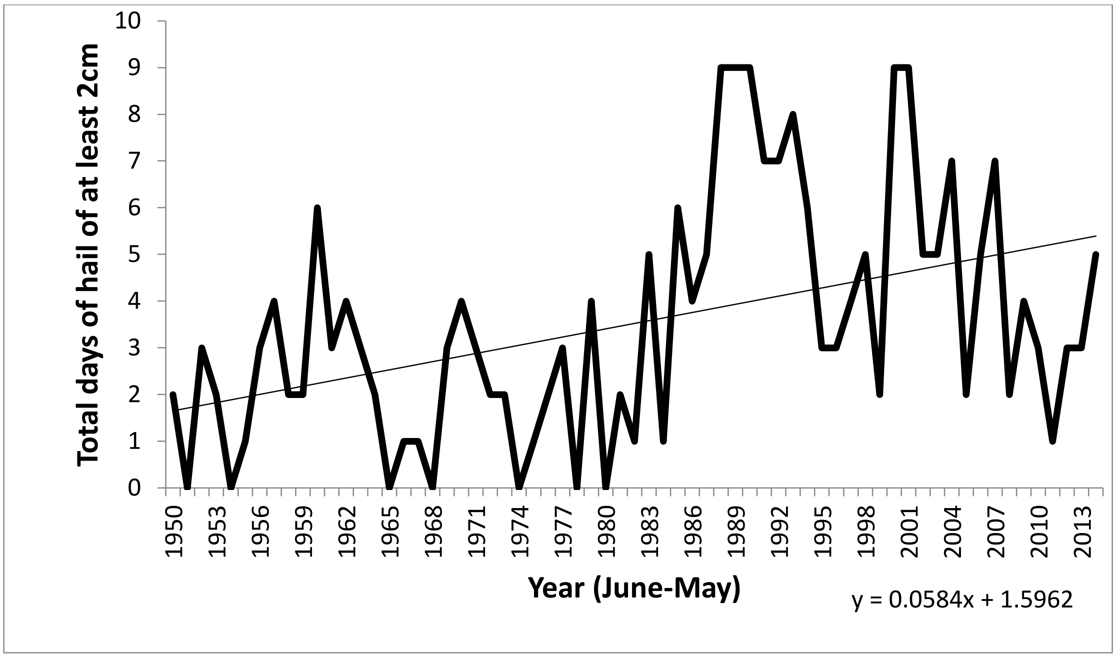

Fig. 3.2. Severe hail (≥ 2 cm) numbers (with trendline) for the Sydney Metropolitan region for the 1950-2014 period.

3.3 Discussion: Trends in hailstorm frequency and variability

3.3.1 Total hail

After extending the database developed by McBurney (2012), a mean of 10.89 ± 1.20 hailstorms per annum was calculated for the 1950-2014 period, with significant inter-annual and inter-decadal variability. These results complement the work of Schuster *et al.* (2005) who found an average of 10.3 hailstorms per annum, with the slightly lower average attributed to a smaller sample region and earlier version of the database. Mean hailstorm numbers have increased slightly from McBurney (2012) who found an average of 10.82 ± 1.26 hailstorms/annum for the 1950-2010 period. However, it was noted in Schuster *et al.* (2005) that there was a statistically significant decline in hailstorm frequency for the 1989-2003 period, which had an average of 7.6 ± 2.8 hailstorms/annum. As displayed in Table 3.1, statistical tests of the new database revealed a similar period of low hailstorm frequency from 1991-2010, with an average of 8.45 ± 1.57 hailstorms per annum.

Table 3.1: Mean hail days per year and mean severe hail days per year (including 95% confidence intervals) for the 1950-2014, 1950-1990, 1991-2010 and 2011-2014 periods.

	All Hail Days/annum	Severe Hail days/annum
1950-2014	10.89 ± 1.20	3.52 ± 0.63
1950-1990	11.98 ± 1.65	2.78 ± 0.76
1991-2010	8.45 ± 1.57	5.15 ± 1.07
2011-2014	12.00 ± 4.68	3.00 ± 2.60

This lower average was partially explained by McBurney (2012), who concluded it was very likely that there were missing small hail reports in 1991-1999 period; however, the 2000-2010 period still displayed slightly lower than average hailstorm frequencies (10.27 ± 2.04 hailstorms/annum). Hailstorm frequency has been shown to be declining in other parts of the globe, including the United States (Changnon and Changnon, 1999), southern parts of Argentina (Mezher *et al.*, 2012) and China *(*Xie *et al., 2008*; Xiaoyan *et al., 2010*). It was suggested by Xie *et al.* (2008) that the decline in hailstorm numbers in China could be attributed to aerosols offsetting instability, as well as an increase in freezing-level height. In Argentina, it was similarly concluded by Mezher *et al.* (2012) that hail numbers were declining due to an increasingly negative difference between the 925 hPa and 250 hPa temperature (i.e. a warming upper troposphere). In Australia, this rise in freezing-level height has also been observed (McBurney, 2012; Santer *et al.*, 2003). McBurney (2012) also showed that active hailstorm periods in Sydney (on decadal scales) were often associated with higher than average vertical wind shear and lower than average geopotential height, whilst quiet hailstorm periods were affiliated with the opposite. Notably however, in the 2003-2009 period (a phase of slightly lower than average hail frequency), near average vertical wind shear and lower than average geopotential height was observed. It was aimed that by extending the database to the 2014/2015 hail season, it would reveal if there had been a continuation in the potential decline in hailstorm frequency across Sydney. However, the 2010-2014 period saw above average hailstorm frequency, averaging 12.00 ± 4.68 hailstorms P.a. Whilst it is recognised that four years is only a small scope of time to do statistical tests, there has been no other four-year period since 1987-1990 (19.00 ± 3.44 hailstorms P.a.) that has had higher hailstorm frequencies. This may suggest hailstorm numbers are recovering, with a return to near-average or above average frequencies likely in the future. Although further analysis will be needed in future years, this suggests that hailstorm frequency is not declining in Sydney, and rather the lower frequency in recent years is more likely related to inter-annual and inter-decadal variability.

3.3.2 Severe hail

A mean of 3.52 ± 0.63 severe hailstorms P.a was calculated for the 1950-2014 period (Table 3.1), with significant inter-annual and inter-decadal variability. This is similar to McBurney (2012), who observed a mean of 3.57 ± 0.67 severe hailstorms P.a. Notably, the 1990-2010 period that saw lower than average total hailstorm frequency experienced higher than average severe hailstorm frequency, with an average of 5.15 ± 1.07 severe hailstorms per annum. The second half of the database revealed higher severe hail frequencies (5.09 ± 0.89 severe hailstorms/annum from 1983-2014) than the first half (2.00 ± 0.53 severe hailstorms/annum from 1950-1982). This increase was largely attributed to a higher frequency of reports from the public, particularly with formation of the BoM storm spotter network in 1990 (McBurney, 2012). It was however noted in Rasuly *et al.* (2015) that there was a significant decline in severe hailstorm frequency in the Sydney Basin in recent years (particularly 2011-2013), with only seven severe hailstorm days reported in this period. The results in this paper complement Rasuly *et al.* (2015), with a noticeable decline in hailstorm frequency in recent years (3.00 ± 2.60 hailstorms/annum). 2011 (1 severe hail day) produced the lowest amount of severe hailstorm days in a June-May hail season since 1984. However, in the 2014 hail season, 5 severe hailstorm days occurred, the highest since 2007. Whilst it is apparent that severe hailstorm frequency has declined in recent years, it is more likely to be attributed to temporal variability than a permanent decline.

CHAPTER 4 SIMULATING THE 9th DECEMBER 2007 SYDNEY HAILSTORM

4.1 Introduction

On the 9th of December, 2007 a supercell thunderstorm containing giant hail devastated western and northern parts of Sydney, causing an estimated AUD$470 million in damage (Davies *et al.*, 2008). As displayed in radar echoes in Fig 4.1, the thunderstorm formed over elevated terrain on the Blue Mountains to Sydney's southwest, before taking an east-northeast path through the Sydney Basin, hitting suburbs including Blacktown, Castle Hill and Hornsby before moving out to sea over the Northern Beaches.

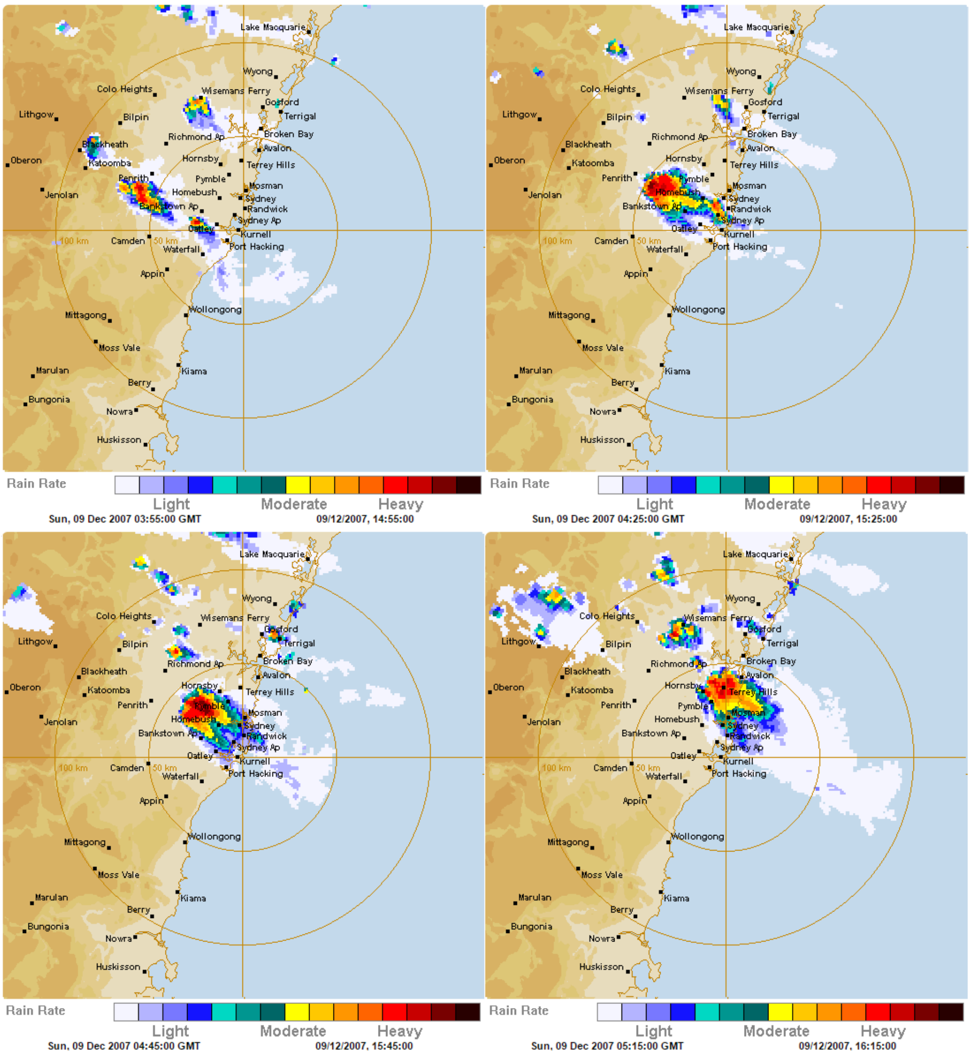

Fig. 4.1. Radar images from the Bureau of Meteorology Sydney (Kurnell) radar at 2:55 pm, 3:25 pm, 3:45 pm and 4:15 pm (EDT) on 9th December, 2007 (obtained from the Bureau of Meteorology).

The storm produced official maximum hail sizes of 8.5 cm in diameter (Davies *et al.*, 2008), although the BoM reported unconfirmed stones of up to 11 cm in diameter at Cherrybrook. Had the storm gone through a more populated part of Sydney, damage would have been much greater (Davies *et al.*, 2008). Rainfall totals across Sydney were generally light, with only 5-10 mm recorded across the Basin (Fig 4.2).

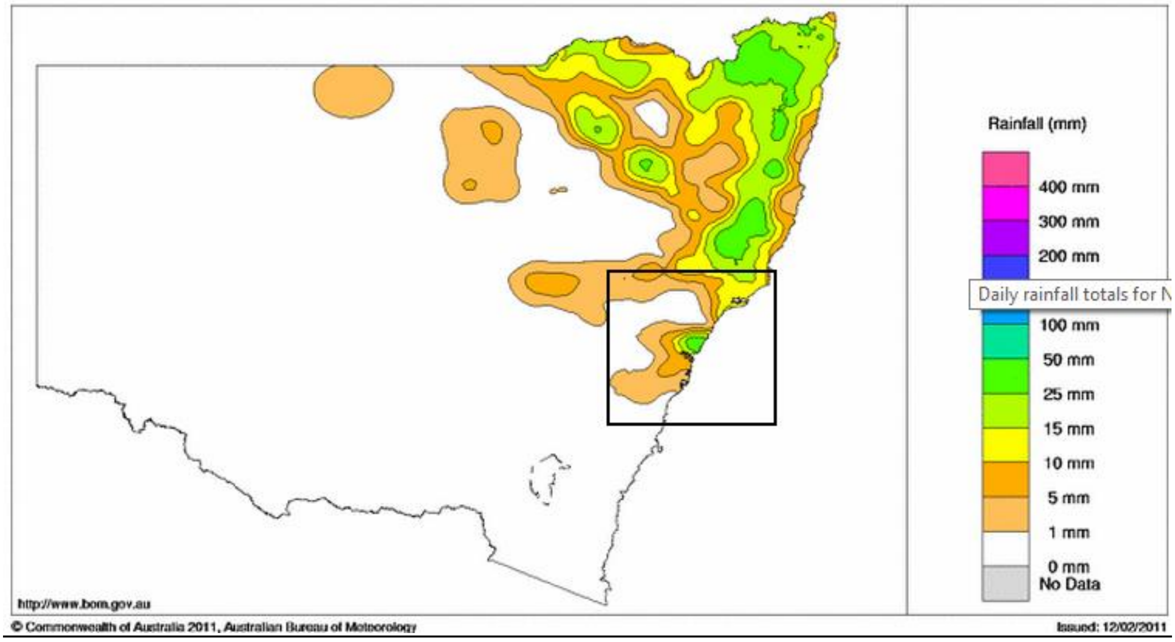

Fig. 4.2. Accumulated precipitation in the 24 hours to 9am on the 10th December, 2007 including the domain 3 region (obtained from the Bureau of Meteorology).

As a case study, this chapter aims to simulate the 9th December 2007 Sydney hailstorm using version 3.6.1 of the WRF model, in order to decipher improvements in NWP models for such local-scale hazardous weather, particularly in Australia. This storm was selected as it is Sydney's most damaging hailstorm since the 14th April, 1999 event, and to-date has not been studied in detail. One of the main focuses of this chapter will be sensitivity tests on cloud microphysics schemes, particularly comparing those incorporating hail as one of the hydrometeors and those that do not. The sensitivity of cloud microphysical schemes for forecasting convective storms is well documented (Liu and Moncrieff, 2007; McCumber *et al.*, 1991; Rajeevan and Bhate, 2010), with factors such as rainfall spectrum, upper-level radiative flux and upper-level cloudiness and condensate most sensitive to changes. As discussed at length in Chapter 1.3, the differences in model output when using a cloud microphysics scheme that incorporates hail as a hydrometeor (or manipulating the graupel hydrometeor to be more representative of hail), has been shown to be significant when compared to a microphysics scheme that does not include hail (Sokol *et al,* 2014; Chevuturi *et al.,* 2014; Speer *et al.,* 2004). It is also noticeable that studies that used higher horizontal resolution had more encouraging results (Speer *et al.,* 2004; Leslie *et al.,* 2008; Sokol *et al.,* 2014).

In order to simulate the storm, the WRF model was fed by 1° latitude/longitude Final Analysis data from the GFS model as initial and boundary conditions. The region was similar to that of Buckley *et al.* (2001) and Speer *et al.* (2004), also incorporating three domains. The parent domain was located over the Australian region at 15 km horizontal resolution which was a coarse enough resolution to use the Kain-Fritsch Cumulus Parametrisation Scheme. The second domain is nested in the parent domain over southeast Australia with a 5 km horizontal resolution, and the third domain over Sydney and surrounding regions (see Fig 2.2 (b)), with a 1 km horizontal resolution. Thirty vertical levels were used, and kept constant throughout the different runs. Besides the sensitivity tests on cloud microphysics schemes (changing between hail and graupel), radiation options were investigated to determine their influences on model output of the hailstorm event. Whilst a significant amount of cloud microphysics schemes were tested (see methods in chapter 2.4), this chapter will focus on output from the Goddard microphysics scheme using the New Goddard Shortwave scheme, comparing the graupel and hail hydrometeors. This option was chosen as it simulated the event most accurately in most aspects, particularly in storm initiation, track and intensity. Encouraging results were also produced by using the WRF Double-Moment 6-class scheme with hail, and the Thompson *et al.* (2008) microphysics scheme, which will also be discussed briefly. It is intended that this simulation will be a step towards improving high-resolution forecasting of severe hailstorm events in Australia, and will assess the potential improvements of NWP models since the last known hailstorm simulation in Australia by Leslie *et al.* (2008).

4.2 Results: Goddard microphysics scheme (hail vs graupel) with New Goddard shortwave scheme

4.2.1 Synoptic pattern and moisture

The Goddard microphysics scheme comparing the graupel and hail hydrometeors coupled with the New Goddard Shortwave scheme will be examined in detail. To establish WRF's ability to simulate the event on a synoptic scale, the surface synoptic setup (including temperature and dewpoint) and 500 hPa synoptic setup on the 9th of December, 2007 were outputted. Data output were compared to the BoM's analysis charts, which for the surface are made four times daily (18:00 UTC, 00:00 UTC, 06:00 UTC and 12:00 UTC) and for 500 hPa twice daily (00:00 UTC and 12:00 UTC). As shown in Fig. 4.3 below, Sea Level Pressure (hPa) was compared at 00:00 UTC (11 am EDT) and 06:00 UTC (5 pm EDT), the times prior to and proceeding the thunderstorm event. Both the hail and graupel options portrayed the synoptic setup well, therefore only the hail option is shown in Fig 4.3. The surface trough was simulated accurately, located over inland NSW during the morning, before lying close to Sydney during the afternoon. The trough was slightly further east at both 00:00 UTC and 12:00 UTC when using the hail option compared to the graupel option, which is more similar to the analysis charts (Fig 4.3c & Fig 4.3d). The pressure was also accurately portrayed, with 1012 hPa ridges separating the 1008 hPa trough at 00:00 UTC and 1008 hPa ridges separating the 1004-1008 hPa trough at 06:00 UTC. The eastern ridge (over the Tasman Sea) helped direct a moist onshore (northeast) flow over the NSW coast, feeding into the trough and bringing instability to the Sydney Basin.

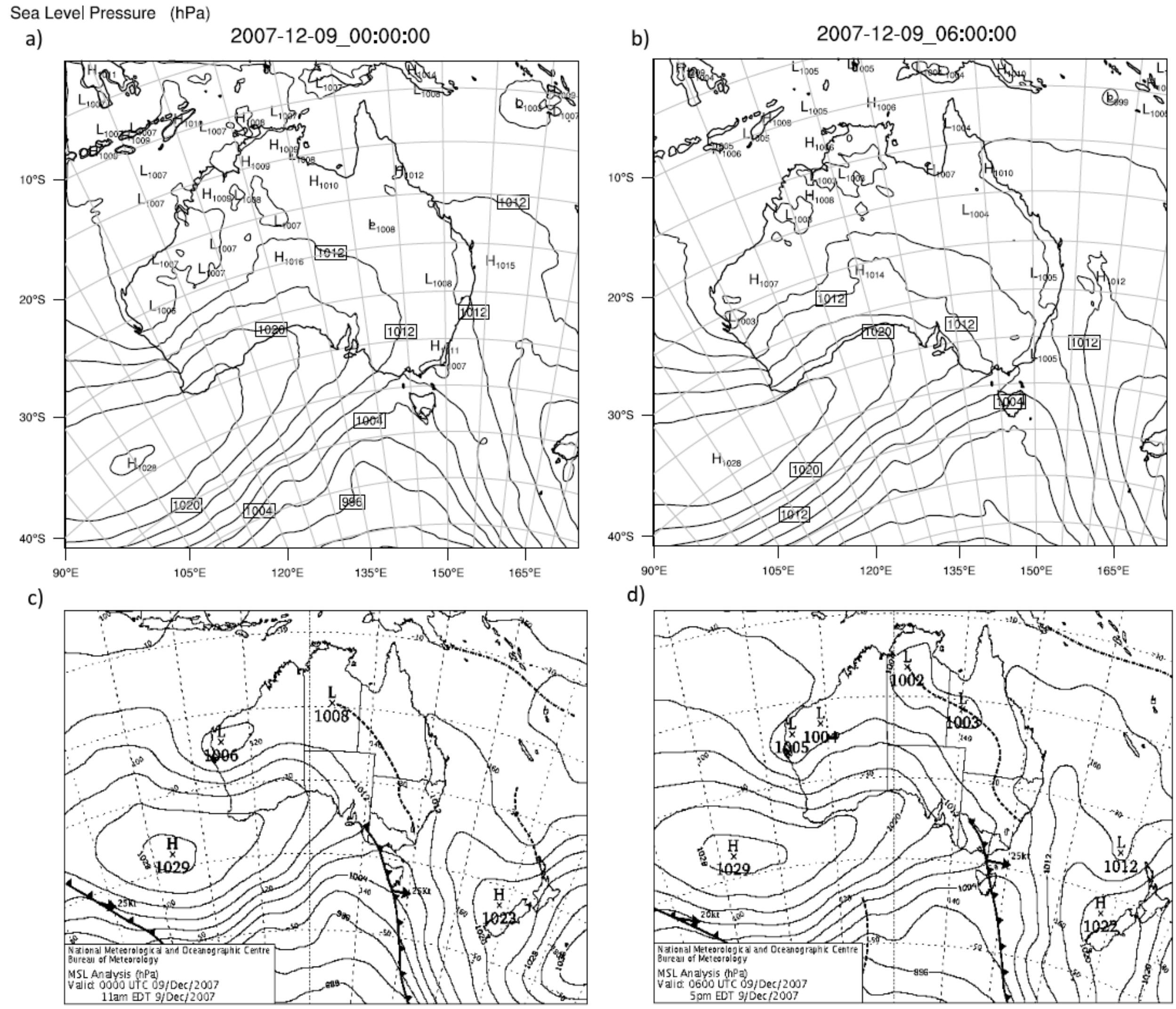

Fig. 4.3. Domain 1 Sea Level Pressure (hPa) at 00:00 UTC (11 am EDT) and 06:00 UTC (5 pm EDT) using the Goddard microphysics scheme with hail **(a & b)** compared to the 00:00 UTC BoM analysis chart **(c)** and the 06:00 UTC analysis chart **(d)**.

Dewpoints ahead of the trough were high (Fig 4.4), reaching around 18-22 °C throughout the Sydney Basin. These dewpoints were high due to winds off the Tasman Sea, with the hail and graupel options showing northeasterly winds throughout much of Sydney at 00:00 UTC, tending more northerly in the Basin's southwest. At 06:00 UTC, both options showed winds reaching up to 20 kts along Sydney's coast, although the hail option showed northeasterly winds compared to east-northeasterly winds with the graupel option. Along the boundary of the troughline there was a noticeable dryline associated with westerly component winds, with dewpoints dropping to around 6 °C behind the trough, which moved closer to the coast by 06:00 UTC. The hail option displayed a more marked boundary between the moist and dry air than the graupel option, which had marginally higher dewpoints behind the trough.

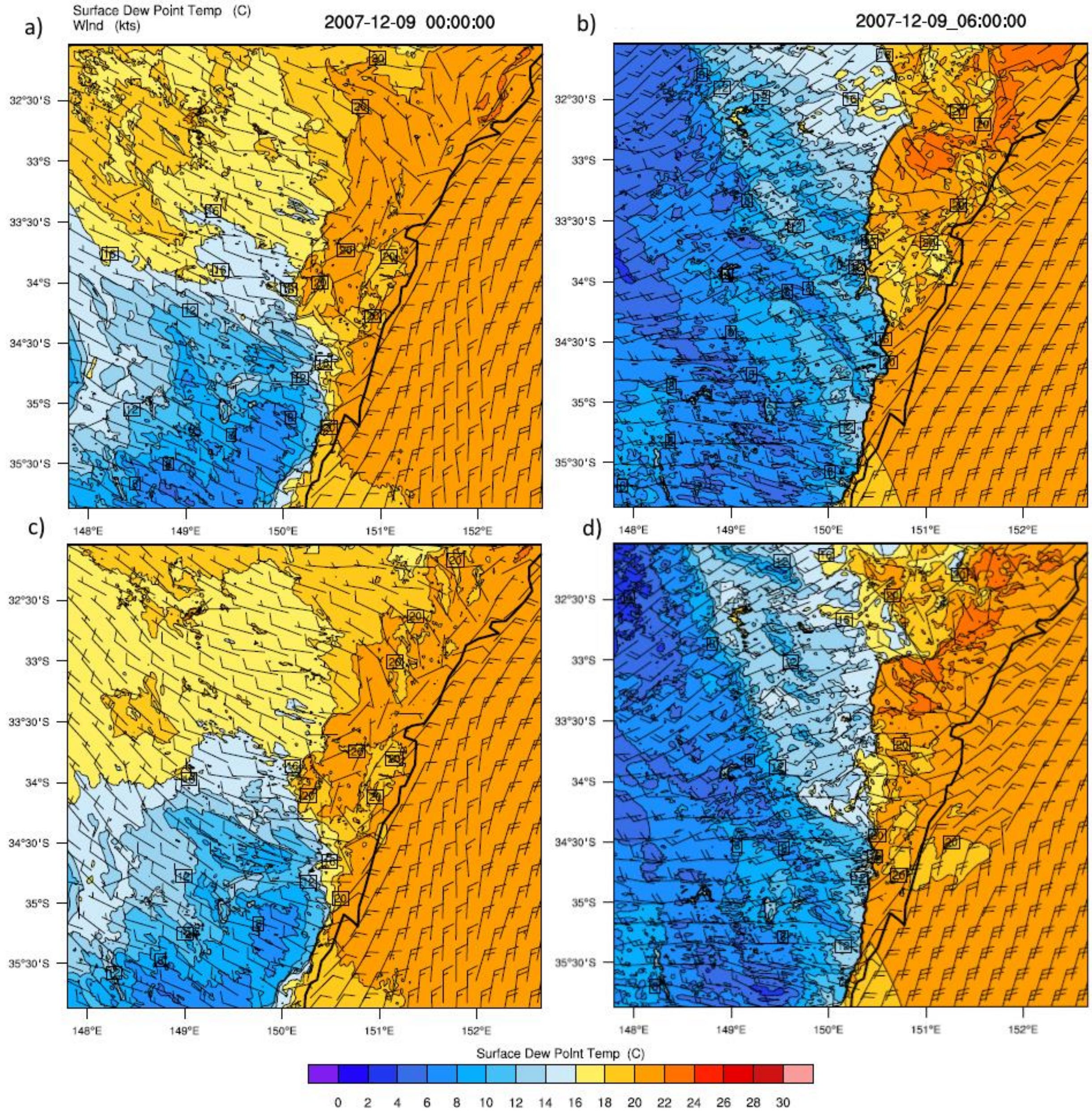

Fig. 4.4. Domain 3 Surface Dew Point Temperature (°C) and vector wind speeds (kts) at 00:00 UTC (11 am EDT) and 06:00 UTC (5 pm EDT) using the Goddard microphysics scheme with hail **(a & b)** and with graupel **(c & d)**.

As shown in Fig. 4.5, the placement and strength of the 500 hPa upper trough at 00:00 UTC and 12:00 UTC was simulated well when compared to the BoM's analysis charts. Only the hail option is displayed as it was almost identical to the graupel option. The upper trough pushes up through the Great Australian Bight, southeastern parts of South Australia and western Victoria in the morning, before moving east and spiking slightly northward along the ranges into southern Queensland by the evening. Whilst the 500 hPa temperatures remain stable (around -10 °C), the geopotential height decreased slightly throughout the day from approximately 5800 m in the morning to 5780 m in the evening, which was similar to the 5760 m on the analysis charts. 500 hPa wind shear increased on both the hail and graupel options from 30 kt westerly at 00:00 UTC to 40 kt west-northwesterly at 12:00 UTC.

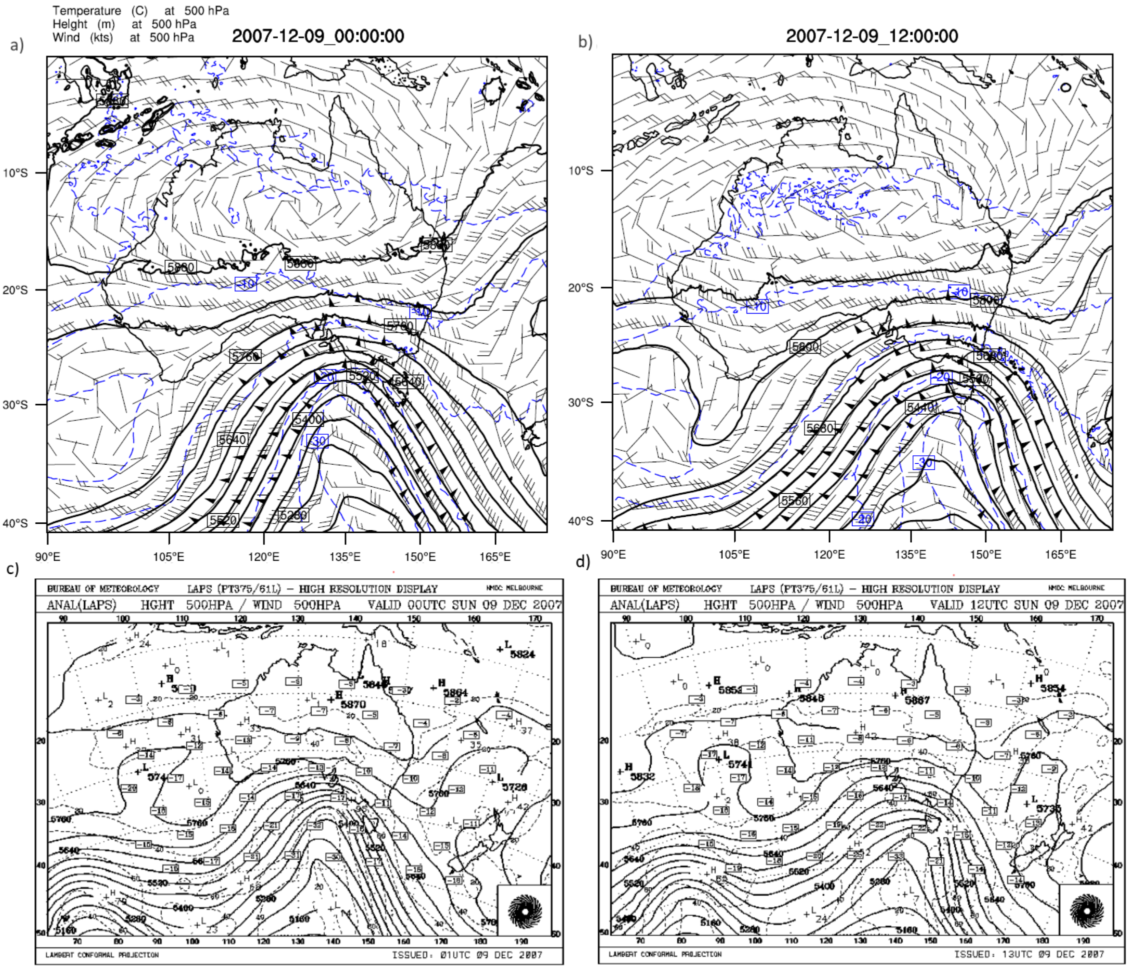

Fig. 4.5. Domain 1 Temperature (°C), Geopotential Height (m) and vector wind speeds (kts) at 500 hPa at 00:00 UTC (11 am EDT) 9 December and 12:00 UTC (11 pm EDT) 9 December using the Goddard microphysics scheme with hail **(a & b)** compared to the 00:00 UTC 9 December 500 hPa analysis BoM chart **(c)** and the 12:00 UTC 500 hPa 9 December BoM analysis chart **(d).**

4.2.2 Skew-T diagrams

Skew-T diagrams (including CAPE) were outputted for Sydney airport in domain 3 at 19:00 UTC (6 am EDT) and 04:00 UTC (3 pm EDT). Fig 4.6 shows the BoM observed diagram at 04:00 UTC, whilst Fig 4.7 shows the simulated soundings. At 19:00 UTC, both the hail and graupel options were similar, with 5-10 kt northeasterly winds as deep as approximately 900 hPa, before turning west-southwest 15 kts at 700 hPa, and west 20 kts at 500 hPa. A low-level inversion layer lay below 700 hPa, whilst a dry layer of air was located between 700 hPa and 500 hPa. At 04:00 UTC, Skew-T diagrams for the hail and graupel options had noticeable differences, with the hail option overall representing the BoM sounding more accurately than the graupel option. Whilst both options had 10-15 kt northeasterly winds as deep as around 900 hPa, the hail option had 30 kt westerly winds at 700 hPa and 35 kt westerly winds at 500 hPa, compared with the graupel option that had 25 kt west-northwest winds at 700 hPa and 25 kt westerly winds at 500 hPa. The hail option produced a deeper layer of moisture to around 800 hPa compared to the graupel option that had dry air intrusion from 850 hPa, whilst both had a sharp dry slot between 500 hPa and 700 hPa. CAPE was much higher using the graupel option than the hail option (3999 J kg^{-1} compared to 2235 J kg^{-1}), although it is worth noting that CAPE values were simulated as high as 4270 J kg^{-1} using the graupel option (03:20 UTC) and 4076 J kg^{-1} using the hail option (02:20 UTC). CAPE was calculated to be 3423 J kg^{-1} from the observational sounding (Fig. 4.6) at 04:00 UTC.

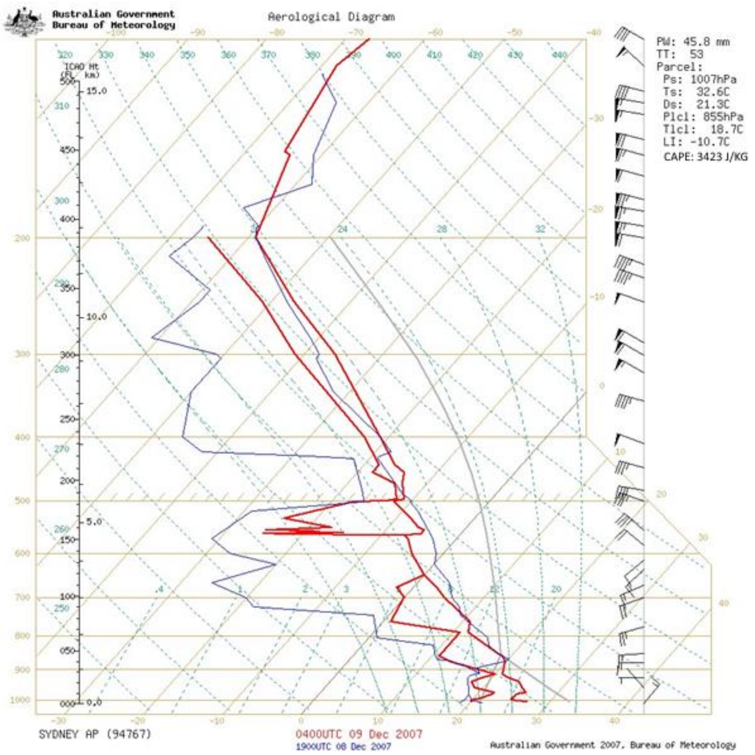

Fig. 4.6. Skew-T diagram from Sydney airport at 3 pm EDT, 9th December 2007 (blue lines represent 5 am EDT temperature and dewpoint), obtained from the Australian Bureau of Meteorology, Sydney.

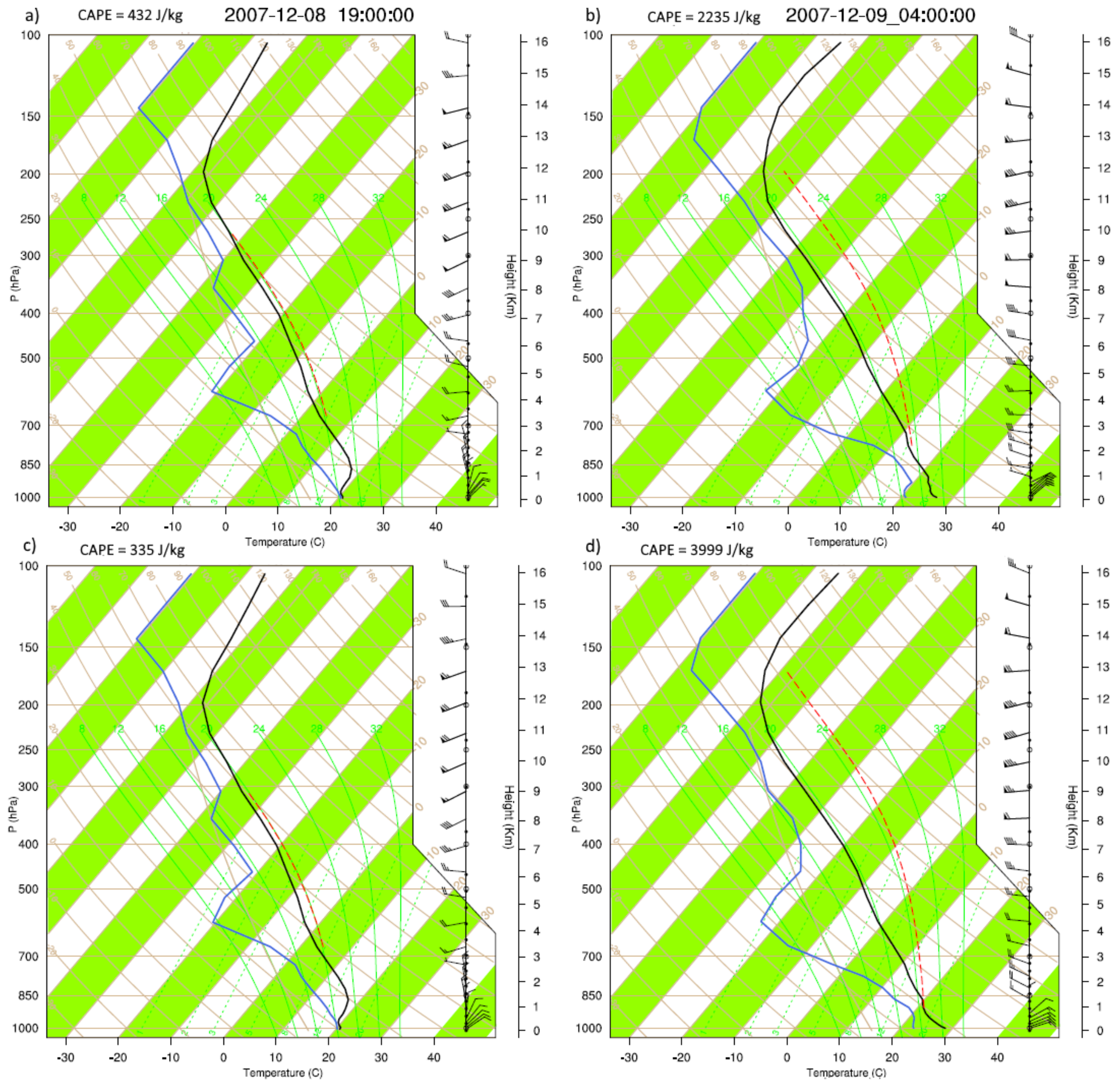

Fig. 4.7. Skew-T diagrams at Sydney airport (Domain 3) with calculated CAPE at 19:00 UTC (6 am EDT) and 04:00 UTC (3 pm EDT) 8 December using the Goddard microphysics scheme with hail **(a & b)** and with graupel **(c & d)** compared to the 04:00 UTC 9 December observed sounding **(f)** that also displays 19:00 UTC temperature and dewpoint (blue lines).

4.2.3 Storm track and precipitation

Precipitation tendency with Sea Level Pressure (hPa) and simulated equivalent radar reflectivity factor [dBZ] were calculated from WRF to determine the trough's role in storm initiation, storm track, intensity and precipitation. Using the hail option, thunderstorm cells were initiated to the southwest of Sydney around the middle of the day, before moving east and intensifying as they moved into the Sydney Basin (Fig. 4.8 and Fig 4.9). The thunderstorm strengthened into a supercell around 03:00 UTC-03:20 UTC (Fig 4.8b, Fig 4.8c, Fig 4.9b & Fig 4.9c) as it took on a northeasterly path, with peak intensity around Sydney's northwest (Castle Hill & Blacktown). A secondary and less intense storm formed on its northwest flank. The storm system remained strong as it moved out of Sydney through the Northern Beaches and Central Coast regions. Total precipitation across the storm path was generally between 20 mm and 40 mm (Fig. A1 & Fig. A2). AFWA_HAIL calculated maximum hail diameters to be 10-12 cm at 03:20 UTC, whilst AFWA_HAILCAST showed a mean maximum diameter of 4-5 cm (Fig. A3).

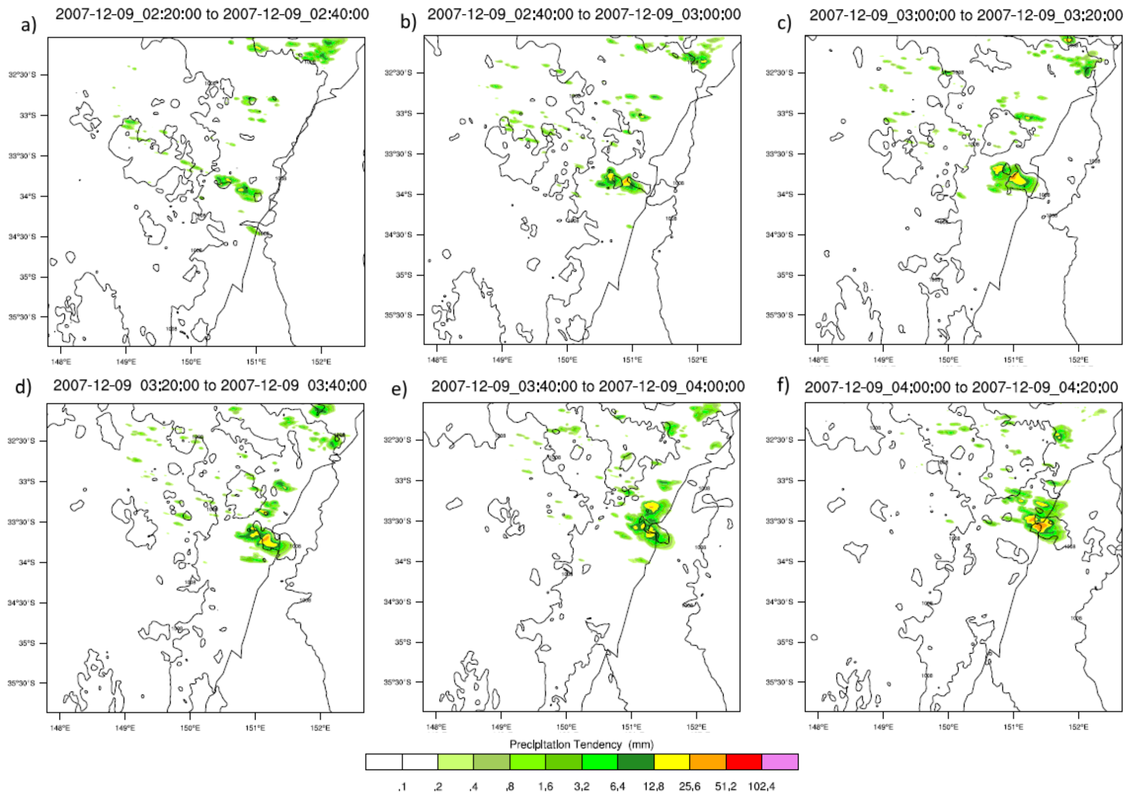

Fig. 4.8. Domain 3 Precipitation Tendency (mm) and Sea Level Pressure (hPa) using the Goddard microphysics scheme with hail from 02:20 UTC 9 December-04:20 UTC 9 December (1:20 pm – 3:20 pm EDT) at 20 minute intervals **(a-f)**

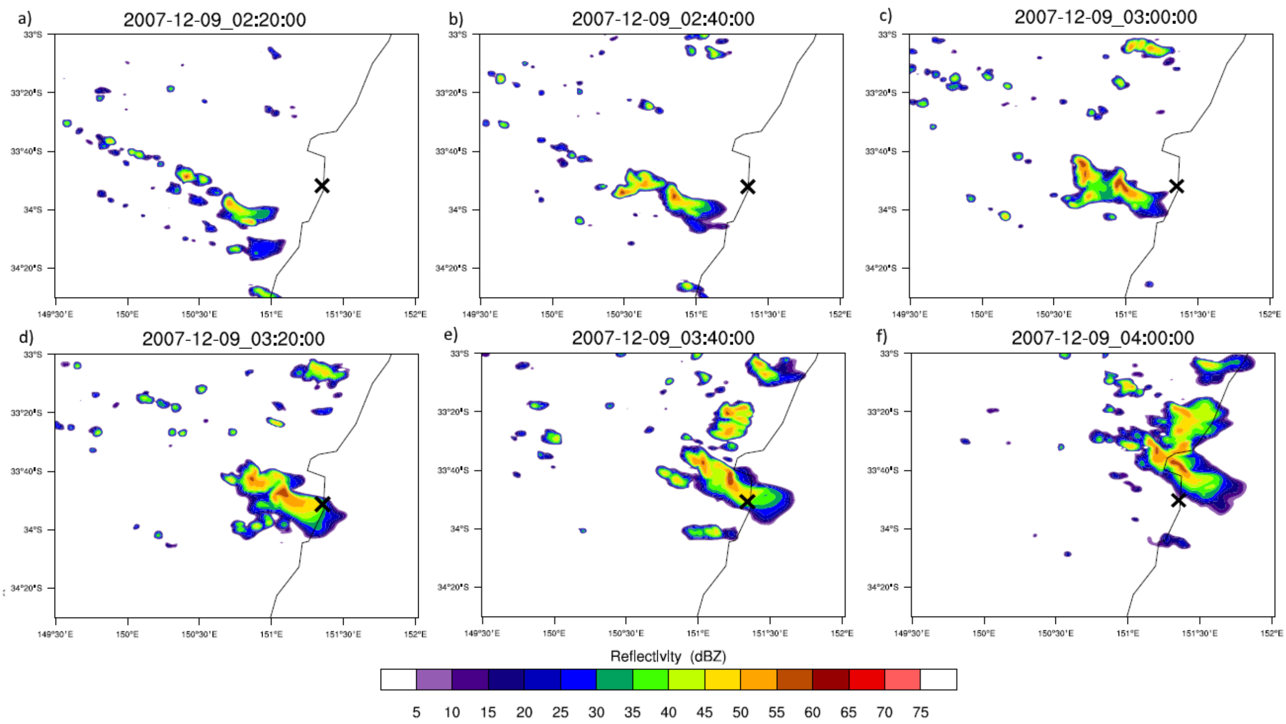

Fig. 4.9. Zoomed domain 3 simulated equivalent radar reflectivity factor [dBZ] using the Goddard microphysics scheme with hail from 02:20 UTC 9 December-04:00 UTC 9 December (1:20 pm – 3:00 pm EDT) at 20 minute intervals **(a-f).** Cross indicates Sydney Central Business District (CBD).

Using the graupel option, multi-cell showers and thunderstorms were initiated on the ranges west of Sydney during the early afternoon, which then moved east into the Sydney Basin (Fig. 4.10 and Fig 4.11). One of the leading cells in the cluster intensified over northwest Sydney and remained on an easterly path, before weakening as it approached the Northern Beaches region, before a second band strengthens as it moved through the Northern Beaches around 05:00 UTC. A secondary, and slightly more intense multi-cell cluster moved through southern Sydney and the Illawarra, maintaining strength until the coast, but did not reach severe intensity. AFWA_HAIL calculated maximum hail diameters to be 7-8 cm at 04:40 UTC, whilst AFWA_HAILCAST showed a mean maximum diameter of 2.5-3.5 cm (Fig. A4). Total precipitation across Sydney was scattered generally between 5 mm and 10 mm, with an isolated pocket in southern Sydney of 20-30 mm. Thus, comparatively the simulation with hail option has better organisation of the convective cells and storm structure as revealed by the precipitation and radar reflectivity. The simulated storm track in the hail option also better agreed with that observed, as shown in Fig. 4.9. However, precipitation was overestimated using the hail option, with the graupel option displaying more accurate totals (Fig. A1 & Fig. A2).

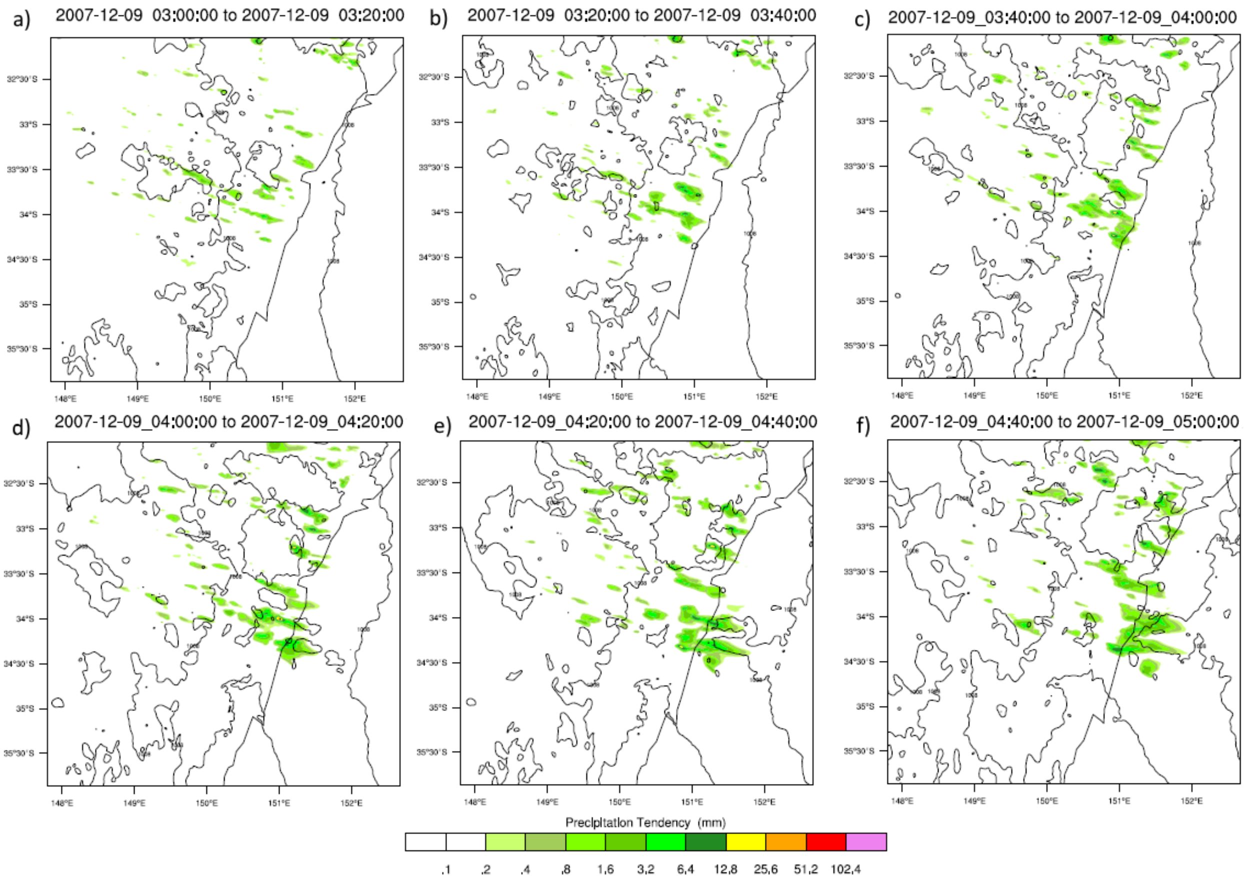

Fig. 4.10. Domain 3 Precipitation Tendency (mm) and Sea Level Pressure (hPa) using the Goddard microphysics scheme with graupel from 03:00 UTC 9 December-05:00 UTC 9 December (2:00 pm-4:00 pm EDT) at 20 minute intervals **(a-f)**

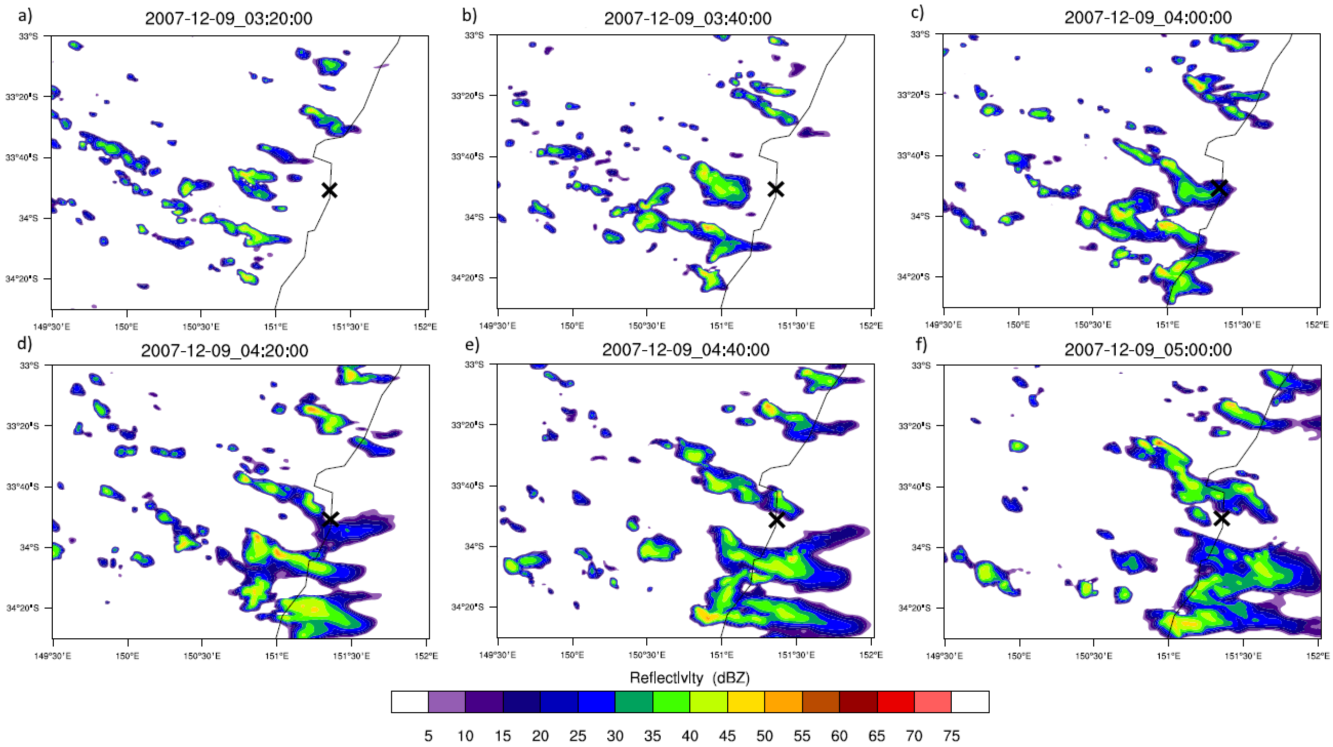

Fig. 4.11. Zoomed domain 3 simulated equivalent radar reflectivity factor [dBZ] using the Goddard microphysics scheme with graupel from 03:20 UTC 9 December-05:00 UTC 9 December (2:00 pm-4:00 pm EDT) at 20 minute intervals **(a-f).** Cross indicates Sydney CBD.

4.2.4 Mixing ratio of hail or graupel

The Hail Mixing Ratio (g kg^{-1}) for the hail option, Graupel Mixing Ratio (g kg^{-1}) for the graupel option and zonal and vertical wind (m s^{-1}) were analysed to determine the amount of hail/graupel in the storm and the vertical motion. 3D simulated radar reflectively (dBZ) was also shown to compare precipitation height and structure. As seen in the longitude-pressure cross section (latitude = 33.7°S) in Fig 4.12a, hail mixing ratios using the hail option suggested there was large amounts of hail at 03:40 UTC (8-10 g kg^{-1}) between 600 mb and 400 mb. These corresponded well to 3D simulated radar reflectively (dBZ) in domain 3 (Fig 4.12b) with the highest mixing ratios being located above the strongest echoes. Using the graupel option, graupel mixing ratios (Fig 4.12c) were highest at 05:00 UTC, with values of around 4.4-6.0 g kg^{-1} between 400 mb and 200 mb. The mixing ratio corresponded well to 3D simulated radar reflectively (Fig 4.12d), with the highest values positioned above the strongest echoes. Noticeably, there was significant vertical upward motion in front of the highest values of the hail mixing ratio (Fig 4.12a), which was not observed in the graupel option (Fig 4.12b).

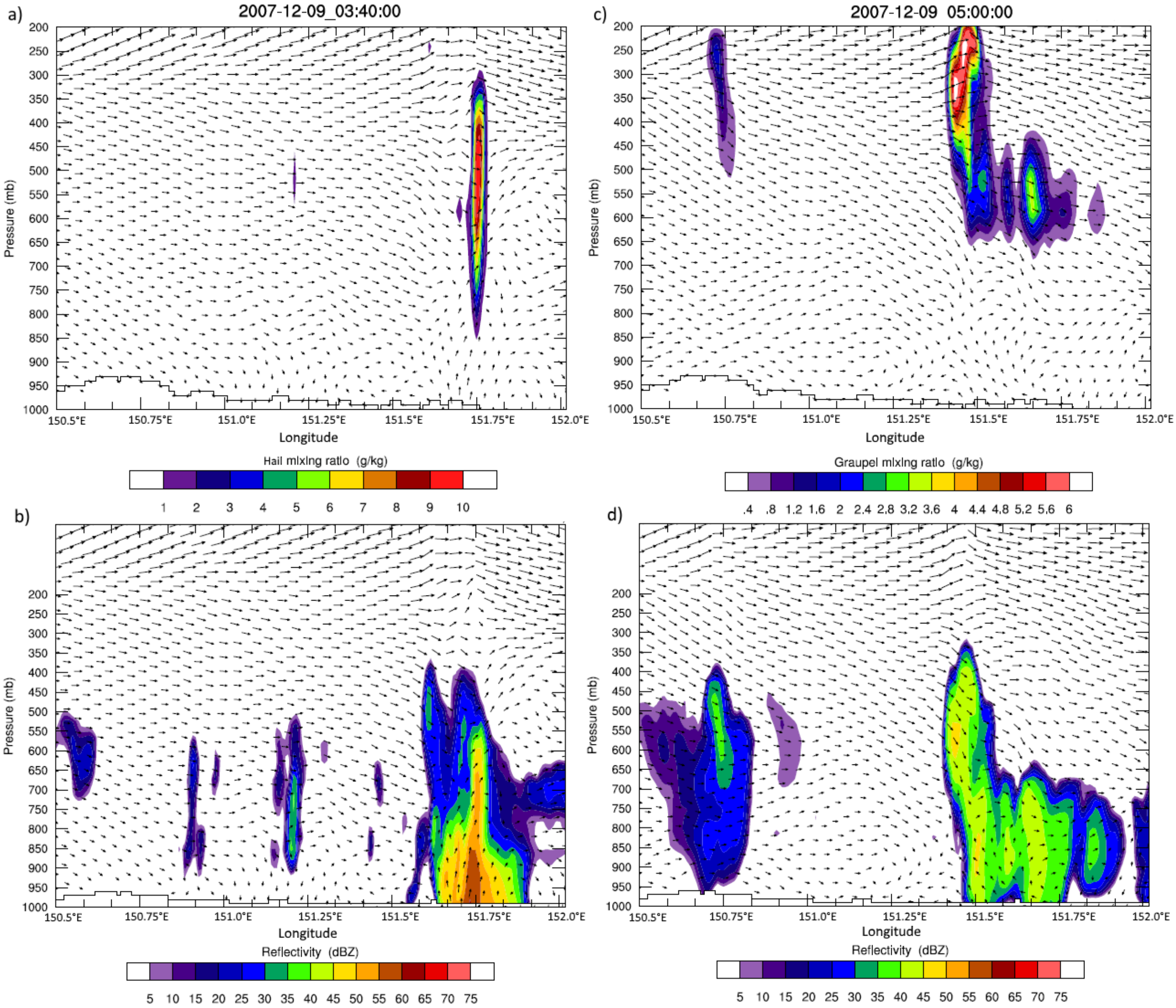

Fig. 4.12. Domain 3 longitude-pressure cross section at latitude 33.7°S showing hail mixing ratio (g kg^{-1}) and zonal and vertical wind (m s^{-1}) using the hail option at 03:40 UTC 9 December **(a)**, with corresponding 3D dBZ at the same time **(b)**. **(c)** and **(d)** the same as **(a)** and **(b)**, except using the graupel option at 05:00 UTC. Times were selected based on maximum mixing ratios of any time step.

4.2.5 Storm relative helicity, absolute vorticity and vertical velocity

Fig 4.13 and 4.14 display storm relative helicity (m^{2}s^{-2}). Storm relative helicity is derived from speed shear, directional shear, and low level wind (see Appendix I), although and is a measure of the potential for storm rotation that has been shown to be useful in forecasting storm longevity, supercells and tornadoes (Davies-Jones *et al.*, 1990; Droegemeier *et al.*, 1993).

Values above 100 m^2s^{-2} can be an indicator for supercells and tornadoes, with the threat growing as numbers are higher. (Rasmussen and Blanchard, 1998). Near the storm, the hail option shows an isolated region of intense negative helicity (consistent with cyclonic vorticity) persisting between 02:40 UTC and 03:40 UTC over northwest Sydney, peaking around 03:00 UTC (stronger than -1000 m^2s^{-2}). In the preceding environment, values were up to 400-600 m^2s^{-2} at times. The graupel option showed no defined or persistent areas of negative helicity. At 03:40 UTC, there are two isolated areas of negative helicity which are no stronger than around -300 to -400 m^2s^{-2}, but these quickly dissipate by 04:00 UTC. A persistent region of intense positive helicity (>1000 m^2s^{-2}) is noticeable throughout the period, particularly from 03:40 UTC as it approached and moved off the Illawarra coastline. In the preceding environment, values were 400-600 m^2s^{-2} at times.

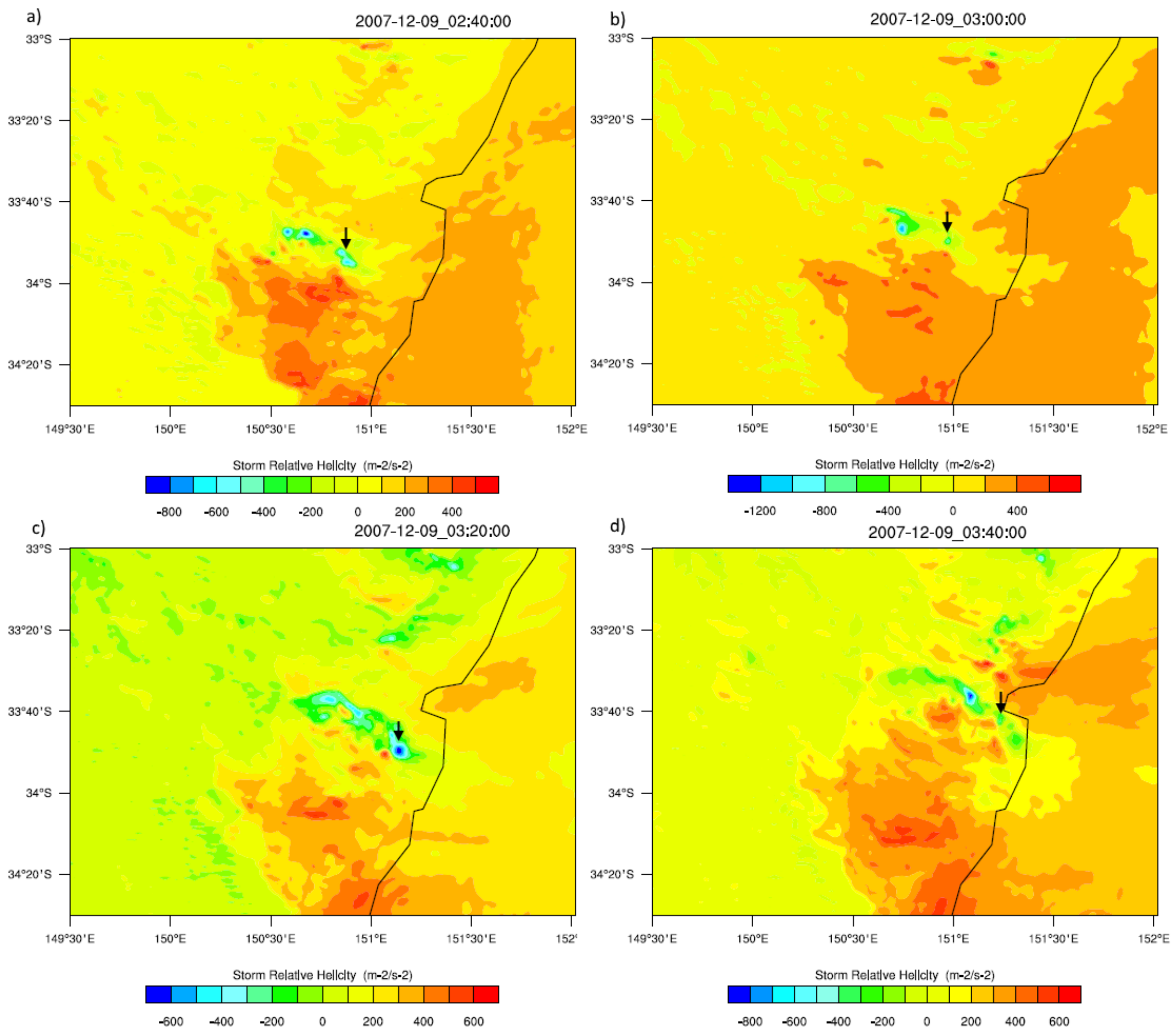

Fig. 4.13. Zoomed domain 3 0-3 km storm relative helicity (m^2s^{-2}) using the Goddard microphysics scheme with hail from 02:40 UTC 9 December-03:40 UTC 9 December (1:40 pm – 2:40 pm) at 20 minute intervals (**a-d)**. Arrows indicate main storm cell.

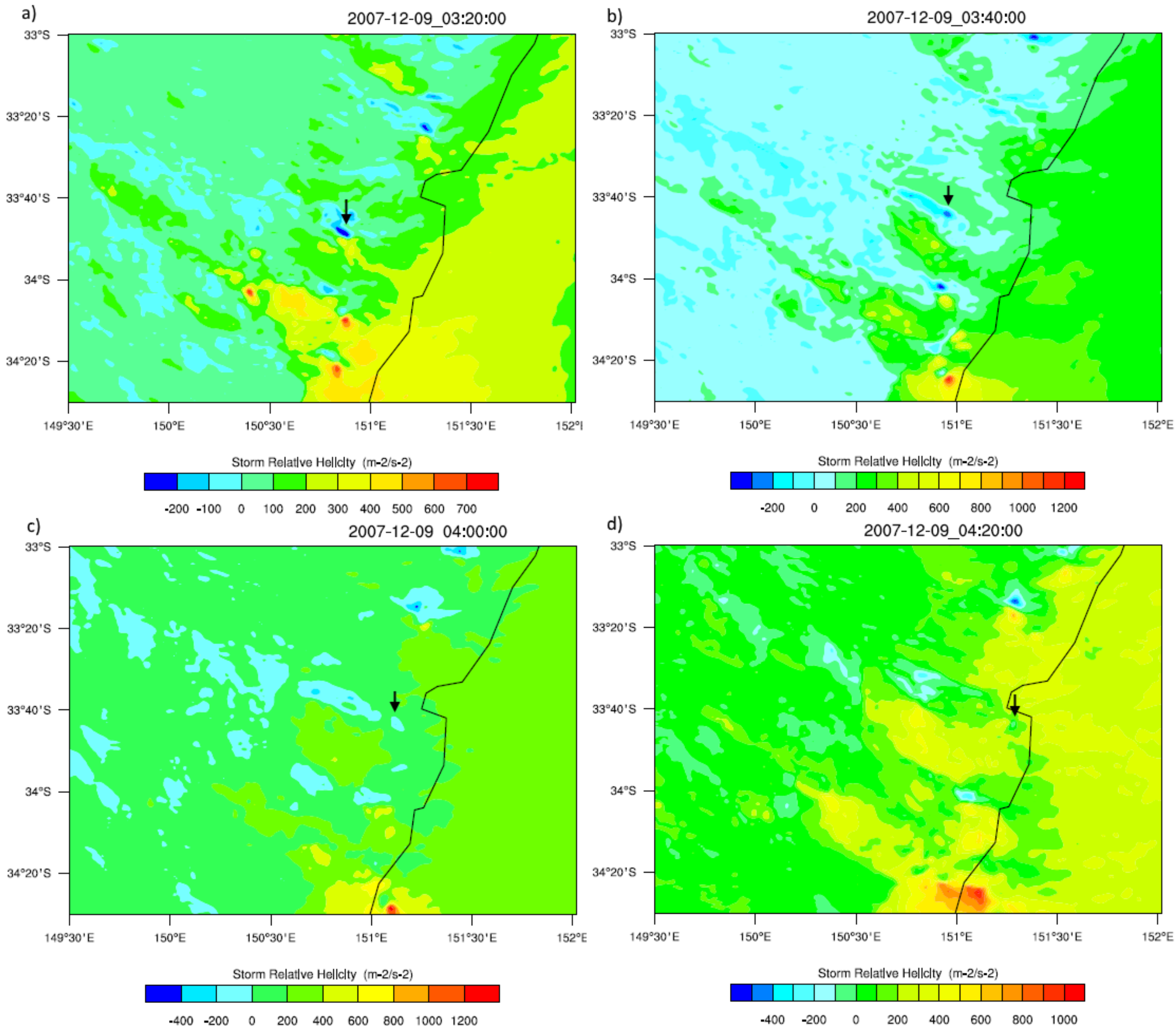

Fig. 4.14. Zoomed domain 3 0-3 km storm relative helicity (m^2s^{-2}) using the Goddard microphysics scheme with graupel from 03:20 UTC 9 December-04:20 UTC 9 December (2:20 pm – 4:20 pm EDT) at 20 minute intervals **(a-d)**. Arrows indicate main storm cell.

To further illustrate the simulated storm development within the trough, absolute vorticity (10^{-5} s^{-1}) and vertical velocity (m s^{-1}) were investigated (Fig 4.15). Across the domain, the hail option showed a greater tendency to develop more isolated patches of vorticity and intense convection, compared to the graupel option which had more scattered, weaker convection. The hail option showed the main cell well, with values of absolute vorticity in excess of 200 10^{-5} s^{-1}, coupled with vertical velocity of 14-16 m s^{-1} between 500 mb and 300 mb. Values in excess of 200 10^{-5} s^{-1} were also observed with the graupel option over the storm region, although vertical velocity values were lower, with 8-10 m s^{-1} between 400 mb and 200 mb. It is not readily clear that how the large difference in the simulated vertical velocity was resulted from the different microphysical treatment in the hail and graupel option, which is an issue deserving further investigation.

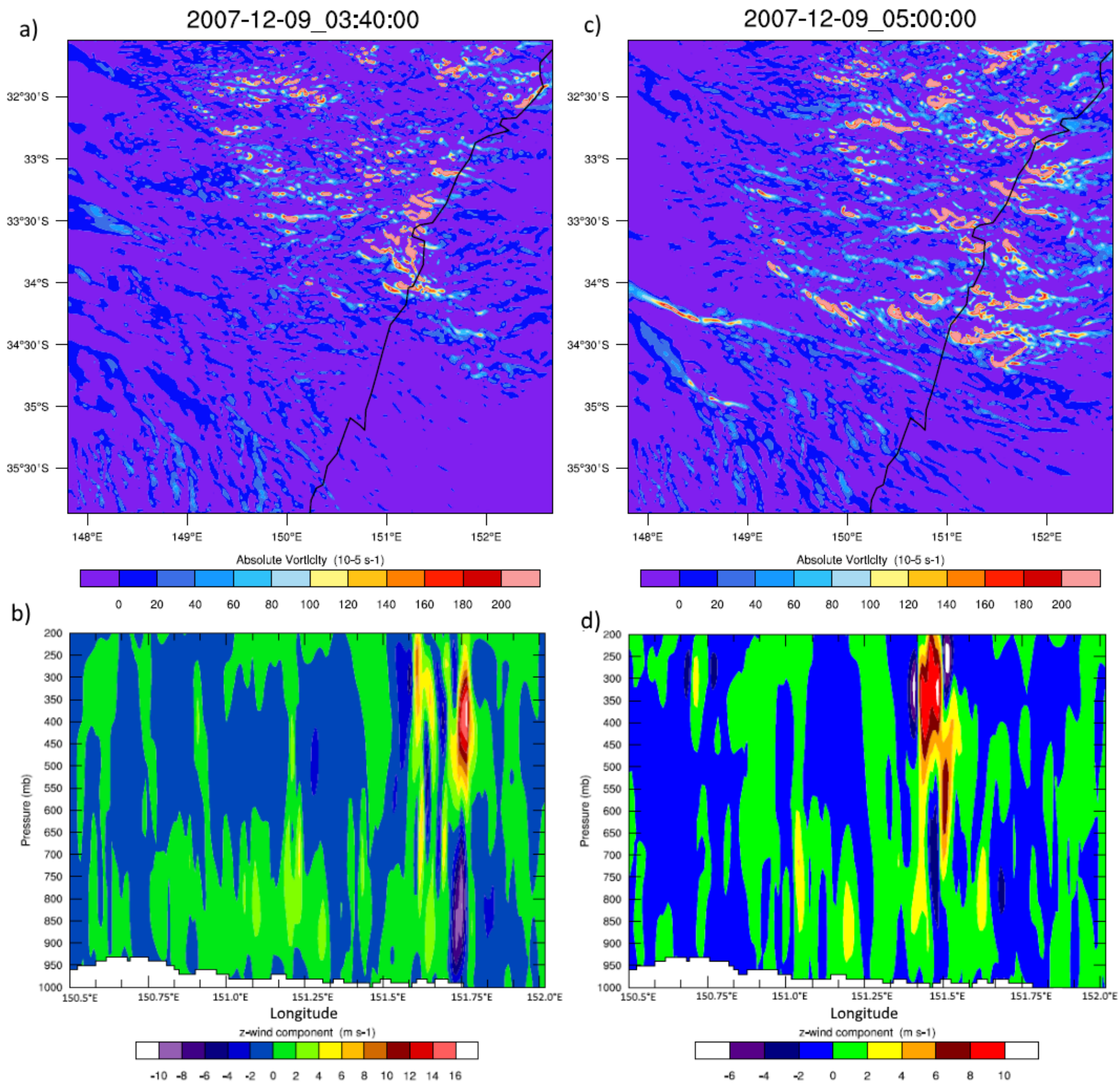

Fig. 4.15. Domain 3 500 hPa absolute vorticity (10^{-5} s^{-1}) and longitude-pressure cross section of vertical velocity (m s^{-1}) using the Goddard microphysics scheme with hail at 03:40 UTC 9 December **(a)** and **(b)** and using the graupel option at 05:00 UTC 9 December **(c)** and **(d).**

4.3 Results: Sensitivities on microphysics schemes

A number of other microphysics schemes were run with WRF, including the Kessler scheme, the Lin *et al.* (1983) scheme, the WRF Single-Moment 3-class scheme, the WRF Single-Moment 6-class scheme, the Thompson *et al.* (2008) scheme, the Morrison double-moment scheme and the WRF Double-Moment 6-class Scheme. The vast majority of these options did not include hail as a hydrometeor, but nevertheless they generally resulted in the environment and synoptic setup being captured well. However, typically the storm was simulated inaccurately, with common scenarios including weak multicell clusters moving through Sydney (with graupel options), or strong thunderstorms well north or west of Sydney (hail options). Since an in-depth discussion of these microphysics options is useful, this section will briefly analyse the WRF Double Moment 6-class scheme and the Thompson *et al.* (2008) scheme. These two microphysics schemes produced the most encouraging results after the Goddard microphysics scheme, although they still had noticeable shortcomings.

4.3.1 WRF Double Moment 6-class scheme

The WRF Double Moment 6-class scheme included hail as a hydrometeor and was run with hail and graupel options. The hail option (Fig. 4.16) produced thunderstorms further south than the graupel option (which only had weak thunderstorms forming over far northern suburbs), with cells forming to the west and south of Sydney. With the hail option, a band of thunderstorms moved into the Sydney Basin from around 1 pm EDT, intensifying as it moved east. The storm became particularly intense around 2 pm near the Central Business District (CBD), before moving out to sea. AFWA_HAIL computed maximum hail diameters to be 10-12 cm using this option at 02:40 UTC, whilst AFWA_HAILCAST showed a mean maximum diameter of 5-6 cm (Fig. A5). The overall synoptic setup and environment was captured well, although wind shear was underestimated by 5 kts at 700 hPa and 10 kts at 500 hPa (04:00 UTC), whilst there was also a lower level inversion (cap) that persisted into the afternoon.

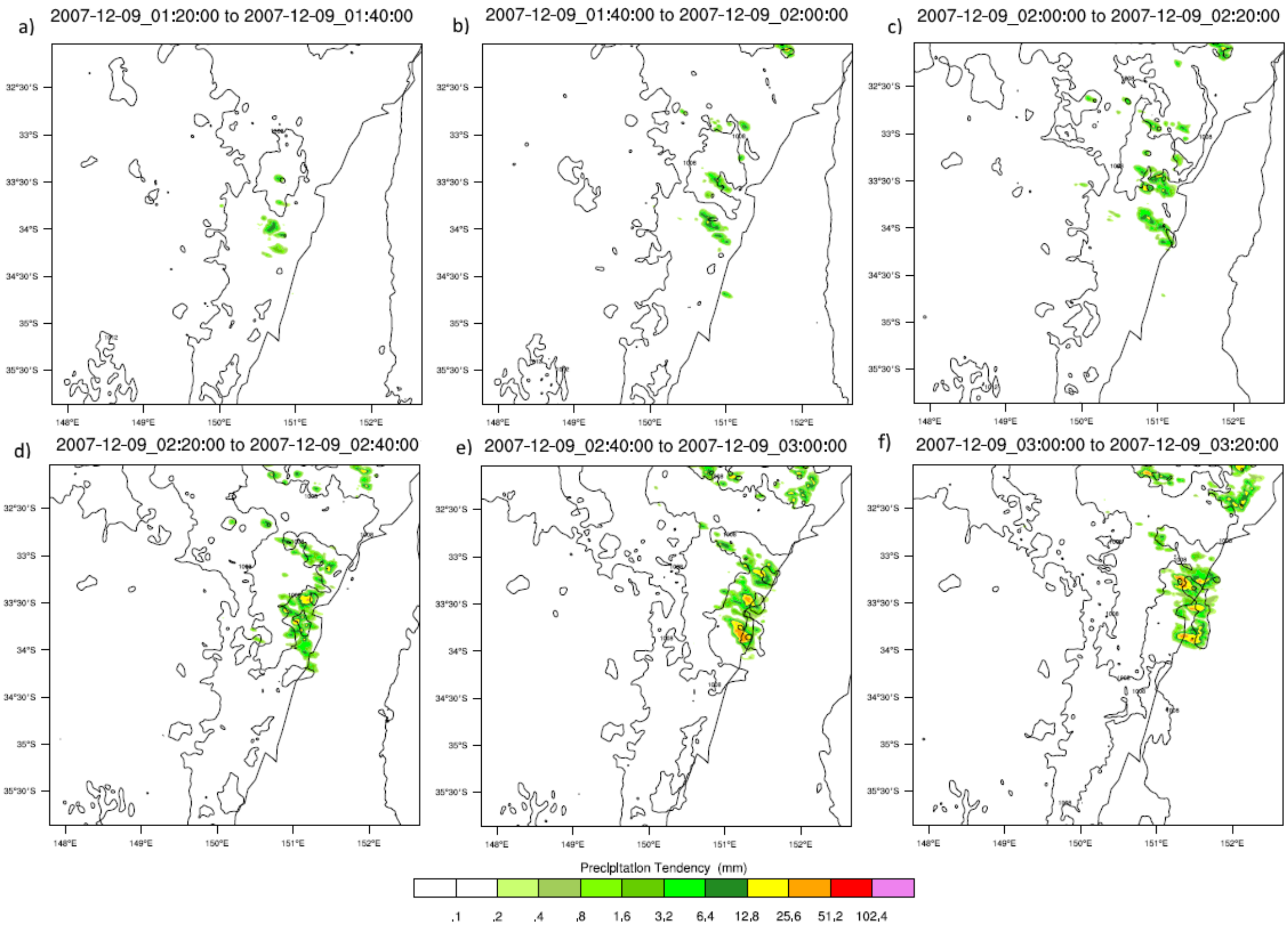

Fig. 4.16. Domain 3 Precipitation Tendency (mm) and Sea Level Pressure (hPa) using the WRF Double Moment 6-class microphysics scheme with hail from 02:20 UTC 9 December- 04:20 UTC 9 December (1:20 pm – 3:20 pm EDT) at 20 minute intervals (**a-f)**

4.3.2 Thompson, Field, Rasmussen and Hall scheme

The Thompson *et al.* (2008) microphysics scheme did not contain hail as a hydrometeor, instead using graupel. Two thunderstorm clusters were initiated over the Blue Mountains west of Sydney, and moved on an eastward trajectory into Sydney (Fig 4.17). The northern Sydney cell was initially slightly more intense than the southern one, but failed to intensify further, as it took on a very slight northeasterly path, before decaying over the Northern Beaches. The southern Sydney cell gradually intensified as it moved east, becoming moderately strong near the coast around the Sutherland Shire (far southern suburbs of Sydney). The synoptic setup and thunderstorm environment were captured well, similar to the Goddard microphysics. CAPE was well simulated at 04:00 UTC with a value of 3092 J kg^{-1}, although wind shear was underestimated by 5 kts at 700 hPa and 10 kts at 500 hPa. AFWA_HAIL calculated maximum hail diameters to be 7-8 cm at 03:40 UTC, whilst AFWA_HAILCAST showed a mean maximum diameter of 2-3 cm (Fig. A6).

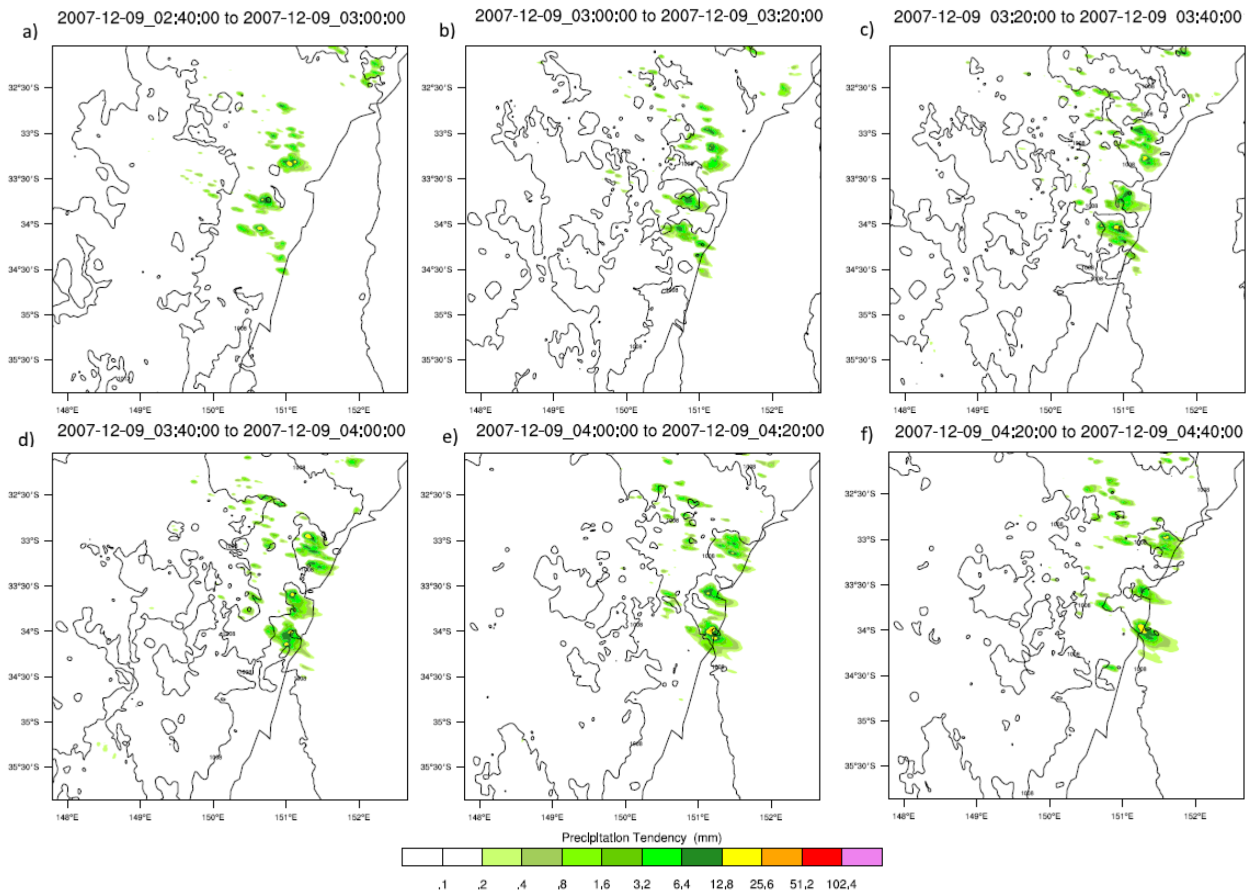

Fig. 4.17. Domain 3 Precipitation Tendency (mm) and Sea Level Pressure (hPa) using the Thompson *et al.* (2008) microphysics scheme from 02:40 UTC 9 December-04:40 UTC 9 December (1:40 pm – 3:40 pm EDT) at 20 minute intervals (**a-f)**

4.4 Discussion

4.4.1 Cloud microphysics schemes and sensitivity tests

Using WRF in conjunction with the Goddard microphysics scheme, and the New Goddard shortwave radiation scheme and Rapid Radiative Transfer Model produced the best results in simulating the 9th December 2007 Sydney hailstorm in comparison to other microphysics options. When used with the hail option (instead of the graupel option), it outperformed all other combinations of cloud microphysics schemes and radiation options (see Table 2.1 for these different schemes). The major differences can be seen in Table 4.1.

Table 4.1: Major differences between the Goddard microphysics scheme with hail and graupel options

	Goddard with hail	Goddard with graupel
Storm intensity & hail size	Strong, isolated supercell thunderstorm, hail 10-12 cm	Multi-cell cluster, hail 7-8 cm
Storm track	Camden – Blacktown – Northern Beaches	Cluster through northern suburbs and southern suburbs
Storm time	1:00 pm – 3:30 pm EDT	1:50 pm – 4:20 pm EDT
Storm Relative Helicity	In excess of -1000 m^2s^{-2} at times in storm area	Above 1000 m^2s^{-2} at times in Illawarra, south of Sydney
Graupel mixing ratio	8-10 g kg^{-1}	4.4-6.0 g kg^{-1}
Moisture	18-22 °C dewpoints, high moisture until 800 hPa	18-22 °C dewpoints, high moisture until 850 hPa
Wind shear	10-15 kt NE at surface, W 30 kt at 700 hPa, W 35 kt at 500 hPa	10-15 kt NE at surface, W/NW 25 kt at 700 hPa, W 25 kt at 500 hPa
CAPE (04:00 UTC and max)	2235 J kg^{-1} (4076 J kg^{-1} max)	3999 J kg^{-1} (4270 J kg^{-1} max)
Vertical velocity	14 - 16 m s^{-1} at 500 – 300 mb (03:40 UTC)	8 - 10 m s^{-1} at 400 mb – 200 mb (05:00 UTC)

The hail option resulted in a much more powerful thunderstorm that was of a similar track and intensity to the observed event, compared to the graupel option that showed a cluster of moderately strong multi-cellular storms (Fig 4.8 – Fig 4.11). The hail option also significantly overestimated precipitation values, with 20-40 mm commonplace within the path of the storm. With the graupel option, scattered falls of 5-10 mm were more common. Mixing ratios (Fig 4.12) indicated a significant amount of hail using the hail option (8-10 g kg^{-1}), with associated upward motion just ahead of the highest values, which is indicative of hail formation (Chevuturi *et al.*, 2014). Graupel mixing ratios (Fig 4.11b) were comparatively lower (4.4-6.0 g kg^{-1}), with no upward motion observed ahead of the highest mixing ratio values. Hail diameters were computed to be larger using the hail option (AFWA_HAIL = 10-12 cm; AFWA_HAILCAST

= 4-5 cm) than the graupel option (AFWA_HAIL = 7-8 cm; AFWA_HAILCAST = 2.5-3.5 cm). The hail option showed strong and sustained negative storm relative helicity (Fig 4.13) indicative of supercell and storm rotation potential (Davies-Jones *et al.*, 1990) between 1:40 pm and 3:40 pm with values in excess of -1000 m^2s^{-2} at times. Conversely, the graupel option (Fig 4.14) had strong positive storm relative helicity (> 1000 m^2s^{-2} at times) over the Illawarra district, which is atypical for the southern hemisphere and well south of the actual storm track. In the preceding environment, values were between 400 and 600 m^2s^{-2} for both options, which is adequate for strong supercells (Rasmussen and Blanchard, 1998). Vertical velocity (Fig 4.15b & Fig 4.15d) was also higher using the hail option (14-16 m s^{-1} between 500 mb and 300 mb) compared to the graupel option (8-10 m s^{-1} between 400 mb and 200 mb). The differences in the portrayal of the storm's intensity between the two options can be explained largely by the different microphysics processes by which hail and graupel develop. Graupel is formed by soft hail processes (dry growth/raindrop freezing), but have a small diameter of less than 5mm (Pruppacher and Klett, 2010). Graupel also has a relatively low density, and high intercept value due to more numerous small particles (Tao and Adler, 2003). Hail is formed by both soft hail processes and hard hail processes (wet growth/shredding), which continuously repeats itself, causing layered ice particles that continue to grow in convective clouds until they are too heavy, and fall as hail (Chevuturi *et al.*, 2014). Hail has a relatively high density and a low intercept value, with more numerous large particles (Tao and Adler, 2003). In the Goddard microphysics scheme, the particle size distribution is changed between the hail and graupel options to account for these processes (Tao and Adler, 2003), which has been shown to have a significant impact on the model's portrayal of storm development (Chevutri *et al.*, 2014; Snook and Xue, 2008). It is plausible that the presence of hail in the storm (using the hail option) had an influence on the storm's evolution and morphology, such as the frictional drag of hail on the storms downdrafts (van den Heever & Cotton, 2004). To understand this aspect of the storm's development further, microphysics options that contain hail would need to be studied in-depth.

However, some of the intensity can also be explained by minor (although significant) differences in the portrayal of the synoptic setup and storm environment. Along the troughline, there was a sharper distinction between the moist and dry air in the hail option (Fig 4.4), resulting in more of a dryline setup. A dryline is a boundary that separates moist air from dry air (Schaefer, 1986) and is often associated with enhanced surface convergence (Ziegler and Rasmussen, 1998); thus may be part of the reason why the hail option portrayed a more intense thunderstorm than the graupel option. In the USA, supercell thunderstorms (including large hail) are often seen on or just ahead of drylines (Burgess and Davies-Jones, 1975). Whilst the storm environment (Fig 4.7) was portrayed fairly accurately using both options, lower-level moisture was simulated to be marginally deeper using the hail option (800 hPa), whereas the graupel option had dry air intruding from 850 hPa. Wind shear (Fig 4.7) was also stronger using the hail option, with 10-15 kt northeasterly winds at the surface, 30 kt westerly winds at 700 hPa and 35 kt westerly winds at 500 hPa, compared with the graupel option that had 10-15 kt northeasterly winds at the surface, 25 kt west-northwest winds at 700 hPa and 25 kt westerly winds at 500 hPa. When calculating the 0-6 km bulk wind shear from these values, a parameter that is indicative of supercell potential (Doswell and Evans, 2003), this leads to noticeable differences. Using the hail option, 0-6 km bulk wind shear was calculated to be 45.4 kts, compared to the graupel option where it was 40.7 kts. Whilst both values are above the 20 m s^{-1} (39.64 kts) regarded as being favourable for supercells (Doswell and Evans, 2003), the stronger 0-6 km bulk shear likely led to a more organised and powerful thunderstorm. Absolute vorticity (Fig 4.15a & Fig 4.15c) suggested activity over the Sydney Basin on the day showed a tendency towards more isolated convection, which meant that the storm could make use of the heat and moisture in an environment free of cold outflow and left-over anvil cloud. One facet in which the graupel option outperformed the hail option was the timing of the storm. Whilst both options had the storm moving through Sydney slower than the actual event, the hail option pushed the storm through Sydney from 1 pm to 3:30 pm, compared to the graupel option that had the multi-cell cluster move through between 1:50 pm – 4:20 pm. Both these options developed the storm too early, however the graupel option finished at a similar time to the observed storm which hit Sydney from 3 pm to 4:30 pm. Incorporating data assimilation (feeding observations into the model using data such as Skew-T diagrams, satellite images and radar images) into the model is planned using surface and upper-level data, and could improve the model's temporal accuracy. Data assimilation has been shown to improve both the temporal and spatial output for a variety of weather phenomena in both high-resolution and ensemble models (Sokol *et al.*, 2014; Fujita *et al.*, 2007; Wilson *et al.*, 2010). It is worth mentioning that the New Goddard longwave radiation option was also tested in conjunction with the New Goddard shortwave radiation option (instead of the Rapid Radiative Transfer Model), due to evidence that using the two together would improve output (Shi and Tao, 2006). Including this radiation option resulted in a powerful thunderstorm and associated weaker multi-cells being simulated (Fig. A7). AFWA_HAIL computed hail in this storm to be as large as 10-12 cm at 03:00 UTC, whilst AFWA_HAILCAST computed maximum diameters of 5-6 cm (Fig. A8). However, the storm track was significantly different to the observed storm, passing to the south of Sydney, and moved to the right of the mean-steering flow.

Other schemes such as the WRF Double-Moment 6-class scheme with hail (Fig 4.16), and the Thompson *et al.* (2008) microphysics scheme (Fig 4.17), which did not contain a hail option, also produced encouraging results (although probably not usable operationally). Whilst an intense thunderstorm was predicted using the WRF Double-Moment 6-class scheme with hail over the Sydney CBD area, the storm was only very short lived (20-40 minutes) at this intensity, and was 10-20 km south of the observed event. However, this was still significantly better than using the graupel option that displayed only weak shower activity developing over far northern parts of Sydney and the Central Coast. The Thompson *et al.* (2008) scheme had two main storm cells moving through Sydney, which arrived approximately 1 hour earlier than the observed storm. However, it spatially outperformed the WRF Double-Moment 6-class scheme with a storm cell in approximately the same area as the observed storm. The Thompson *et al.* (2008) scheme does not incorporate hail as a hydrometeor into its microphysics, and it is inferred that this scheme would have been one of the optimum schemes for simulating the 9th December 2007 event if it did.

4.4.2 Reconstructing the 9 December 2007 Sydney hailstorm

Simulating the 9th December 2007 severe hailstorm using WRF allowed an in-depth analysis of the factors that led to the storm's development and intensity to be carried out. The time of the year at which the thunderstorm developed was well within the severe thunderstorm season, occurring in Sydney's second-most hail prone month (Schuster *et al.*, 2005). Instability was generated by a surface trough that was located over central-inland NSW during the morning, with its southern flank approaching Sydney during the afternoon and moving through the city during the evening. There was also increasing instability in the upper atmosphere due to an upper level trough, which lay over the Great Australian Bight during the morning, before moving east during the day and spiking northward along the Great Diving Range. The upper trough caused the 500 hPa geopotential height to decrease slightly throughout the day (5800 m in the morning to 5780 m in the evening), although the 500 hPa temperature was stable throughout the day, remaining around -10 °C. This is not unusually cold for December, however combining with very warm air at the surface (above 30 ° C in western parts of Sydney), resulted in steep lapse rates, which is often associated with explosive convection and severe thunderstorms (Doswell *et al.*, 1985; Sherburn and Parker, 2014). Cool upper level temperatures are frequently associated with hail (Biedenger, 1984), however warm air accompanying this cold upper level is often required for severe hail (Longley and Thompson, 1965). A deep layer of moisture (as high as 900 hPa) was fed over the NSW coast ahead of the surface trough, with dewpoints reaching above 20 °C across Sydney. Deep-layer moisture near the surface is common in large hail events (McBurney, 2012**;** Kunz *et al.,* 2009). In the wake of the trough, there was much drier air, with dewpoints dropping to around 6 °C. This resulted in somewhat of a dryline setup, which caused enhanced surface convergence. The storm developed on the Great Dividing Range west of Sydney, where the higher terrain forced lifting to help break the lower level inversion. The role of topography in initiating thunderstorm formation is well documented (Spanos, 1993; Manzato, 2012; McBurney, 2012; Changnon, 2000), particularly when conditions are not unstable enough to break inversions in the lower levels.

As the storm came off the higher ground and moved into the Sydney Basin, it intensified rapidly into a supercell, moving in an east-northeast direction left of the mean steering flow, which is typical of Australian supercells (Dickins, 1994). Very large CAPE values likely between 3000 J kg^{-1} and 4000 J kg^{-1}, occurred in the pre-storm environment. These values are exceptionally high for Australian standards and are more readily observed in the United States (Tucker, 2002; Johns and Doswell, 1992). In many severe hail cases in Sydney, large CAPE has not been required (McBurney, 2012), and rather strong vertical wind shear aiding in updraft alignment is more important (Mitchell and Griffiths, 1993; McBurney, 2012). The role of CAPE on severe hail is debatable. Large CAPE has been suggested to encourage the formation of strong updrafts (Sánchez *et al.,* 2008) and is also essential for tropical hailstorm formation (Cecil and Blankenship, 2012). However, many studies suggest European hailstorms are typically associated with only low-to-moderate CAPE (Lopez *et al*., 2001**,** Tucker, 2002; Houze *et al.,* 1993), as are those that regularly in the United States (Sherburn and Parker, 2014). Some studies argue that CAPE can be used to determine whether a thunderstorm contains severe hail (Ryan, 1992; Niall and Walsh, 2005), whilst other studies found there was little difference in CAPE values between large and small hail events (McBurney, 2012; Knight and Knight, 2001). It is therefore inferred than the large CAPE on this day likely contributed somewhat to the thunderstorm's severity, most likely through aiding in the formation of strong updrafts (Sánchez *et al*., 2008). However, it is more likely that the combination with strong vertical wind shear that contributed most towards the thunderstorm's intensity. Vertical wind shear is a crucial component for severe thunderstorm formation, aiding in the organisation and longevity of storm structure (Allen *et al*., 2011; Spark and Casinader, 1995). Over the Sydney Basin, a deep 10-15 kt northeasterly wind persisted until the 850 hPa layer, before backing with height to 25 kts at 700 hPa and 35 kts at 500 hPa. This resulted in 0-6 km bulk wind shear of 45.4 kts, higher than the values of 20 m s^{-1} (39.64 kts) regarded as being favourable for supercells (Doswell and Evans, 2003). It likely that the storm became supercellular as it encountered these northeasterly winds in Sydney (compared to northwesterly winds on the ranges), dropping large hail across western and northern Sydney. A sharp dry slot between 600 hPa and 500 hPa would have been a pivotal factor in the size of the hail, with dry slots found to significantly enhance updraft strength (Browning and Ludlam, 1962) and are often associated with giant hail events (Colquhoun, 1987). The cell eventually weakened over the Northern Beaches of Sydney as it encountered cooler outflow from storms over the Central Coast.

McBurney (2012) inferred that hailstorms in Sydney were typically associated with factors such as strong vertical wind shear, cool 500 hPa temperatures, a dry slot between 400 – 600 hPa, a deep layer of low-level moisture and only low-to-moderate CAPE. This thunderstorm fulfilled all of these criteria, apart from CAPE, which was exceptionally high for Sydney and Australia (Tucker, 2002; McBurney, 2012; Allen *et al.,* 2011). This thunderstorm also met the discriminants proposed by Allen *et al.* (2011) to differentiate between environments with an increased likelihood of severe thunderstorm environments and other thunderstorm environments, based on CAPE and 0-6 km bulk shear (S06). For example, the third discriminant, CAPE x $S06^{1.67} \geq 11500$ was found to equal 660442.86, well above the threshold. This significantly larger value can be attributed to the unusually high CAPE for Australian standards, the limits of pseudo-proximity soundings to reproduce CAPE found in Allen *et al.* (2011), and the nature of the discriminants found to be relatively small to differentiate between severe and non-severe environments.

CHAPTER 5 CONCLUSIONS

Hailstorms are Australia's costliest natural disaster and pose a significant threat to loss of life and property, particularly in the nation's east. Sydney, the most densely populated part of Australia, is arguably Australia's most hailstorm-prone capital city, with a number giant hail events contributing to large insurance losses over the last three decades. However, despite the high frequency and consequences of these hailstorms, there has been limited research done on this area of study in Australia. Schuster *et al.* (2005) produced the first in-depth climatology of Sydney from 1791-2003, which was extended to 2010 in McBurney (2012), which provided a significant understanding of the spatial and temporal distribution of hail in the city. However, findings suggested that hail frequency may be decreasing since the early 1990s, which has been observed in some other parts of the world, including China and Argentina. Studies by Buckley *et al.* (2001), Speer *et al.* (2004) and Leslie *et al.* (2008) lay strong foundations for further research into high-resolution hailstorm forecasting in Sydney, simulating a number of severe hailstorm events in Sydney. This paper aims to build on this literature in order to improve high-resolution hailstorm forecasting in Australia, and evaluate advancements in NWP models for such local-scale hazardous weather.

In Chapter 3, the hybrid hailstorm database for Sydney developed by Schuster *et al.* (2005) and McBurney (2012) was extended to the end of the 2014/2015 June-May hail season. This was undertaken to assess whether an apparent decline in hailstorm frequency between 1991 and 2010 (8.45 ± 1.57 hailstorms per annum) had persisted in recent years. Hailstorm numbers had significant temporal variability over annual and decadal scales and were found to average 10.89 ± 1.20 per annum from 1950-2014. However, during 2011-2014 the average increased to 12.00 ± 4.68 hailstorms per annum. Severe hailstorm numbers had declined in recent years, with only 3.00 ± 2.60 per annum from 2011-2014, compared to the 1991-2010 average of 5.15 ± 1.07 severe hailstorms/annum. 2011 had the lowest total of severe hailstorms in a season since 1984. However, in the 2014/2015 season severe hail numbers were the highest since 2007. It was inferred that the apparent decline in total hail frequency and severe hail frequency is more likely inter-annual and inter-decadal variability, rather than a long-term reduction in frequency. More research is needed to explore the importance of the climatic and oceanic oscillations that may help explain this variability.

In Chapter 4, as a case study, a high-resolution numerical simulation of the 9th December 2007 severe hailstorm event was conducted using version 3.6.1 of the WRF model. This event was chosen as it had not been analysed in detail, despite devastating western and northern suburbs and resulting in unofficial reports of hail up to 11 cm in diameter and AUD$470 million dollars in damage. WRF was fed by 1° latitude/longitude Final Analysis data from the GFS model as initial and boundary conditions. Sensitivity tests were conducted primarily on cloud microphysics schemes, but also included radiation schemes to determine their impacts on the simulations. It was found that microphysics options that included hail as one of their hydrometeor more accurately reproduced the storm than those that relied on graupel, although those did that not contain hail as a hydrometeor can still be used to an extent. The Goddard microphysics scheme with the hail option coupled with the Goddard shortwave radiation scheme most accurately simulated the storm on both synoptic and mesoscales, although the storm arrived approximately 1.5 hours earlier than the actual event. Other schemes such as the WRF Double-Moment 6-class scheme with hail, and the Thompson, Field, Rasmussen and Hall microphysics scheme (which did not contain a hail option) also produced encouraging results, however storm track and intensity was noticeably less accurate than the Goddard microphysics scheme.

Simulating this event made it possible to carry out a comprehensive analysis of the mechanisms that led to the formation and severity of the thunderstorm. The event occurred well within the severe thunderstorm season for Sydney in December, one of the most active months for severe hail. A surface trough approached from the west during the day, passing through Sydney during the evening, enhancing lifting. An upper level trough which was located over the Great Australian Bight during the morning approached during the day, lowering the 500 hPa geopotential height slightly (5800 m in the morning to 5780 m in the evening), but keeping the 500 mb temperature around -10 °C. These 500 hPa temperatures are not unusually cold for December. However, with the surface temperature rising above 30 °C in western Sydney, these resulted in steep lapse rates which led to severe convection. The trough had very humid air ahead of it with dewpoints reaching above 20 °C, however significantly drier air in the trough's wake resulted in a dryline setup which has been found to be commonly associated with severe hail events. The thunderstorm formed over higher ground west of Sydney where there was forced lifting to help break the lower level inversion. As the storm entered the Sydney Basin it became severe, taking on supercell structure and moving left of the mean steering flow in an east-northeast direction. Very large CAPE values likely between 3000 J kg^{-1} and 4000 J kg^{-1} in the pre-storm environment (which are unusual for Sydney) were believed to be a factor towards the storms severity, encouraging the formation of sustained powerful updrafts. However, it was the large CAPE's combination with strong vertical wind shear that contributed most significantly to the storm's intensity, with deep northeasterly winds below 850 hPa backing with height to 35 kts at 500 hPa, creating 'turning' in the atmosphere. A sharp dry slot between 600 hPa and 500 hPa was also an important factor in the storm's intensity, encouraging the formation of severe hail due to powerful updrafts. The parameters leading up to the storm event, such as adequate instability, a deep layer of moisture in the lower levels, strong vertical wind shear and a dry slot in the mid-troposphere were typical of those found in severe hailstorms in McBurney (2012), and in severe thunderstorm environments in Australia (Allen *et al.,* 2011).

The results from this paper are encouraging given the model simulated a thunderstorm close to the actual track of the event with similar intensity. Whilst it is recognised that the simulated storm arrived around 1.5 hours earlier than actual event, this study did not incorporate data assimilation, which may have improved the model's ability to reproduce the storm on a temporal scale. However, these outcomes were encouraging given the issues of some Australian simulations to accurately capture hailstorms on spatial scales due to resolution issues. This suggests that there have been improvements over the last 5-10 years in the ability of high-resolution NWP models to simulate hailstorms in Australia, and that their application operationally could greatly improve hail forecasting throughout the country. However, limitations to current effective operational use of such high-resolution NWP models may include, (i) a general unavailability of extra observations for data assimilation in data sparse areas of Australia, and (ii) computer time constraints in running NWP models in real time.

REFERENCES

Allen, J.T., Karoly, D.J., and Mills, G.A.., 2011: A severe thunderstorm climatology for Australia and associated thunderstorm environments, *Australian Meteorological and Oceanographic Journal*, **111**, 143-158

Andrews, K.E., and Blong, R.J., 1997: March 1990 Hailstorm Damage in Sydney, Australia, *Natural Hazards*, **16**, 113-125.

Baldi, M., Ciardini, V., Dalu, D.D., De Filippis, T., Maracchi, G., and Dalu, G., 2014: Hail occurrence in Italy: Towards a national database and climatology, *Atmospheric Research*, **138**, 268-277.

Berthet, C., Dessens, J., and Sanchez, J.L., 2011: Regional and yearly variations of hail frequency and intensity in France, *Atmospheric Research*, **100**, 391-400.

Biedenger, R.E., 1984: July Thunderstorm Produces Large Hail in Miami Florida, NOAA Technical Memorandum NWS-SR 111, 5 pp.

BoM (Bureau of Meteorology): Stormy Weather, A century of storms, flood and drought in New South Wales, Australian Government, 2011.

Browning, K.A., and Ludlam F.H., 1962: Airflow in convective storms, Quarterly Journal of the Royal Meteorological Society, 88, (376), 117-135.

Buckley, B.W., Leslie, L.M., and Wang, Y., 2001: The Sydney hailstorm of April 14, 1999: Synoptic description and numerical simulation, *Meteorology and Atmospheric Physics*, **86**, 167-182

Bureau of Meteorology, 2006: *Report on the 14 April 1999 Sydney Severe Hailstorm*, © Commonwealth of Australia, Australia Government Bureau of Meteorology .

Burgess, D.W., and Davies-Jones, R.P., 1979: Unusual Tornadic Storms in Eastern Oklahoma on 5 December 1975, *Monthly Weather Review*, **107**, 451-457.

Cecil, D.J., and Blankenship, C.B., 2012: Toward a Global Climatology of Severe Hailstorms as Estimated by Satellite Passive Microwave Imagers, Journal of Climate, **25**, 687-703.

Changnon, S.A., and Changnon, D., 2000: Long-term Fluctuations in Hail Incidences in the United States, Journal of Climate, **13**, 658-664.

Chevuturi, A., Dimri, A.P., and Gunturu, U.B., 2014: Numerical simulation of a rare winter hailstorm event over Delhi, India on 17 January 2013, *Natural Hazards Earth System Sciences*, **14**, 3331-3344.

Chou, M.-D., and M. J. Suarez, M.J., 1999: A solar radiation parameterization (CLIRAD-SW) developed at Goddard Climate and Radiation Branch for Atmospheric Studies, Goddard Space Flight Center, Greenbelt, *NASA Technical Memorandum, NASA/TM-1999-104606*(15)

Cintineo, J.L., Smith, T.M, Lakshmanan, V., Brooks, H.E, and Ortega, K.L., 2012: An Objective High-Resolution Hail Climatology of the Contiguous United States, *Weather and Forecasting*, **27**, 1235-1248.

Colquhoun, J.R., 1987: A decision tree method of forecasting thunderstorms, severe thunderstorms and tornadoes, *Weather & Forecasting*, **1**, 337-345.

Crompton, R.P., 2011: Normalising the Insurance Council of Australia Natural Disaster Event List: 1967–2011, Risk Frontiers, Macquarie University

Davies, B., Logan, M., Ling, M., Cinque, P., Fry G., Leigh, R., 2008: *The Western Sydney Hailstorm 2007,* Risk Frontiers & New South Wales State Emergency Service

Davies-Jones, R., Burgess, D., and Foster, M., 1990: The test of energy helicity as a tornado forecast parameter. *Preprints 16th Conference on Severe local storms,* Kananaskis Park AB Canada, Amer. Met. Soc., 588-592.

Dickins, J., 1994: South Australian supercells—A composite hodograph. Preprints, *Fourth Severe Thunderstorm Conference.*, Mount Macedon, Victoria, Australia, Bureau of Meteorology, 1–9
Doswell III, C. A., Caracena, F., and Magnano, M., 1985: Temporal evolution of 700-500 mb lapse rate as a forecasting tool--a case study, *Preprints, 14th Conf. on Severe Local Storms*, Indianapolis, American Meteorological Society, 398-401.
Doswell III, C.A., and Evans, J.S., 2003: Proximity sounding analysis for derechos and supercells: An assessment of similarities and differences, *Atmospheric Research*, **67-68**, 117-133
Droegemeier, K.K, Lazarus, S.M., and Davies-Jones, R., 1993: The Influence of Helicity on Numerically Simulated Convective Storms, *Monthly Weather Review*, **121**, 2005–2029.
Dudhia, J., 1989: Numerical Study of Convection Observed during the Winter Monsoon Experiment Using a Mesoscale Two-Dimensional Model, *Journal of the Atmospheric Sciences*, **46**, 3077–3107.
French, A.J., and Parker, M.D., 1987: Numerical Simulations of Bow Echo Formation Following a Squall Line-Supercell Merger, *Monthly Weather Review*, **142**, 4791-4822.
Fujita, T., Stensrud, D.J., and Dowell, D.C., 2007: Surface Data Assimilation Using an Ensemble Kalman Filter Approach with Initial Condition and Model Physics Uncertainties, *Monthly Weather Review*, **135**, 1846–1868.
Garcia-Ortega, E., Fita, L., Romero, R., López, L., Ramis, C., and Sánchez, J.L., 2007: Numerical simulation and sensitivity study of a severe hailstorm in northeast Spain, *Atmospheric Research*, **83**, 225–241.
Hong, S.-Y., and Pan, H.-L., 1996: Nonlocal Boundary Layer Vertical Diffusion in a Medium-Range Forecast Model, Monthly Weather Review, **124**, 2322–2339
Hong, S.-Y., Dudhia, J., and Chen, S.-H., 2004: A Revised Approach to Ice Microphysical Processes for the Bulk Parameterization of Clouds and Precipitation. *Monthly Weather Review*, **132**, 103–120.
Hong, S.-Y., and Lim, J.-O., J., 2006: The WRF Single-Moment 6-Class Microphysics Scheme (WSM6), *Journal of the Korean Meteorological Society*, **42**, 129–151.
Hong, S.-Y., Noh, Y., and Dudhia, J., 2006: A New Vertical Diffusion Package with an Explicit Treatment of Entrainment Processes. *Monthly Weather Review*, **134**, 2318–2341.
Houze, R.A., Schmid W., Fovell R.G., and Schiesser H.H., 1993: Hailstorms in Switzerland: left movers, right movers, and false hooks, *Monthly Weather Review*, **121**, 3345–3370.
Jewett, B.F., Wilhelmson, R.B., 1996: Numerical simulation of severe squall line thunderstorms. Preprints, 18th Conference on Severe Local Storms, *American Meteorological Society*, 268-272
Ji, F., Riley, M., Clarke, H., Evans, J.P., Argüeso, D., Fita, L. High-resolution rainfall projections for the Greater Sydney Region. 20th International Congress on Modelling and Simulation (MODSIM2013), Adelaide (Australia). December 2013
Johns, R.H., and Doswell, C.A., 1992: Severe local storms forecasting, *Weather and Forecasting*, **7**, 588-612.
Kain, J.S., and Fritsch, J.M., 1990: A one-dimensional entraining/detraining plume model and its application in convective parameterization, *Journal of Atmospheric Sciences*, **47**, 2784–2802.
Kessler, E., 1969: *On the Distribution and Continuity of Water Substance in Atmospheric Circulations, Meteorological Monographs*, No. 32, American Meteorological Society, 84 pp.
Knight, C.A., and Knight N.C, 2001: Hailstorms. Severe Convective Storms, Meteorological Monographs, Chapter 6, American Meteorological Society, **28**, 570 pp.

Kunz, M., Sander J., and Kottmeier Ch., 2009: Recent trends of thunderstorm and hailstorm frequency and their relation to atmospheric characteristics in southwest Germany, *International Journal of Climatology*, **29,** 2283-2297.

Lim, K.-S.S., and Hong, S.-Y., 2010: Development of an Effective Double-Moment Cloud Microphysics Scheme with Prognostic Cloud Condensation Nuclei (CCN) for Weather and Climate Models, *Monthly Weather Review*, **138**, 1587–1612.

Lin, Y.-L., Farley, R.D., and Orville, H.D., 1983: Bulk parameterization of the snow field in a cloud model. *Journal of Applied Meteorology and Climatology*, **22**, 1065–1092

Liu, C., and Moncrieff, M. W., 2007: Sensitivity of cloud-resolving simulations of warm-season convection to cloud microphysics parameterizations, *Monthly Weather Review*, **135**, 2854–2868

Longley, R.W., and Thompson, C.E., 1965: A study of causes of hail, *Journal Applied Meteorology*, **4,** 69-82.

López, L., Marcos, J.L., Sánchez, J.L., Castro, A., and Fraile, R., 2001: CAPE values and hailstorms on northwestern Spain, *Atmospheric Research,* **56,** 147-160.

Leslie, L.M., Leplastrier, M., and Buckley, B.W., 2008: Estimating future trends in severe hailstorms over the Sydney Basin: A climate modelling study, *Atmospheric Research*, **87**, 37-51.

Manzato, A., 2012: Hail in Northeast Italy: Climatology and Bivariate Analysis with the Sounding-Derived Indices, *Journal of Applied Meteorology and Climatology*, **51,** 449-467.

McBurney, B.M., 2012: Meteorological Parameters Controlling Hailstorm Development in the Sydney Metropolitan Region, *Honours Dissertation (unpublished)*, Macquarie University

McCumber, M., Tao, W. K., Simspon, J., Penc, R., and Soong, S. T., 1991: Comparison of ice-phase microphysical parameterization schemes using numerical simulations of tropical convection, Journal of Applied Meteorology and Climatology, **30**, 985–1004

Mezher, R., Doyle, M., and Barros, V., 2012: Climatology of hail in Argentina, Atmospheric Research, **114-115**, 70-82.

Milbrandt, J. A. and. Yau, M.K., 2005: A multimoment bulk microphysics parameterization. Part I: Analysis of the role of the spectral shape parameter, *Journal of the Atmospheric Sciences*, **62**, 3051-3064.

Mills, G.A., and Colquhoun, J.R., 1998: Objective prediction of severe thunderstorm environments: preliminary results linking decision tree with an operational NWP model, *Weather Forecasting*, **13**, 1078-1092.

Mitchell, E., and Griffiths D., 1993: Report on the Sydney Hailstorm March 1990, Sydney Regional Office, © Commonwealth of Australia, Australian Government Bureau of Meteorology.

Mlawer, E.J., Taubman, S.J., Brown, P.D., Iacono, M.J., and Clough, S.A., 1997: Radiative transfer for inhomogeneous atmospheres: RRTM, a validated correlated-k model for the longwave, *Journal of Geophysical Research*, **102**, 16663-16682

Morrison, H., "An overview of cloud and precipitation microphysics and its parameterization in models", National Centre for atmospheric Research (NCAR), 11th WRF Users' Workshop, June 2010.

Niall, S., and Walsh K., 2005: The impact of Climate Change on hailstorms in Southeastern Australia, *International Journal of Climatology*, **25**, 1933-1952.

Pruppacher, H. R., and Klett, J. D., 2010: Microphysics of clouds and precipitation, 2nd edition, *Atmospheric and Oceanographic Sciences Library*, **18,** Springer, New York, USA, 976 pp.

Rajeevan, M. and Bhate, J., 2009: A high resolution daily gridded rainfall dataset (1971–2005) for mesoscale meteorological studies, Current Science, **96**, 558–562
Rasmussen, E. N., and Blanchard, D.O., 1998: A Baseline Climatology of Sounding-Derived Supercell and Tornado Forecast Parameters, Weather and Forecasting, **13**, 1148-1164.
Rasuly, A.A., Cheung, K.K.W., and McBurney, B., 2015: Hail events across the Greater Metropolitan Severe Thunderstorm Warning Area, *Natural Hazards and Earth System Sciences*, **15**, 973-984.
Reisner, J., Rasmussen, R.J., and Bruintjes, R.T., 1998: Explicit Forecasting of Supercooled Liquid Water in Winter Storms Using the MM5 Mesoscale Model, *Quarterly Journal of the Royal Meteorological Society*, **124**, 1071-1107.
Risk Frontiers, 2011, *PerilAus*, https://www.riskfrontiers.com/perilaus.htm, Last accessed 8th October, 2015
Ryan, C.J., 1992:, Dynamical Classification of Australian Thunderstorms, BOM Meteorological Study, No. 40, Monash University, 61 pp.
Santer, B. D., Wehner, M.F., Wigley, M.L., Sausen, R., Meehl, G.A., Taylor, K.E., Ammann, C., Arblaster, J., Washington, W.M., Boyle, J.S., and Brüggemann, W., 2003: Contributions of anthropogenic and natural forcing to recent tropopause height changes, *Science*, **301**, 479– 483.
Sánchez, J.L., López, L., Bustos, C., Marcos, J.L., García-Ortega, E., 2008: Short-term forecast of thunderstorms in Argentina, *Atmospheric Research*, **88**, 36-45.
Schaefer, J.F., 1986: The dryline, *Mesoscale Meteorology and Forecasting*, P.S. Ray, Ed. Amererican Meteorological Society, 549-572.
Schuster, S.S., Blong, R.J., and Speer, M.S., 2005: Climatology of the Greater Sydney area and New South Wales, Australia, *International journal of climatology*, **25**, 1633-1650.
Seifert, A., and Beheng, K.D., 2006: A two-moment cloud microphysics parameterization for mix-phase clouds. Part 1: model description, *Meteorology and Atmospheric Physics*, **92**, 67-82.
Sherburn, K.D., and Parker, M.D., 2014: Climatology and Ingredients of Significant Severe Convection in High-Shear, Low-CAPE Environments, *Weather and Forecasting*, **29**, 854–877.
Shi, J. J., and Tao, W-K., 2006: Implementation of NASA/GSFC Cloud Microphysics Schemes into WRF, available at: http://www2.mmm.ucar.edu/wrf/users/workshops/WS2006/presentations/Session5/5_4.pdf (last access: 25 September 2015)
Skamarock, W.C., Klemp, J.B., Dudhia, J., Gill, D.O., Barker, D.M., Duda, M.G., Huang, X-Y., Wang, W. and Powers, J.G., 2008: A description of the advanced research WRF version 3. NCAR Technical Note TN-475+STR
Snook, N. and Xue, M., 2008: Effects of microphysical drop size distribution on tornadogenesis in supercell thunderstorms, *Geophysical Research Letters*, **35**, L24803, doi:10.1029/2008GL035866.
Sokol, Z., Zacharov, P., and Skripniková, K., 2014: Simulation of the storm on 15 August 2010, using a high resolution COSMO NWP model, *Atmospheric Research*, **137**, 100111.
Spanos, S.J., 1993: A severe hailstorm in Northern Greece, *Meteorological Magazine*, **122**, 270-277.
Spark, E., and Casinader T., 1995: The 21 January 1991 Sydney Severe Thunderstorm,© Bureau of Meteorology of Australia, Australia Government Bureau of Meteorology.

Speer, S.J., Leslie, L.M., Qi, L., Buckley, B.W., 2004: Urban scale modelling: The Sydney hailstorm of 14 April 1999, *Meteorology and Atmospheric Physics*, **87**, 161-166.

Tao, W. K., and Adler, R., 2003: Cloud Systems, Hurricanes, and the Tropical Rainfall Measuring Mission (TRMM): A Tribute to Dr. Joanne Simpson, *American Meteorological Society,* **29,** 51, Springer, 110 pp.

Tao, W. K., Simpson, J., and McCumber, M., 1989: An ice-water saturation adjustment, *Monthly Weather Review*, **117**, 231-235

The Mesoscale and Microscale Meteorology Division, 2015a, *Chapter 5 WRF Model*, http://www2.mmm.ucar.edu/wrf/users/docs/user_guide_V3/users_guide_chap5.htm/, Last accessed 8th October, 2015

The Mesoscale and Microscale Meteorology Division, 2015b, *AFWA Diagnostics in WRF* http://www2.mmm.ucar.edu/wrf/users/docs/AFWA_Diagnostics_in_WRF.pdf, Last accessed 22nd October, 2015

Thompson, G., Field, P.R., Rasmussen, R.M., and Hall, W.D., 2008: Explicit forecasts of winter precipitation using an improved bulk microphysics scheme. Part II: Implementation of a new snow parameterization. *Monthly Weather Review*, **136**, 5095–5115

Tucker, D.F., 2002: Characteristics of severe hail events in eastern Australia, *21st Conference on Severe Local Storms*, 12-16 August 2002, University of Kansas

Tuovinen, J.P., 2007: Suurien rakeiden klimatologia Suomessa 1930–2006 (The severe hail climatology in Finland 1930–2006), M.S. thesis, Department of Physics, University of Helsinki, 86 pp.

Van den Heever, S.C., and Cotton, W.R., 2004: The Impact of Hail Size on Simulated Supercell Storms, *Journal of Atmospheric Science,* **61**, 1596-1609

Vinet, F., 2001: Climatology of hail in France, *Atmospheric Research*, **56**, 309–323.

Wang, W., Kavulich, M., Bruyère, C., Duda, M. G., Dudhia, J.,Gill, D. O., Michalakes, J., Keene, K., Lin H., Zhang, X., Berner, J, Fossell, K and Rizvi S., 2010: WRF Version 3 Modeling System User's Guide, MMM, UCAR, available at: http://www2.mmm.ucar.edu/wrf/users/docs/user_guide_V3/ARWUsersGuideV3.pdf (last access: 24 September 2015)

Webb, J., Elsom D. M., and Reynolds D.J., (2001), Climatology of severe hailstorms in Great Britain, *Atmospheric Research*, **56**, 291–308.

Wilson, J. W., Feng, Y., and Chen, M., 2010: Nowcasting challenges during the Beijing Olympics: Successes, failures, and implications for future nowcasting systems, *Weather and Forecasting*, **25**, 1691-1714.

Xiaoyan, C., Song, L., and Yang, L., (2010), Analysis of Temporal and Spatial Distribution Characteristics and Environental Conditions of Hail in Southwest Guizhou, *Torrential Disasters*, **29**, 49–53.

Xie B., Zhang Q., Wang, Y., 2008: Trends in hail in China during 1960-2005, *Geophysical Research Letters*, **35**, L13801, doi:10.1029/2008GL034067.

Ziegler C. L., and Rasmussen, E.N., 1998: The initiation of moist convection at the dryline: Forecasting issues from a case study perspective, *Weather and Forecasting*, **13**, 1106–1131.

APPENDIX I

Definitions of meteorological terms		
Term	**Abbreviation**	**Definition**
Convective Available Potential Energy	CAPE	Positive buoyancy of an air parcel; the amount of energy available for convection.
Lifted Index	LFTX	The temperature difference between an air parcel lifted adiabatically and the temperature of the environment at a given pressure height in the troposphere
Bulk Richardson Number	BRN	Non-dimensional number which divides vertical stability (CAPE) by vertical wind shear
Horizontal Wind Shear	HWS	Change of horizontal wind direction and/or speed with horizontal distance
Vertical Wind Shear	VWS	Change of horizontal wind direction and/or speed with height. Calculated by a vector difference between two levels in the atmosphere.
Dry Slot	N/A	A layer of air in the vertical profile that is significantly drier than surrounding layers.
Geopotential Height	N/A	Approximates the actual height of a pressure surface above mean sea level.
Mean Sea Level Pressure	MSLP	Atmospheric pressure observed at sea level, which has a mean value of one atmosphere (1013hPa).
Helicity	N/A	The transfer for vorticity from the environment to an air parcel in convective motion.

APPENDIX II

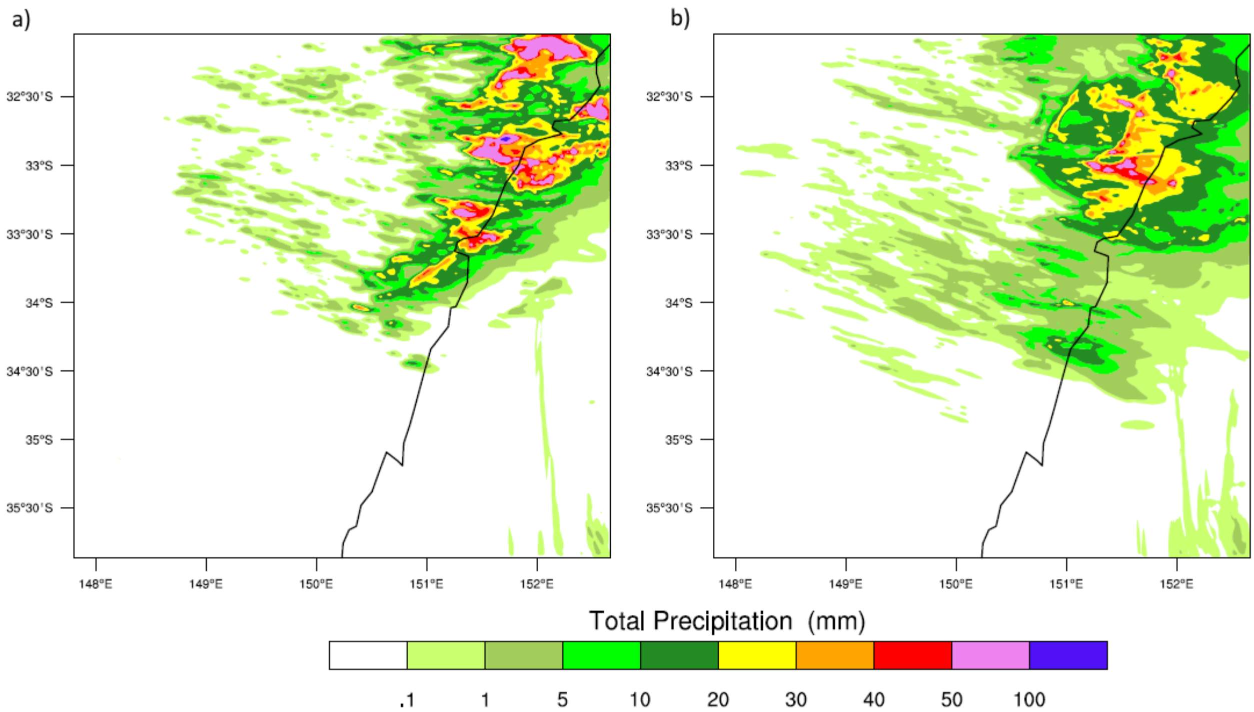

Fig. A1. Domain 3 accumulated precipitation for the Goddard microphysics scheme with the hail option **(a)** and with the graupel option **(b)** from 23:00 UTC 8 December until the end of the simulation (12:00 UTC 9 December)

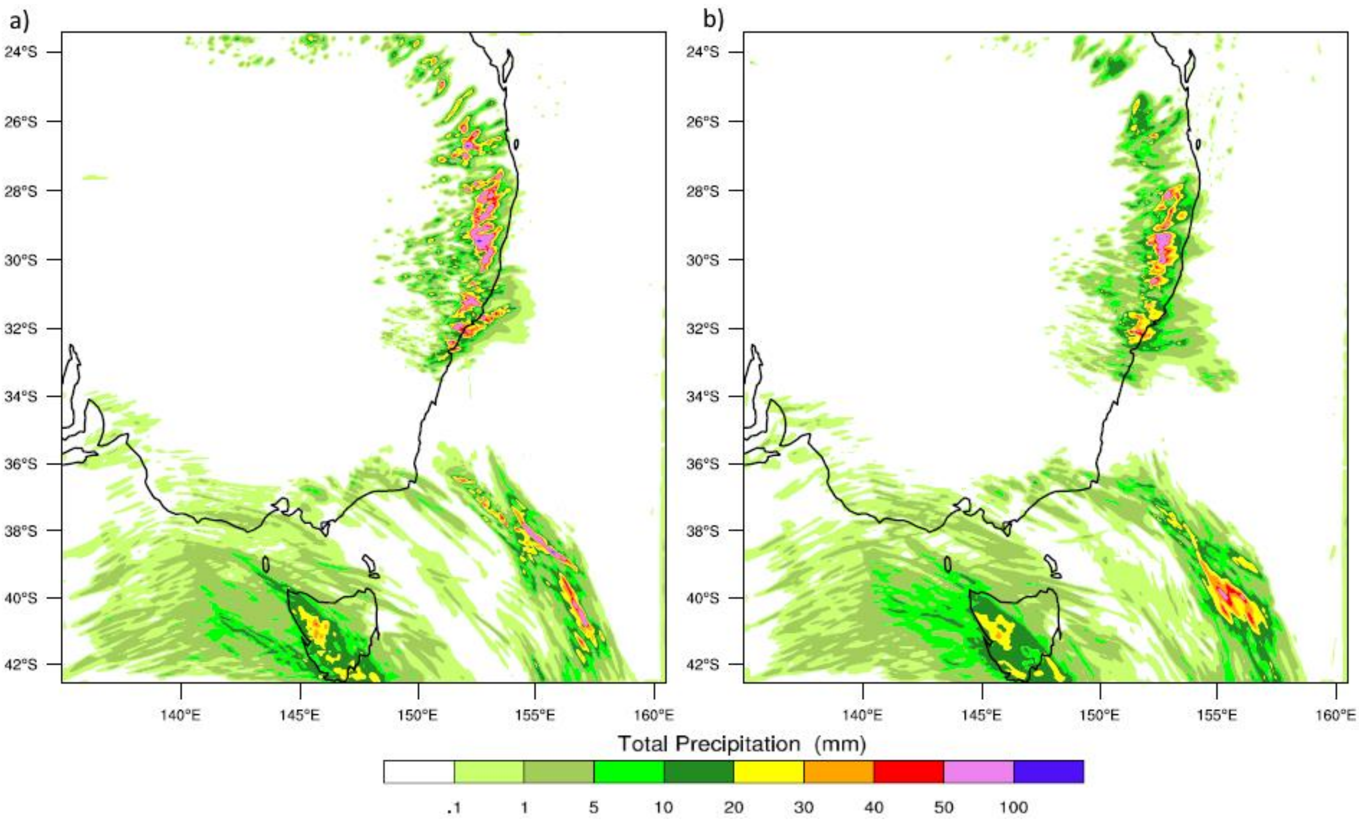

Fig. A2. Domain 2 accumulated precipitation for the Goddard microphysics scheme with the hail option **(a)** and with the graupel option **(b)** from 23:00 UTC 8 December until the end of the simulation (12:00 UTC 9 December)

APPENDIX III

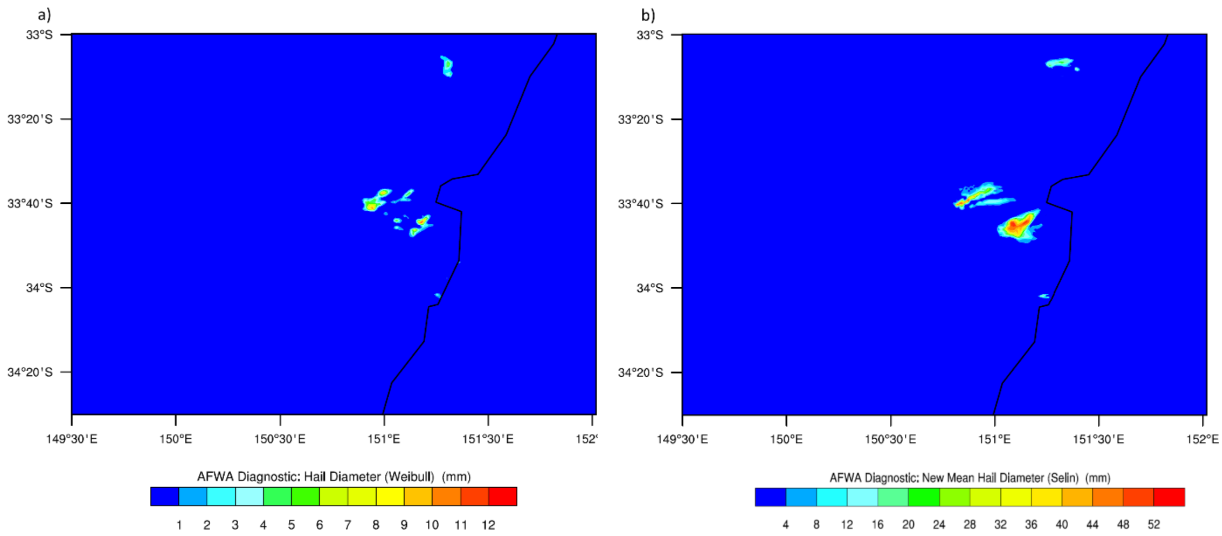

Fig. A3. Zoomed domain 3 AFWA hail diagnostics using the Goddard microphysics scheme with hail showing AFWA_HAIL **(a)** and AFWA_HAILCAST **(b)** at 03:20 UTC

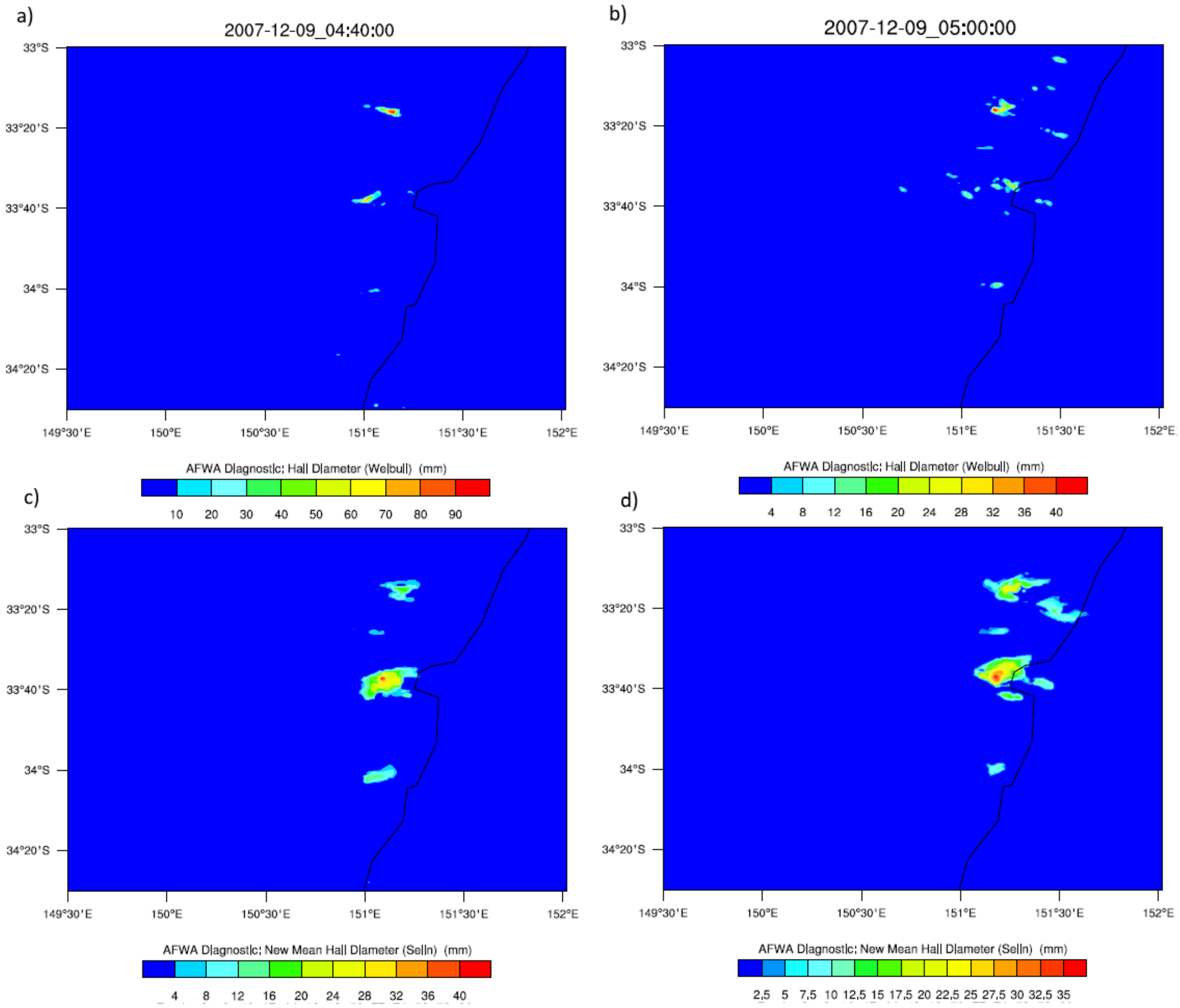

Fig. A4. Zoomed domain 3 AFWA hail diagnostics using the Goddard microphysics scheme with graupel showing AFWA_HAIL and AFWA_HAILCAST at 04:40 UTC **(a)** & **(c)** and 05:00 UTC **(b)** & **(d)**

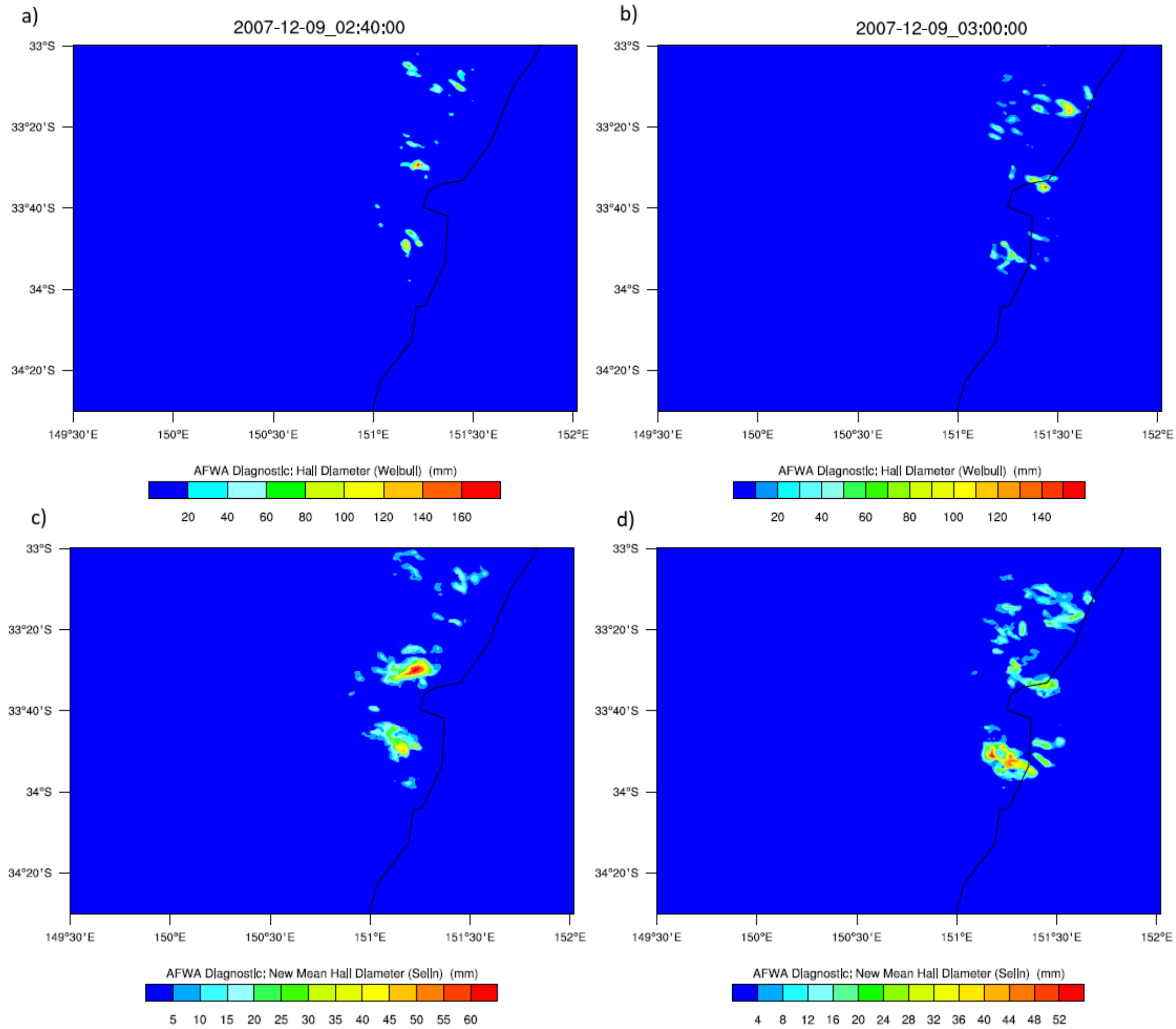

Fig. A5. Zoomed domain 3 AFWA hail diagnostics using the WRF Double Moment 6-class microphysics scheme with hail showing AFWA_HAIL and AFWA_HAILCAST at 02:40 UTC **(a)** & **(c)** and 03:00 UTC **(b)** & **(d)**

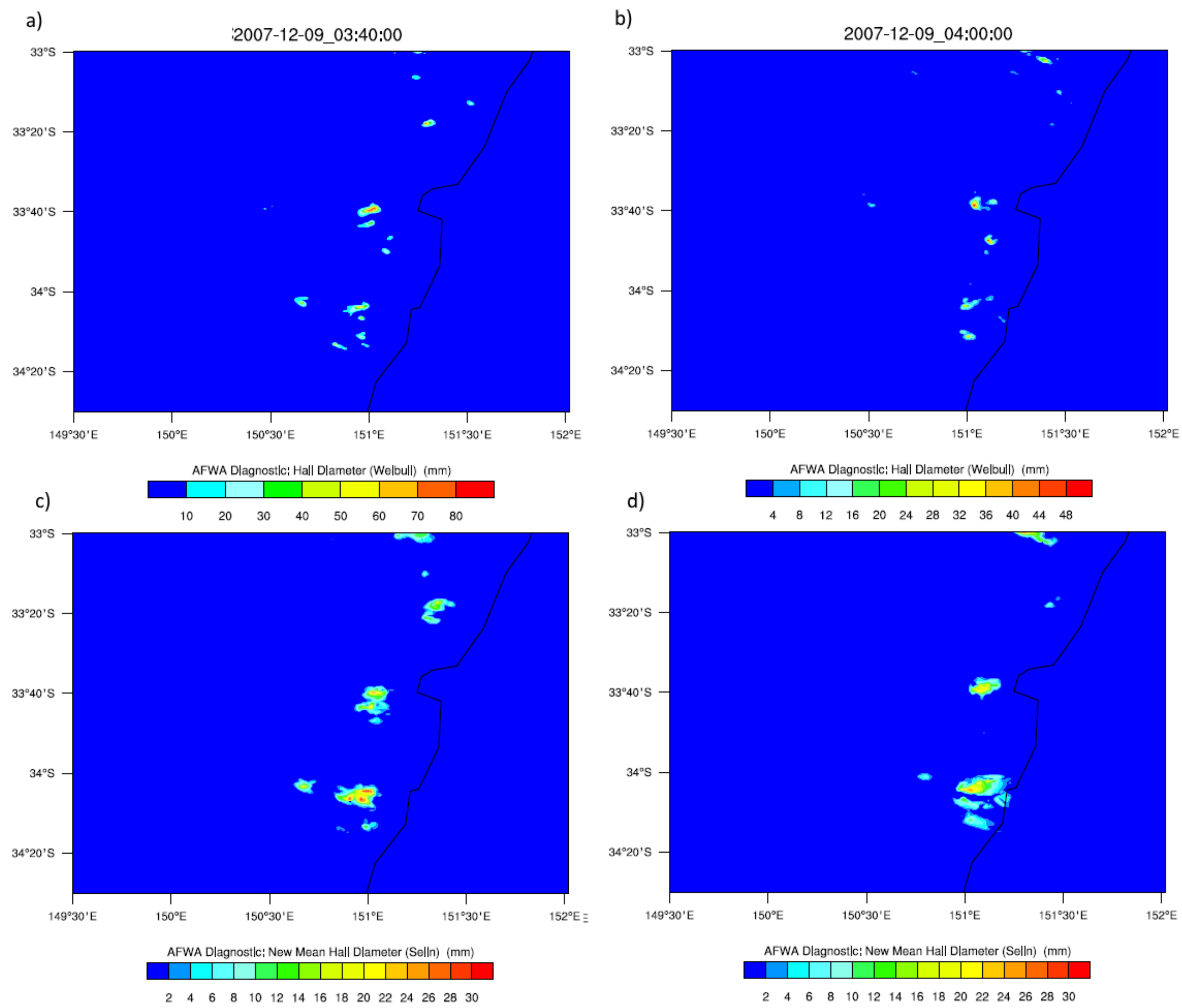

Fig. A6. Zoomed domain 3 AFWA hail diagnostics using the Thompson et al. (2008) microphysics scheme showing AFWA_HAIL and AFWA_HAILCAST at 03:40 UTC **(a)** & **(c)** and 04:00 UTC **(b)** & **(d)**

APPENDIX IV

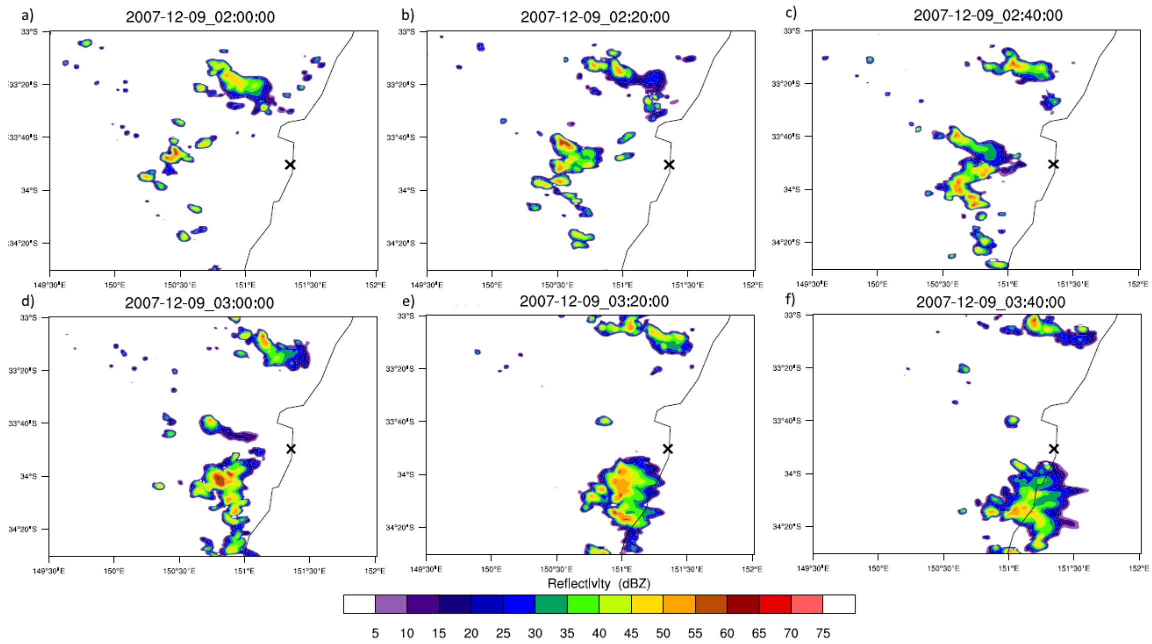

Fig. A7. Simulated equivalent radar reflectivity factor [dBZ] using the Goddard microphysics scheme with hail, the New Goddard shortwave radiation scheme and New Goddard longwave radiation scheme from 02:00 UTC 9 December-03:40 UTC 9 December (1:00 pm – 2:40 pm EDT) at 20 minute intervals **(a-f).** Cross indicates Sydney CBD.

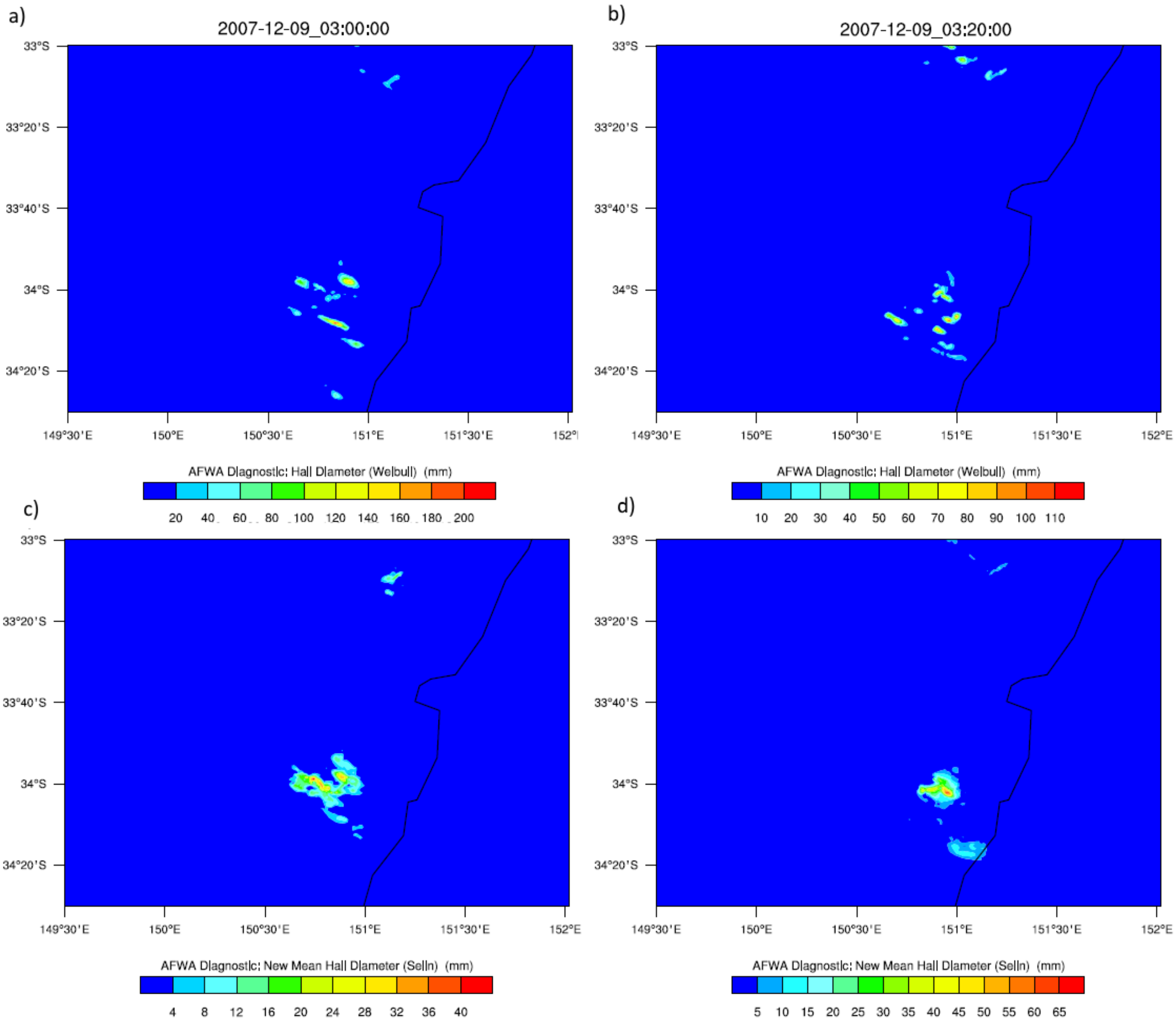

Fig. A8. Zoomed domain 3 AFWA hail diagnostics using the Goddard microphysics scheme with hail, the New Goddard shortwave radiation scheme and New Goddard longwave radiation scheme microphysics scheme showing AFWA_HAIL and AFWA_HAILCAST at 03:00 UTC **(a)** & **(c)** and 03:20 UTC **(b)** & **(d)**